Mohamed Edfawy Soliman Hussien

DISSECTING THE ROLE OF GPRASP2 IN AUTISM SPECTRUM DISORDER AND INTELLECTUAL DISABILITY

Tese de Doutoramento em Biologia Experimental e Biomedicina, ramo de Neurociências e Doença, orientada pelo Doutor João Peça e co-orientação da Doutora Ana Luísa Carvalho, apresentada ao Instituto de Investigação Interdisciplinar da Universidade de Coimbra.

Junho/2017

· U C ·

UNIVERSIDADE DE COIMBRA

Mohamed Edfawy Soliman Hussien

Dissecting the role of GPRASP2 in autism spectrum disorder and intellectual disability

A importância do papel da GPRASP2 na perturbação do espectro do autismo e défice intelectual

2017

Thesis submitted to the Institute of Interdisciplinary Research of the University of Coimbra to apply for the degree of Doctor in Experimental Biology and Biomedicine, specialization in Neuroscience and Disease

• U  C •

This work was conducted at the Center for Neuroscience and Cell Biology (CNC) of University of Coimbra, under the scientific supervision of Doctor João Miguel Peça Lima Novo Silvestre, Assistant Investigator at the Center for Neuroscience and Cell Biology and co-supervision of Doctor Ana Luísa Monteiro de Carvalho, Assistant Professor at the Department of Life Sciences, University of Coimbra.

Mohamed Edfawy was supported by a fellowship (SFRH/BD/51958/2012) awarded by the Doctoral Programme in Experimental Biology and Biomedicine of the Center for Neuroscience and Cell Biology (CNC) and funded by the Portuguese Foundation of Science and Technology (FCT). The work was supported by the Portuguese Foundation for Science and Technology (FCT) and FEDER/COMPETE with FCT grants Pest-C/SAU/LA0001/2013-2014 and UID/NEU/04539/2013; BrainHealth 2020 (CENTRO-01-0145-FEDER-000008); and grants award to João Peça from the FCT Investigator Program (IF/00812/2012), Marie Curie Actions (PCIG13-GA-2013-618525), the Brain & Behavior Research Foundation and FCT grant PTDC/NEU-SCC/3247/2014.

For my Father,

whom I love and miss so much,

I dedicate this thesis to your soul.

I know that you would be proud of me.

You are always in my heart.

"Don't ever let somebody tell you you can't do something. Not even me. You got a dream, you gotta protect it. People can't do something' themselves, they wanna tell you you can't do it. If you want something', go get it. Period."

— The Pursuit of Happyness —

Acknowledgments

Almost five years ago, I left my country, my family, and my friends filled with determination to begin a journey I never thought would be this breathtaking at so many levels! I would never have chosen a better landscape for this adventure; Portugal and specifically Coimbra. It's a long journey getting to the end of a PhD and I'd like to thank everyone who has been a part of that journey.

It gives me immense pleasure to thank my mentor and supervisor João Peça for his support, continuous guidance, astute criticism during the practical phase and for his inexhaustible patience during the correction phase of this dissertation. Despite the challenges since I started my PhD, he always provided me with all the necessary means for the success. Since the beginning, he encouraged me to be independent giving me the freedom to pursue different ideas without objection. I have been extremely lucky to have a supervisor who cared so much about my work, and who responded to my questions and queries so promptly.

I will forever be thankful to my co-supervisor Ana Luisa Carvalho for her support, beneficial discussion and suggestions. She was and remains a role model as a scientist and mentor.

I must express my gratitude to Professor Carlos Duarte not only for his guidance and encouragement, but also for his warmth and kindness. Since I arrived Portugal, he made me feel as being at home.

Completing this work would have been even virtually impossible without the support and friendship of all JP lab members. Special thanks to Lara and Marta for your tremendous help in animal behavior experiments. I cannot forget all the "old fellows" Bruno Cruz, Joao Calmeiro and Renato Sousa. Many thanks to Mario Carvalho and Tiago Reis for their support and friendship. I would like to thank Mariana Laranjo who helped me with manual behavior quantification. Last but not least, I would like to show my appreciation for Joana Guedes who performed all the electrophysiological experiment in this study. Your invaluable input is much appreciated and it was a pleasure working with you.

I want to thank the "laboratory family with whom I shared the lab over the years and who contributed to the accomplishment of this work: Tatiana, Sandra, Dominique, Susana Louros, Joana Ferreira, Pedro Alves, Carlos Matos, Joana Pedro, Mariline, Luis Martins, Pedro Afonso, Miranda, Rui Costa, João Costa, Débora, Marina, Beatriz, Graciano and Catarina Seabra.

Many thanks to Joana Fernandes (minha irmã) for putting me up when I needed a break from thesis work.

I am also very thankful to Lara and Gladys not only for their friendship, but also for the useful assistance through the "dark phases" of my PhD.

I wish to express my gratitude to Ana Teresa, Sara Amaral. I will never forget the many wonderful lunches and fun activities we did done together.

My sincere thanks also go to all my colleagues at 11th BEB edition Ivan, Ravi, Susana Sampaio, Lara Franco, Sofia Morais, Sofia Ferreira, Sara Oliveira, Andrea Gomes, Dina Pereira, Gladys, all of whom I shared the ups and downs of this experience over the years, thank you for your support and friendship.

I would like to extend my appreciations to all members at the animal care facility, especially Carmen and Sandra for their dedication to animal welfare and invaluable support in colony management and husbandry.

I would like to thank Dona Céu, Sara lopes and Elisabete for their indispensable help and expert technical support.

I would express a deep sense of gratitude to my dearest mom, Shadiaa, who has always stood by me like a pillar in times of need and to whom I owe my life, for her constant love, encouragement, moral support and blessings. Special thanks are due to my brother, Ahmed, and loving sister, Sara, who always strengthened my morale by standing next to me in all situations.

Finally, this thesis is dedicated to the memory of my father who would have been happy to see me reaching this goal.

Table of Contents

Abbreviations list

Actinin1	F-actin cross-linking protein 1
AKT	AKT8 virus oncogene cellular homolog
AGRP	agouti-related peptide
AMCA	aminomethylcoumarin acetate
AMPA	α-amino-3-hydroxy-5-methyl-4-isoxazolepropionic acid receptor
ANOVA	analysis of variance
ATP	adenosine-5'-triphosphate
BCA	bicinchoninic acid
BCIP	5-bromo-4-chloro-3-indolyl-phosphate
BSA	bovine serum albumin
CaMKII	calcium/calmodulin-dependent protein kinase II
CDPPB	3-cyano-*N*-(1,3-diphenyl-1*H*-pyrazol-5-yl)benzamide
CNV	copy number variation
CSPD	disodium 3-(4-methoxyspiro {1,2-dioxetane-3,2'-(5'-chloro)tricyclo [3.3.1.1^{3,7}]decan}-4-yl)phenyl phosphate
CTNNB1	catenin beta-1
CTP	cytidine triphosphate
DEPC	diethyl pyrocarbonate
DHPG	(S)-3,5-Dihydroxyphenylglycine
DIG	digoxigenin
DIV	days in vitro
DMSO	dimethyl sulfoxide
DNA	deoxyribonucleic acid
ECL	enhanced chemiluminescence
EDTA	ethylenediaminetetraacetic acid
eIF4E	eukaryotic translation initiation factor 4E
ER	endoplasmic reticulum
ERK	extracellular signal-regulated protein kinase
FBS	fetal bovine serum
fEPSP	field excitatory postsynaptic potential

FMRP	fragile X mental retardation protein
GFP	green fluorescent protein
GKAP	guanylate kinase-associated protein
GluA1	glutamate ionotropic receptor AMPA type subunit 1
GluN2B	glutamate ionotropic receptor NMDA type subunit 2B
GPRASP2	G protein-coupled receptor associated sorting protein 2
GTP	guanosine-5'-triphosphate
HEK	human embryonic kidney cells
HEPES	N-(2-hydroxyethyl)-1-piperazine-N'-(2-ethanesulfonic acid)
HOMER	homer scaffold protein
IL1RAPL1	interleukin 1 receptor accessory protein like 1
IP3R	inositol 1,4,5-trisphosphate receptor type 1
LAMP1	lysosomal associated membrane protein 1
LB	Luria-Bertani
LIF	leukemia inhibitory factor
LTD	long term depression
LTP	long term potentiation
MAP	microtubule-associated protein
MCF2	cell line derived transforming sequence
MECP2	methyl-CpG binding protein 2
mGluR	metabotropic glutamate receptors
MPEP	2-Methyl-6-(phenylethynyl)pyridine hydrochloride
mTOR	mechanistic target of rapamycin
NaOH	sodium hydroxide
NBT	4-nitro blue tetrazolium chloride
NMDA	N-methyl-D-aspartate
NR1	glutamate ionotropic receptor NMDA type subunit 1
OPHN1	oligophrenin-1, Rho-GTPase activating protein
PBS	phosphate-buffered saline
PDZ	post synaptic density protein (PSD95), Drosophila disc large tumor suppressor (Dlg1), and zonula occludens-1 protein (zo-1)

PFA	paraformaldehyde
PI3K	phosphatidylinositol 3-kinase
POMC	pro-opiomelanocortin
PPP1R3F	protein phosphatase 1 regulatory subunit 3F
PSD	postsynaptic density
PSD95	postsynaptic density protein 95
PSMD10	proteasome 26S Subunit, Non-ATPase 10
PTEN	phosphatase and tensin homolog
PVDF	polyvinylidene fluoride
RFP	Red fluorescent protein
RNA	ribonucleic acid
SAPAP	synapse-associated protein 90/postsynaptic density-95-associated protein
SDS	sodium dodecyl sulfate
SHANK1	SH3 and multiple ankyrin repeat domains protein 1
SHANK2	SH3 and multiple ankyrin repeat domains protein 2
SHANK3	SH3 and multiple ankyrin repeat domains protein 3
SH3	SRC homology 3 domain
Siah-1A	Siah E3 ubiquitin protein ligase 1
SLITRK2	SLIT and NTRK-like family member 2
SSC	the saline-sodium citrate buffer
TBST	Tris-buffered saline and Tween-20
TEMED	tetramethylethylenediamine
TM4SF2	T-cell acute lymphoblastic leukemia-associated antigen
tRNA	aminoacyl-transfer RNA
TRPC1	transient receptor potential channel 1
TSC1	tuberous sclerosis protein 1
UBE3A	ubiquitin protein ligase E3A
UTP	uridine-5'-triphosphate
VGLUT1	vesicular glutamate transporter 1

Keywords

Autism spectrum disorder

Intellectual disability

Metabotropic glutamate receptors

GPRASP2

LTD

Palavras-chave

Perturbação do espectro do autismo

Défice intelectual

Receptores metabotrópicos do glutamato

GPRASP2

LTD

Abstract

Autism spectrum disorder (ASD) is diagnosed based on the presence of persistent behavioral deficits affecting social communication, social interactions, and repetitive or restricted interests. ASD poses an immense burden to society, since in some countries it may afflict up to 1 in 68 children. Recent genetic and genomic studies have identified a multitude of mutations in proteins related to synapse formation, maturation, glutamate receptor activity and synaptic plasticity associated with ASD and intellectual disability (ID). In these neurodevelopmental disorders, neurons exhibit deficiencies in spine morphology and neuronal complexity which can correlate with the behavioral and intellectual deficits. Two complexes of particular importance to neuronal spines and synaptic processes have been of recent interest in the field. One is the trans-synaptic macromolecular assembly composed of the Neurexin/Neuroligin/PSD-95/SAPAP/SHANK/HOMER family of proteins. The other module includes proteins directly and indirectly linked to the mTOR signaling pathway and the regulation of cellular growth and protein synthesis, such as TSC1, TSC2, FMRP and PTEN. Together, these molecular complexes share as a common feature the regulation of mGluR signaling.

Altered mGluR signaling has been strongly implicated in the pathophysiology of ASD and ID, however, research centering on the intracellular partners that directly regulate the trafficking and surface availability of these receptors has not been widely explored. In this context, the G Protein-Coupled Receptor Associated Sorting Proteins (GPRASPs) are an interesting target, as this family of proteins have been shown to regulate the trafficking of diverse GPCRs, such as the delta opioid, oxytocin, mGluR1 and mGluR5 receptors. In particular, *GPRASP2* has been recently associated to autism and neurodevelopmental disorders in humans. However, the exact role of GPRASP2 in the nervous system and the consequences of its dysregulation remain unknown.

To address some of these questions, we developed a novel conditional knockout mouse model. We demonstrate that mice lacking *Gprasp2* expression display several phenotypes reminiscent of autism and ID, including abnormal social behavior, altered anxiety levels and enhanced mGluR-LTD. We show that GPRASP2 is expressed in several brain regions including hippocampus, thalamus, and hypothalamus which can be related to the behavioral deficits found in the knockout mice. Additionally, we found that changing the expression levels of GPRASP2 *in vitro* can bidirectionally affect dendritic spine morphology, neuronal complexity

and interfere with mGluR5 trafficking in hippocampal neuronal cultures. Together, our data suggest that *Gprasp2* mutations may contribute to the pathogenesis of neurodevelopmental disorders, affecting dendritic and spine morphology via disruption of mGluR5 trafficking.

Resumo

A perturbação do espectro do autismo (PEA) é diagnosticada com base na presença de défices comportamentais persistentes que afectam a comunicação social, as interações sociais e interesses repetitivos ou restritos. A PEA tem um imenso custo para a sociedade, sendo que em alguns países pode afectar cerca de 1 em cada 68 crianças. Estudos recentes na área de genética e genómica identificaram uma multiplicidade de mutações em proteínas relacionadas com a formação e maturação de sinapses, com a função do receptor do glutamato e com plasticidade sináptica, que estão associadas à PEA e ao défice intelectual (DI). Nestes distúrbios do neurodesenvolvimento, os neurónios apresentam anomalias na morfologia das espículas e complexidade neuronal, que se podem correlacionar com as alterações comportamentais e intelectuais. Dois complexos proteicos de particular relevância para a regulação de espículas e processos sinápticos têm sido o foco na investigação da PEA e DI. O primeiro é o complexo macromolecular trans-sináptico composto pela família de proteínas Neurexina/Neuroligina/PSD-95/SAPAP/SHANK/HOMER. O segundo módulo inclui proteínas direta ou indiretamente ligadas à via de sinalização mTOR e da regulação do crescimento celular e síntese proteica, como TSC1, TSC2, FMRP e PTEN. Juntos, estes complexos macromoleculares têm como uma característica comum a regulação da sinalização dos receptores metabotrópicos de glutamato (mGluR).

A alteração da sinalização pelos mGluR tem sido fortemente implicada na fisiopatologia da PEA e DI, no entanto, investigação centrada nas proteínas que regulam diretamente o tráfico e a disponibilidade destes receptores à superfície da célula não está ainda amplamente explorada. Neste contexto, um alvo interessante é a família de proteínas GPRASP, visto que estas demonstraram regular o tráfico de diversos *GPCRs*, como por exemplo os receptores delta opióide, oxitocina, mGluR1 e mGluR5. Desta família, o gene GPRASP2 é particularmente interessante pois foi recentemente associada ao autismo e a distúrbios do desenvolvimento neurológico em humanos. Porém, o papel deste proteína no sistema nervoso e as consequências da sua desregulação são ainda desconhecidas.

Para adereçar algumas destas questões, desenvolvemos um novo modelo de murganhos *knockout* (KO) condicional para o gene GPRASP2. Usando este modelo, conseguimos demonstrar que, na ausência de Gprasp2, os animais apresentam vários fenótipos característicos de PEA e DI, incluindo comportamento social anormal, alterações de ansiedade e aumento da depressão sináptica de longa duração associada aos mGluRs. Mostramos também que a

GPRASP2 é expressa em várias regiões do cérebro, incluindo o hipocampo, o tálamo e o hipotálamo, regiões relevantes para os défices comportamentais encontrados nos murganhos *knockout*. Além disso, descobrimos que a alteração dos níveis de expressão de GPRASP2 *in vitro* pode afectar bidirecionalmente a morfologia das espículas dendríticas, assim como a complexidade neuronal por interferir com o tráfico de mGluR5. No seu conjunto, os nossos dados sugerem que mutações no gene GPRASP2, por via de uma desregulação de mGluR5, contribuem para a patogénese de distúrbios do desenvolvimento neurológico, afetando o comportamento animal, as propriedades sinápticas dos circuitos e a morfologia neuronal.

Chapter 1 | Introduction

Part of this chapter is under preparation for submission as a review.

Edfawy M., Peça, J. The role of the mGluR network of proteins in autism spectrum disorder and intellectual disability (in preparation)

1.1. Autism Spectrum Disorder

Autism spectrum disorder (ASD) is characterized by persistent deficits in social behavior and communication, and the presence of restricted interests and repetitive behavior (American Psychiatric Association, 2013a). It is one of the most prevalent neurodevelopmental disorders, which in the US affects 1 in each 68 children at a 4:1 male to female incidence ratio (CDC, 2014). Manifestations of ASD start early in life, but the clinical profile varies widely due to the presence of other co-morbid conditions such as abnormal gait and motor function, epilepsy, sensorial abnormalities (up to 90%), sleep disturbances, attention deficit hyperactivity disorder, obsessive-compulsive disorder, mood disorders and intellectual disability (ID, up to 70%) (Geschwind, 2009; Charman et al., 2011; Zoghbi and Bear, 2012a; Belardinelli et al., 2016; de la Torre-Ubieta et al., 2016).

In terms of etiology, ASD is a complex, heterogenous disorder and in a majority of patients, it is also idiopathic. While environmental factors may play a role in increasing risk (Grabrucker, 2013), ASD is considered among the most heritable of all brain diseases. In support of this view, studies with twins showed concordance rate as high as 90% for monozygotic pairs and 30% for dizygotic pairs (Bailey et al., 1995; Rosenberg et al., 2009). More recent work points to heritability in the range of 50-60%, still strongly suggesting that the bulk of risk for ASD stems from genetic influence (Huguet et al., 2013). Moreover, recurrence within the same family is seen in up to 18% of infants with at least one affected older sibling (Ozonoff and Young, 2011). Finally, there is also strong prevalence of ASD in patients diagnosed with genetic syndromes (de la Torre-Ubieta et al., 2016). Indeed, at the molecular and cellular level, some of the best described forms of ASD and ID arise from the studies on Fragile X, Rett, Phelan-McDermid, Tuberous Sclerosis and Angelman syndrome, and their associated genes, FMR1, MECP2, SHANK3, TSC1/2 and UBE3A, respectively (Peça and Feng, 2012; de la Torre-Ubieta et al., 2016). Not surprisingly, human studies have found a wide pleiotropism in genes simultaneously responsible for ASD and ID (Volk et al., 2015).

The emerging picture in the genetic architecture of ASD suggests that various types of alterations play a role in disease etiology, these can range from autosomal recessive and dominant mutations, copy number variations (CNVs), large genomic translocations and rearrangements, as well as *de novo* rare variants (de la Torre-Ubieta et al., 2016). Nevertheless, while more than 100 protein-coding genes have been highlighted as ASD susceptibility genes (Betancur, 2011), it is still unclear if most cases arise from deleterious rare variants, CNVs or from combinations of common polymorphisms (Sebat et al., 2007; Gaugler et al., 2014).

Recent evidence has found strong prevalence of ASD candidate-genes with critical roles in synaptic function. Several of these candidates encode proteins that play an essential role in protein-protein interaction and neurotransmitter signaling, such as postsynaptic scaffolding proteins (e.g. SHANK, HOMER, SAPAP) and transmembrane proteins (neuroligin, cadherin or contactin) (Peça and Feng, 2012; Ting et al., 2012). One hypothesis is that the disruption of any of these elements perturb the synapse and the signaling hub that brings together ionotropic (iGluR) and metabotropic glutamate receptors (mGluR) in excitatory spines (Peça and Feng, 2012; O'Connor et al., 2014).

1.2. Spine pathology in ASD and ID

Changes in spine morphology and spine dynamics mediate connectivity within neuronal circuits and are critically important for brain functions involving memory, cognition and regulation of behavior (Holtmaat and Svoboda, 2009; Kasai et al., 2010). The expression of long-term potentiation (LTP) and long-term depression (LTD) represent plastic changes in synaptic strength that correlate with alterations in the number or morphology of spines (Holtmaat and Svoboda, 2009). In particular, LTD has been linked to decreases in spines number through the removal of weak synapses (i.e. synaptic pruning) (Nägerl et al., 2004; Wiegert and Oertner, 2013). This interplay between LTD and synaptic pruning is critically important in normal brain developmental and its dysfunction may represent a pathognomonic event underlying ASD and ID. Moreover, there is evidence supporting the hypothesis that aberrant synaptic pruning is a core feature in disease pathogenesis (Penzes et al., 2011; Zoghbi and Bear, 2012a). Several animal models of ASD and ID, such as the Fragile X, 15q11-13 duplication, Tuberous sclerosis, SYNGAP1, SHANK3 or Neuroligin mutant lines manifest impairment in LTD and abnormal spine rearrangements (Huber et al., 2002a; Auerbach et al., 2011; Peça et al., 2011; Piochon et al., 2014; Barnes et al., 2015; Zhang et al., 2015; Wang et al., 2016b).

Alterations in spines are also found in other mental illnesses, including neurodegenerative and neuropsychiatric disorders (Fiala et al., 2002; Penzes et al., 2011). Postmortem imaging and gene expression studies in ASD patients have highlighted potential dysregulations in cortical developmental (Schumann et al., 2010; Voineagu et al., 2011; Willsey et al., 2013; Chen et al., 2015). These changes include: increased number of neurons, decreased white matter, as well as dendritic abnormalities (Chen et al., 2015). Recent studies also showed that spine density in ASD patients may be higher than what is found in controls (Hutsler and

Zhang, 2010; Tang et al., 2014). From these studies, one group showed that spine density was inversely correlated with cognitive function (Hutsler and Zhang, 2010), while the other showed that spine deficits correlated with impaired autophagy and hyperactive mTOR signaling (Tang et al., 2014). Considering the strong association between ASD and ID it is also important to mention the seminal work of Dominick Purpura showing the presence of spine dysgenesis and reduced spine density in patients with intellectual disability (Purpura, 1974). Nevertheless, the broad etiology and complexity of ASD may preclude any general conclusions on spine density changes without *a priori* knowledge of the underlying genetic insult.

Specifically, this is where animal models of ASD, with well-defined genetic lesions, may provide clearer mechanistic insights towards the link between this cellular feature and pathological behaviors and cognitive dysfunction. In the next section, some of the genes involved in ASD are highlighted and explored in terms of overlapping and converging deficits on synapse function and plasticity, altered signaling pathways and behaviors relevant to ASD and ID.

1.3. Synaptic proteins involved in ASD and ID

Several of the rare mutations and CNVs found in ASD and ID patients encode for synaptic proteins localized at the postsynaptic density (PSD) (Penzes et al., 2011; Volk et al., 2015). This compartment sits in dendritic spines as a highly organized and prominent structure juxtaposed to the synaptic membrane. The PSD is comprised of a large number of proteins involved in protein-protein interactions, scaffolding, cellular adhesion, neurotransmitter signal transduction, endo- and exocytosis, intracellular trafficking and the regulation of the actin cytoskeleton (Sheng and Hoogenraad, 2007). The PSD proteome is composed of about 1500 different proteins, and mutations or alterations to some 200 of these elements have been linked to various human brain diseases (Bayés et al., 2011). In particular, multiples classes of core PSD scaffolding proteins have been strongly linked to autism and ID (Ting et al., 2012; Volk et al., 2015). This convergence reflects the functional interdependence between overlapping molecular elements. Indeed, the postsynaptic density provides a prime example of a complex network model for human diseases (Goh et al., 2007; Peça and Feng, 2012). Two pathways of particular importance for neuronal spines and synaptic processes have been the focus of recent interest. One is the trans-synaptic macromolecular complex composed of the Neurexin/Neuroligin/PSD-95/SAPAP/SHANK/HOMER family of proteins (Ting et al., 2012). The other module includes proteins directly or indirectly linked to the mTOR signaling

pathway and regulation of cellular growth (Peça and Feng, 2012). Together, these molecular complexes share as a key feature the regulation of mGluR signaling (Fig.1) (O'Connor et al., 2014).

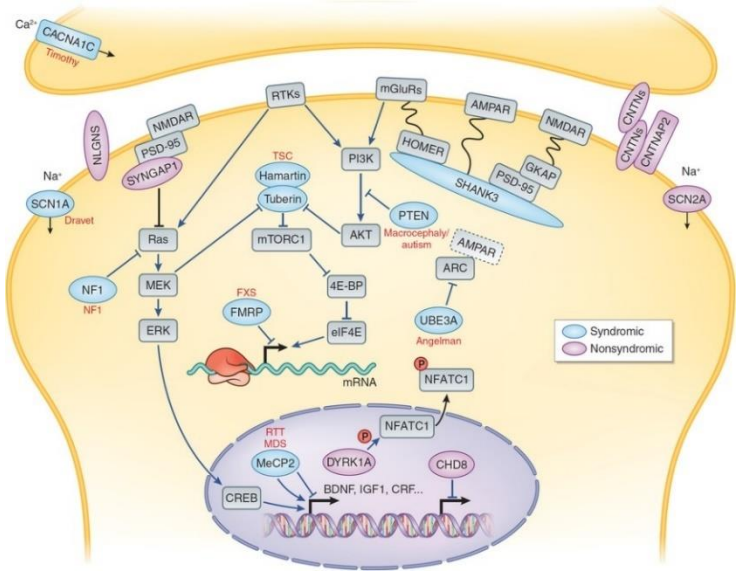

Figure 1 | Synaptic signaling proteins encoded by ASD-related genes. Examples of signaling proteins encoded by genes associated with ASD. A common property of many of these genes is in their modulation of synaptic structure and function as well as their connection to mGluR signaling. NF1, neurofibromatosis type 1; FXS, fragile X syndrome; RTT, Rett syndrome; MDS, MECP2 duplication syndrome; TSC, tuberous sclerosis complex; NLGNs, neuroligins; CNTNs, contactins; RTKs, receptor tyrosine kinases; mGluRs, metabotropic glutamate receptors; AMPAR, AMPA receptor; NMDAR, NMDA receptor; PSD-95, postsynaptic density protein 95; GKAP, guanylate kinase-associate protein; HOMER, homer protein homolog; PI3K, phosphoinositide kinase-3; PTEN, phosphatase and tensin homolog; SCN1A, sodium channel voltage gated type 1 a-subunit; CNTNAP2, contactin associate protein-like 2. Adapted from (Sztainberg and Zoghbi, 2016).

1.3.1. HOMER

HOMER is an important scaffolding protein that is enriched at the PSD of excitatory synapses, where it regulates the cross-talk between cell surface receptors, signaling pathways and scaffolding proteins (Whistler et al., 2002). At the N-terminal, HOMER proteins displays an Ena-Vasp-Homology (EVH1) domain that binds membrane receptors, such as mGluR1 and mGluR5 (Brakeman et al., 1997), TRPC1 and IP_3R (Yuan et al., 2003), and other cytosolic partners such as SHANK (Tu et al., 1999), dynamin (Gray et al., 2003) or oligophrenin (Govek et al., 2004). In longer isoforms, the C-terminal displays a coiled-coil domain responsible for homomeric interactions (Hayashi et al., 2009a). The formation of higher-order tetramers through interactions with SHANK was shown to create a polymeric matrix within the PSD

(Hayashi et al., 2009b). In humans, HOMER isoforms are coded by three genes, *HOMER1, HOMER2,* and *HOMER3*. Some of the best-studied isoforms include for example, HOMER1b/c, HOMER2a/b and HOMER3, which contain the coiled-coiled domain; and the short isoform HOMER1a which was originally described as an immediate early gene and only expresses the EVH1 domain (Brakeman et al., 1997; Shiraishi-Yamaguchi and Furuichi, 2007). Long forms of HOMER act as a scaffold that modulate mGluR activity by promoting clustering of the receptors and bringing them in close proximity to intracellular signaling machinery. Conversely, HOMER1a competes with the longer isoforms to influence the ligand-dependent activity of mGluR1 and mGluR5 (Kammermeier, 2008). Thus, while HOMER1b/c regulates the constitutive activity of mGluRs, HOMER1a functions as a dominant negative protein in disrupting the mGluR-HOMER1b/c complex (Ango et al., 2001).

Additionally, HOMER1b/c modulates a third signaling pathway of these receptors that is Ca^{2+}-independent, by linking mGluR5 to ERK1/2 activation (Mao et al., 2005). Recent evidence have highlighted the impairment in HOMER-mGluR interaction in various mouse models of ASD (Guo *et al.*, 2016; Wang *et al.*, 2016). In particular, *Shank3* knockout mice (KO) displayed abnormal expression and distribution of Homer1b/c and mGluR5 in striatal neurons (Wang *et al.*, 2016). This abnormal expression was not found in the neocortex and hippocampus, which may be explained by the non-redundant role Shank3 in the striatum (Peça et al., 2011).

A popular model to study autism is the *Fmr1* mouse model of Fragile X syndrome (FXS) (discussed in detail below), in this model, a key dysfunction is found in mGluR-dependent long-term depression (Huber et al., 2002a). In *Fmr1* mice there is reduced association of mGluR5 with the HOMER1b/c isoforms but the association with HOMER1a is maintained (Giuffrida, 2005). In line with this, introducing a genetic deletion of *Homer1a*, rescued some of the abnormal phenotypes present in *Fmr1* mice, including neocortical hyperexcitability (Ronesi et al., 2012). Similarly, the *Ube3A* mouse model for Angelman syndrome also exhibits exaggerated mGluR-LTD linked to a dysfunctional association between mGluR5 and HOMER isoforms (Pignatelli et al., 2014).

Interestingly, direct manipulation of HOMER1a levels via over-expression in the amygdala was shown to perturb normal social behavior in rats (Banerjee et al., 2016). Also, HOMER1 levels were found reduced in the superior cortex and in the cerebellar vermis in postmortem human samples (Fatemi et al., 2013). Finally, direct evidence for the role of *HOMER1* in disease has emerged from a genetic screening, which revealed the presence of rare

and potentially deleterious mutations is ASD patients (Kelleher et al., 2012). Together, these lines of evidence support a direct involvement of *HOMER* in ASD and ID-relevant disorders such as Fragile X and Angelman syndromes.

1.3.2. SHANK family of proteins

SHANK proteins are synaptic scaffolding proteins that anchor various other proteins to the PSD. SHANK1, SHANK2 and SHANK3 possess multiple protein-protein interaction domains including ankyrin repeats, SH3, PDZ, proline-rich region, and a sterile alpha motif domain that coordinates the binding of SHANK to other scaffolding protein, receptors and elements of the actin cytoskeleton (Boeckers et al., 1999; Naisbitt et al., 1999). Of particular interest, SHANKs connect: i) NMDA receptors via the PSD-95/GKAP complex (Naisbitt et al., 1999), ii) mGluRs via Homer (Tu et al., 1999), and iii) AMPA receptors via PSD-95/Stargazin (Schnell et al., 2002). Although SHANK protein family members (SHANK1-3) share the same binding domains, they display a complex array of isoforms, expression profiles, and binding partners. Particularly, SHANK3 has a unique expression pattern as it is highly expressed in the striatum while SHANK1 and SHANK2 are not (Böckers et al., 2004; Peça et al., 2011).

1.3.3. SHANK1

SHANK1 plays a role in the regulation of spine morphology and its over-expression is associated with spine enlargement and maturation (Sala et al., 2001). Deletion of *Shank1* in mice leads to a thinning of the PSD and a decrease in levels of SAPAP and HOMER as well as a reduction in synaptic transmission and spine density in the hippocampus (Hung et al., 2008). SHANK1 and HOMER1b interact to link mGluR1/5 and IP_3R to regulate Ca^{2+} homeostasis at the synapse and disruption of this complex is thought to underlie the spine alteration seen in *Shank1* mutant mice (Sala et al., 2005). At the behavioral level, *Shank1* knockouts showed normal sociability in reciprocal social interaction, increase anxiety-like behavior and abnormal motor coordination (Silverman et al., 2011). When pups, these mice manifest reduced ultrasonic vocalization as well as impaired social learning and increased self-grooming in social contexts (Wöhr et al., 2011; Sungur et al., 2014).

In humans, a familial *SHANK1* deletion was found to propagate across four generation where male carriers were diagnosed with high functioning ASD (Sato et al., 2012b), also,

SHANK1 rare mutations have also been found in ASD patients (Krumm et al., 2015; Wang et al., 2016a).

1.3.4. SHANK2

Several studies have found mutations and alterations in CNVs in the *SHANK2* gene in individuals with ASD and ID (Berkel et al., 2010; Pinto et al., 2010; Sanders et al., 2012). Some of these mutations have been shown to reduce spine volume, the size of SHANK2 clusters in the synapse, as well as spine density (Berkel et al., 2012; Leblond et al., 2012). Much like other SHANK family members, SHANK2 is a scaffolding protein involved in spine morphology via the regulation of the actin cytoskeleton. Mice lacking *Shank2* exhibit autistic-like behavior alterations including impairment in social behavior, increased locomotor activity and repetitive grooming (Schmeisser et al., 2012). Consistent with its effect on spine formation, *Shank2* knockout animals display a reduction in spine density and impaired synaptic transmission (Schmeisser et al., 2012). Similar result was obtained in a second mutant line carrying a deletion of exons 6 and 7 (Won et al., 2012). In this line, disruption in NMDAR-associated signaling was shown to be rescued by administration D-cycloserine, a partial agonist of NMDARs, which recovered NMDA-dependent synaptic plasticity and improved the social interaction deficits associated with *Shank2* deletion. Additionally, treatment with CDPPB a positive modulator of mGluR5 normalized NMDA/AMPA ratio and also promoted greater recovery in social interactions, when compared to D-cycloserine (Won et al., 2012). These findings solidify the hypothesis that glutamatergic transmission is a critical focal point in ASD and ID, highlighting also a contribution from NMDA receptors and convergence in terms of mGluRs function.

1.3.5. SHANK3

SHANK3 is the leading candidate gene for the major neurobiological alterations occurring in the Phelan-McDermid syndrome (22q13.3 microdeletion syndrome) due to the presence of a recurrent breakpoint within the *SHANK3* gene that is found across multiple patients (Bonaglia et al., 2006). The role of *SHANK3* as a *bona fide* ASD gene is further supported by the discovery of a deleterious mutation in patients afflicted with social behavior deficits, language and social communication deficits (Durand et al., 2007; Moessner et al., 2007; Gauthier et al., 2010). Some authors have highlighted that approximately 1% of all ASD cases derive from mutations in the *SHANK3* gene (Moessner et al., 2007). Moreover, *SHANK3* has

also been implicated in non-syndromic cases of intellectual disability (Hamdan et al., 2011; Gong et al., 2012b; Gilissen et al., 2014).

Besides expression in mouse cerebral cortex and cerebellum, SHANK3 displays a strong expression in the striatum, whereas SHANK1 and SHANK2 are not as prevalent, suggesting a potentially non-redundant role of SHANK3 in corticostriatal connectivity (Peça et al., 2011). SHANK3 is also a target for rapid bidirectional regulation since on one hand its mRNA is dendritically enriched and on the other hand, SHANK proteins are regulated via ubiquitination in response to activity (Ehlers, 2003; Böckers et al., 2004). Also, several lines of evidence have documented the role of SHANK3 in the maturation and stabilization of dendritic spines either by overexpression or knockdown (Roussignol et al., 2005; Durand et al., 2012).

Several genetically modified mouse models targeting *Shank3* have now been generated (Bozdagi et al., 2010; Peça et al., 2011; Wang et al., 2011). Different groups performed unique manipulations in the gene structure of *Shank3* gene, but most *Shank3* models displayed a combination of behavioral deficits attributed to ASD, such as social interaction deficits, increased repetitive behaviors, and altered vocalizations. In particular, *Shank3*$^{e4–9}$ (exon 4-9 deletion) mutant mice showed increased grooming and repetitive behavior, alteration in locomotor activity and reduced interaction in a social dyadic test (Wang et al., 2011). Bozdagi and colleagues pointed to alterations in social communication, manifested by reduced social sniffing and decrease ultrasonic vocalization when placed in a cage with an estrus wild-type female (Bozdagi et al., 2010). From the two *Shank3* mouse lines created by Peça et al, the *Shank3B* line deleting exons 13-16, displayed severe self-injurious repetitive grooming, deficits in social interaction, anxiety-like behavior and a striking impairment in corticostriatal circuits (Peça et al., 2011). Deletion of major SHANK3 isoforms in this mouse line altered the molecular composition of the postsynaptic assembly in the striatum along with perturbed medium spiny neuron morphology. Recordings in cortico-striatal synapses also showed a decrease in pop spike amplitude measured by extracellular field recordings (Peça et al., 2011). Hippocampal neurons from *Shank3*$^{e4–9}$ homozygous mice also showed an impairment in LTP linked to a reduction in NMDA and AMPA subunits (Wang et al., 2011).

Recently, two novel mutant mice with *Shank3* point mutations associated with ASD (InsG3680) mutation or schizophrenia (R1117X) displayed both common and distinct biochemical and behavioral alterations (Zhou et al., 2016). Interestingly, the ASD-linked mutation mimicked the phenotype of *Shank3B* knockout line in terms of juvenile social deficits and disruption of corticostriatal circuits, while on the line carrying the schizophrenia mutation

displayed social dominance behavior and an impairment in prefrontal cortical circuits (Zhou et al., 2016).

In line with its interaction with HOMER, altered SHANK3 expression leads to abnormal mGluR5 signaling and impaired synaptic plasticity via an inhibition of mGlu5-Homer complex formation (Verpelli *et al.*, 2011; Wang *et al.*, 2016). This is in contrast with the up-regulation of hippocampal mGluR5 receptors found in mutant mouse models for Fragile-X and Angelman syndromes (Ronesi et al., 2012; Pignatelli et al., 2014). However, different *Shank3* mouse models have also shown differential response to mGluR manipulations (Vicidomini *et al.*, 2016; Wang *et al.*, 2016). Vicidomini and colleagues found that potentiation of mGluR5 signaling rescued behavioral phenotypes in *Shank3*^{e11} KOs, such as grooming and social behaviors via administration of a positive allosteric mGlu5 agonist (CDPPB). Conversely, Wang and colleagues described that MPEP (a mGluR5 negative allosteric modulator), but not CDPPB, could ameliorate the grooming behavior in their *Shank3* null line (*Shank3*$^{e4\text{-}22}$) (Wang *et al.*, 2016). The latter also showed alterations in PSD composition, reorganization of Homer and mGluR5 association and a decreased spine density in striatal neurons (Wang *et al.*, 2016). A possible reconciliation of these findings could be ascribed to different Shank3 isoforms being disrupted in different mouse lines leading to perturbations that are cell-type specific or that affect different brain regions (Wang et al., 2017).

Lastly, a recent addition to the repertoire of *Shank3* mouse models is the conditional knockout-first line created in the laboratory of Guoping Feng. This line allowed the introduction of SHANK3 protein expression only in the adult mouse in a Cre-dependent manner. Using this strategy the authors showed that they could revert the synaptic alterations, social deficits and repetitive grooming behavior when the correction of the genetic lesion was performed in 2-4 month-old mice (Mei et al., 2016).

1.4. mTOR, protein synthesis and ASD-associated genetic syndromes

Dysregulated mTOR signaling is found in ASD, FXS, Tuberous Sclerosis, Cowden syndrome and in patients with ID (Ehninger et al., 2009; Zhou et al., 2009; Troca-Marín et al., 2012). In a group of ASD patients, hyperactive mTOR activation was connected with deficient synaptic pruning (Tang et al., 2014). Additionally, *Tsc2*$^{+/-}$ mice also showed spine pruning dysfunction and autophagy inhibition due to excessive mTOR activation (Tang et al., 2014). Administration of rapamycin (mTOR inhibitor) corrected autophagy and recovered normal spine density suggesting that mTOR signaling and autophagy are required for normal spine

pruning (Tang et al., 2014). Aueurbach and colleagues also demonstrated that excessive mTOR signaling abolished the necessity of *de novo* protein synthesis for mGluR mediated LTD (Auerbach et al., 2011). Overall changes in protein synthesis linked to autism have also been identified in eIF4E-transgenic mice, where overexpression of eIF4E leads to upregulation in mGluR- dependent LTD in the hippocampus, an increase in spine density and ASD-like behaviors (Santini et al., 2013). More generally, this suggests that alterations in protein translation and synaptic abnormalities are core hallmarks in ASD subtypes.

1.4.1. Fragile X syndrome

Fragile X syndrome is an X-linked dominant disorder caused by an expansion of unstable CGG repeats within the *FMR1* gene resulting in transcriptional silencing and loss of fragile X mental retardation protein (Verkerk et al., 1991). FXS is the leading genetic cause of intellectual disability in humans and affects approximately 1:5000 in males (Gustavson *et al.*, 1986). Due to the high incidence of ASD in FXS patients, mutations in *FMR1* are one of most common known causes of ASD (Hatton et al., 2006). The role of FMRP in the regulation of synaptic protein synthesis via its ability to transport mRNA cargo to dendrites while playing a part in translational repression (Dictenberg et al., 2008; Darnell et al., 2011). Consistent with its proposed biochemical function, absence of FMRP causes an upregulation of hippocampal protein synthesis, in what is considered a core feature of FXS neurophysiology (Huber et al., 2002a; Hagerman et al., 2009; Osterweil et al., 2010). Interestingly, some of the synaptic alterations in FXS arise from loss of translational constraint on other ASD-related transcripts such as Neuroligin-3, Neurexin-1, SHANK3, PTEN, TSC2 and NF1 (Darnell et al., 2011) (Fig. 2).

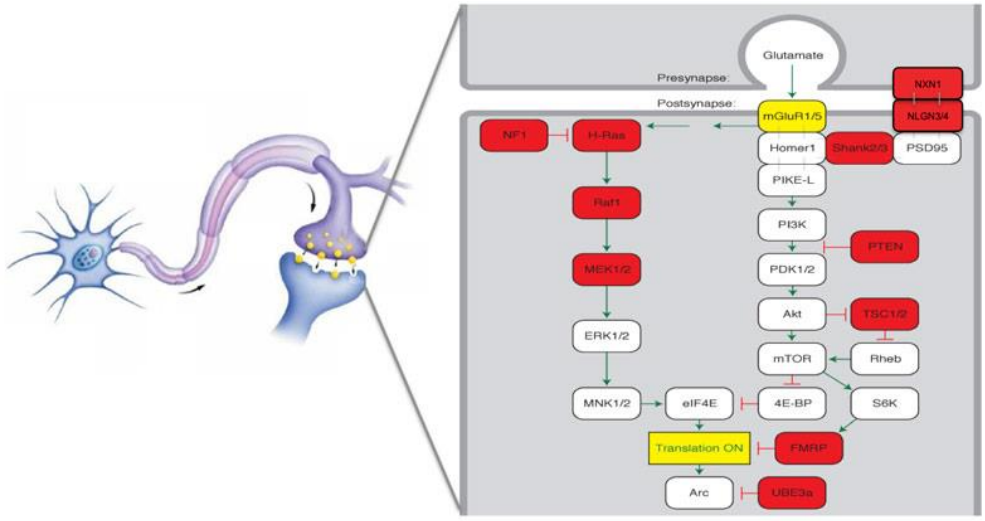

Figure 2 | Schematic drawing showing examples of proteins involved in local protein synthesis at excitatory synapses. Disruption of the gene products indicated in the colored boxes significantly increases the risk of ASD/ID. Syndromic disorders that involve dysregulation in protein synthesis include Neurofibromatosis type 1 (NF1); Costello syndrome (H-Ras, MEK1); Cowden syndrome (PTEN); Cardio-facio-cutaneous (CFC) syndrome (MEK1/2); Tuberous sclerosis complex (TSC1 and TSC2); Fragile X syndrome (FMRP); Angelman syndrome (UBE3a); Rett syndrome (MeCP2); and Rubinstein-Taybi syndrome (CREB binding protein, p300). Adapted from (Zoghbi and Bear, 2012a).

A central hypothesis in FXS is the so-called "mGluR theory of fragile X", which proposes that loss of FMRP provokes an increase in mGluR activation and exaggerated LTD (Huber et al., 2002a; Bear et al., 2004; Chuang, 2005). A corollary to this hypothesis is that the attenuation of mGluR signaling would provide a plausible approach to alleviate many of the abnormalities associated with FXS. Indeed, in recent years, this has been tested via direct modulation of mGluR5 activity (Huber, 2011). Specifically, administration of mGluR5 antagonists have been shown to correct the excitatory/inhibitory imbalance and restore normal magnitude of hippocampal LTD, as well as promote an amelioration of some behavioral deficits in *Fmr1* KO mice (Yan et al., 2005; Dölen et al., 2010; Michalon et al., 2012). Furthermore, mGluR5 heterozygosity in FMRP KOs (*mGlur5*$^{+/-}$ *FMR1*$^{-/y}$) was also shown to correct the excessive mGluR signaling and normalize synaptic protein levels, leading to a rescue of the dendritic spine alteration and behavioral abnormalities (Dölen et al., 2007). However, the exact behaviors being modified or rescued by mGluR5 heterozygosity remain controversial (Thomas et al., 2011).

Since translational imbalance is another potential cause for FXS, it has been proposed that the recovery of translation homeostasis might correct several of the associated pathologies

(Osterweil et al., 2010; Bhattacharya et al., 2012). In addition to deregulation of mGluRs activity, mTOR signaling upregulation is another feature in FMRP mice (Sharma et al., 2010). Similarly to mGluR5 depletion approach, interfering with mRNA stability by targeting the cytoplasmic polyadenylation element binding protein (CPEB), to generate *Fmr1*$^{-/y}$ *CPEB*$^{-/-}$ double knockout mice led to the recovery of excessive protein translation and rescued FMRP audiogenic seizures, anxiety-like behavior and exaggerated mGluR-LTD (Udagawa et al., 2013).

The presence of a potential mechanism prompted clinical research into the amelioration of FXS symptoms via negative modulation of mGluR5 receptors. However, despite early promising results in human trials using fenobam, a selective negative allosteric modulator of mGluR5 (Berry-Kravis et al., 2009), the latest pharmacological studies aimed at negatively modulating mGluR5 failed to produce significant results in FXS patients (Williams, 2012; Mullard, 2015). Still, there is ongoing controversy regarding effective doses used in the latest trials as well as the development of an unexpected drug tolerance and the age at which patients were treated (Mullard, 2015).

Interestingly, while most studies on FMRP have focused on the hippocampus, Koekkoek and colleagues showed that both global or cell-specific *Fmr1* deletion were sufficient to induce spine elongation and produce enhanced LTD in Purkinje cells (Koekkoek et al., 2005), suggesting that the cellular mechanism of FXS is shared across different brain regions and cellular types. This could suggest that modification in mGluR5 alone, due to its specific regional expression, may not be sufficient to ameliorate deficits in humans.

1.4.2. Tuberous sclerosis complex

Tuberous sclerosis complex (TSC) is an autosomal dominant disorder characterized by general central nervous system dysfunction and by the formation of benign tumors in multiple organs (Prather and de Vries, 2004). Strongly linked to mutations in the genes *TSC1*/harmatin or *TSC2*/tuberin, TSC patients often display epilepsy, ID and ASD (Kelleher and Bear, 2008). Interestingly, the presence of social interaction deficits and repetitive behavior in TSC was observed even prior to the description of autism by Leo Kanner (CRITHCHLEY and EARL, 1932; Kanner, 1943). Reciprocally, there is a high incidence of TSC mutations among autistic samples and the prevalence of ASD in TSC is in the range of 50-60% (Shepherd et al., 1991; Hunt and Shepherd, 1993; Ahlsen et al., 1994; de la Torre-Ubieta et al., 2016).

At the cellular level, TSC1 and TSC2 proteins form a complex that negatively regulates cell growth via the mTOR pathway (The European Chromosome 16 Tuberous Sclerosis Consortium, 1993; van Slegtenhorst et al., 1997; El-Hashemite et al., 2003). Dysfunction of the TSC1-TSC2 complex in individuals with TSC has been shown to lead to excessive mTOR activation in hamartomatous tissues (El-Hashemite et al., 2003; Kwiatkowski, 2003). It has also been shown that mTOR plays a major role in maintaining different forms of synaptic plasticity that require de novo protein synthesis (Tang et al., 2002). These evidence further support Akt/mTOR signaling and regulating of translation at dendritic spines as a central molecular mechanism in ASD and ID (Kelleher and Bear, 2008; Troca-Marín et al., 2012).

TSC/mTOR signaling is crucial during development since it is involved in synaptogenesis, the growth of dendrites and axons and the regulation of cell proliferation (Swiech et al., 2008; Dazert and Hall, 2011). Perturbation of TSC1 or TSC2 in hippocampal pyramidal neurons leads to an alteration in dendritic spine morphology including a decrease in spine density (Tavazoie et al., 2005). This is also seen with the upregulation of mTOR found in *Tsc2*$^{+/-}$ mice (Ehninger et al., 2009). Moreover, mice lacking TSC1 in Purkinje cells presented increase in spine density (Tsai et al., 2012), while TSC mutation in cortex and hippocampus showed decreased spine density (Tavazoie et al., 2005; Meikle et al., 2008; Bateup et al., 2011) suggesting that TSC1/2 complex regulates spine morphology through different mechanisms across different circuits. Taken together, these results highlight the synaptic function of the TSC1/2 complex in regulation neuronal of morphology.

Interestingly, the several shared interaction partners between TSC1 and SHANK3, such as ACTININ1 and HOMER3, again point to an overlap in the molecular pathways between ASD-associated conditions (Sakai et al., 2011). At the synaptic level, TSC1 mutant mice display decreased spine density with enhancement in AMPA/NMDA ratios (Tavazoie et al., 2005), while an heterozygous mutation in TSC2 has shown to promote altered hippocampal synaptic plasticity through a mTOR protein-synthesis dependent mechanism (Auerbach et al., 2011). Additionally, there are learning and memory impairment in both *Tsc1* and *Tsc2* heterozygous mutant mice (Goorden et al., 2007; Ehninger et al., 2009). Notably, this disruption in synaptic plasticity could be rescued by the mTOR inhibitor rapamycin again suggesting that the cognitive impairment in TSC are be caused by disinhibited mTOR signaling (Ehninger et al., 2009).

As in several other ASD associated condition, *Tsc* mutant mice also presented a component of abnormal mGluR signaling (Ehninger and Silva, 2011). Postnatal deletion of *Tsc1 in vivo* showed impairment in hippocampal mGluR-LTD with no significant alterations in

NMDA receptor-dependent LTD (Bateup et al., 2011). Similarly, several lines of evidence confirmed the impairment in mGluR-LTD in *Tsc2* mutant mice (Ehninger et al., 2009; Chévere-Torres et al., 2012). Mutations in *Tsc2* are also associated with increased protein synthesis consistent with an elevated mTor activity, altered hippocampus-dependent learning well as impaired mGluR-LTD (Auerbach et al., 2011). Together, this suggests that deregulation of protein synthesis is a mechanism underlying TSC and that mTOR plays a role in this dysfunction.

Augmenting mGluR5 signaling with a positive allosteric modulation (CDPPB) managed to restore the magnitude of mGluR LTD in $Tsc^{+/-}$ mice to normal level besides improving the cognitive impairments (Auerbach et al., 2011). In *Tsc2*, mGluR-LTD exhibits opposing direction dysfunction when compared to *Fmr1-/y* mice and what is striking is that crossing the two strains together (double mutants) cancels out both mGluR-LTD dysfunction as well as behavioral deficits (Auerbach et al., 2011). One hypothesis arising from these observations is that the increased translation of specific transcripts at the synapse in different animal models may produce differential effects, nevertheless, the precise mechanisms regulates these putative pools remains unknown.

Recent findings have shown that circuit dysfunction underlying ASD lead to disruption in excitatory/inhibitory (E/I) balance in human (Bejjani et al., 2012; van de Lagemaat et al., 2014) as well as in animal models (Chih et al., 2005; Paluszkiewicz et al., 2011; Han et al., 2013). Perturbation of TSC expression in mice has been shown to affect the balance between excitatory and inhibitory synaptic activity in cerebellum and hippocampus (Tavazoie et al., 2005; Tsai et al., 2012) and this abnormal neuronal excitability is implicated in the seizures and the cognitive impairment characteristic of TSC (Zeng et al., 2007; Curatolo, 2015). Bateup and colleagues suggested that deletion of *Tsc1* from CA1 pyramidal neurons reduces inhibitory input to pyramidal neurons and this cell-autonomous deficit was the initiating factor in disrupting excitatory/inhibitory (E/I) balance towards increased excitation. Notably, the hippocampal hyperexcitability and other phenotypes associated with *Tsc1* deletion in neurons were rescued by mTOR inhibitor rapamycin (Bateup et al., 2013). Tavazoie et al. pointed towards the elevation of AMPA-mediated synaptic current in absence of TSC2 as a possible mechanism responsible for this hippocampal hyperexcitability (Tavazoie et al., 2005).

In sum, genetic manipulation of *Tsc1* and *Tsc2 in vivo* revealed distinct features of ASD including social interaction deficits (Goorden et al., 2007; Waltereit et al., 2011), stereotypic behaviors and impaired social communication (Tsai et al., 2012; Reith et al., 2013) besides

profound cognitive dysfunction (Sato *et al.*, 2012). A recent study with conditional deletion of *Tsc2* from the forebrain revealed upregulation in mTOR signaling associated with increased seizures, repetitive behavior and impaired social interaction (McMahon et al., 2015). The authors also proposed that the frequent seizures seen in TSC mutant mice are linked to the hyperactivity of mTOR in 5-HT neurons (McMahon et al., 2015). Taken together, the discovery of the relationship between *TSC1/TSC2* and mTOR has resulted in important clinical advances in the use of mTOR inhibitors in the treatment of several TSC manifestations.

1.4.3. Cowden syndrome and PTEN

Phosphatase and tensin homolog (PTEN) is a tumor suppressor gene found in a broad spectrum of human cancers (Ali et al., 1999). Additionally, individuals with PTEN mutations are more susceptible to several neurological disorders including macrocephaly, ID, epilepsy and ASD (Goffin et al., 2001; Butler et al., 2005; Endersby and Baker, 2008). Several clinical studies have reported the presence of PTEN mutations among autistic individuals (Buxbaum et al., 2007; Redfern et al., 2010) and most of these correspond to rare nonsense and missense mutations (Butler et al., 2005; Endersby and Baker, 2008). PTEN is a negative regulator of the PI3K/AKT signaling pathway which has also been linked to schizophrenia (Emamian et al., 2004) and ASD (Lv et al., 2013). The PI3K/AKT pathway regulates several cellular processes such as dendritic arborization, neurite growth and neuronal polarity (Crowder and Freeman, 1998; Jaworski et al., 2005; Jiang et al., 2005).

PTEN is expressed both at presynaptic and postsynaptic sites where it plays an important role in regulation of synaptic plasticity (Jurado *et al.*, 2010; Weston *et al.*, 2012). For example, Weston and colleagues found that *Pten* deletion increases evoked synaptic release in both inhibitory and excitatory neurons in the hippocampus (Weston et al., 2012), meanwhile, others have shown that PTEN is an essential component for NMDA-dependent LTD (Jurado *et al.*, 2010).Together these findings provide new insights towards the role of PTEN in regulating hippocampal synaptic function.

At early stages of development, PTEN also controls multiple physiological processes including neuronal migration and proliferation (Endersby and Baker, 2008). Due to the significant role of PTEN during development, it has been reported that loss of PTEN significantly increases dendrite size and results in an enlarged hippocampus, which is in the line with macrocephaly in patients. (Backman et al., 2001; Kwon et al., 2001). Supporting this view,

it was shown that the knockdown of PTEN in a specific subset of hippocampal cells induced increased excitatory synaptic function (Luikart et al., 2011).

When PTEN is deleted only in a subset of postmitotic neurons in the cortex and hippocampus, mice displayed anxiety-like behavior and social interaction deficits (Kwon et al., 2006). Additionally, deletion of PTEN in neurons and astrocytes was associated with increased cell sized due to upregulation of AKT/mTOR signaling (Fraser et al., 2004; Kwon et al., 2006), and this neuronal hypertrophy could be rescued by blocking TSC/mTORC1 (Zhou et al., 2009). Indeed, mutations associated with PI3K/AKT/mTOR intracellular signaling pathway play a significant role in mediating several abnormalities that mimic ASD (Enriquez-Barreto and Morales, 2016). Changes to synaptic plasticity, both LTP and LTP, were found to be impaired by manipulations of PTEN expression *in vivo* and *in vitro* (Wang et al., 2006; Fraser et al., 2008; Jurado et al., 2010a). Together with FXS and TSC animal models, *Pten* mutant mice also showed impairment in mGluR signaling in the hippocampus (Lugo et al., 2014). This is in agreement with a previous study showing that the deletion of PTEN in the hippocampus was associated with impairments in both LTP and mGluR-LTD in perforant pathway synapses (Takeuchi et al., 2013). With the above, these findings highlight the importance of the mechanisms regulating protein synthesis and proteostasis in the context of ASD and ID.

Table 1 | Synaptic and cellular dysfunction in ASD/ID mouse models

Mouse	Brain area	mGluR-dependent LTD	mTOR activity	Dendritic phenotype	Neuronal translation	References
Fmr1 KO	Hippocampus	Enhanced	Increased	Increased density of spines; (immature spines)	Increased	(Comery et al., 1997; Huber et al., 2002b)
Pten cKO	HippocampusCortex	Impaired (TBS/mGluR-LTD)	Enhanced PI3K pathway	Neuronal hypertrophy	ND	(Takeuchi et al., 2013; Lugo et al., 2014)
Tsc2+/− mouse	Hippocampus	Reduced	Increased	Increased density of Spines	Slightly decreased	(Tavazoie et al., 2005; Auerbach et al., 2011)
eIF4E transgenic	Hippocampus	Enhanced	ND	Increased density of Spines	increased	(Santini et al., 2013)
MECP2	Hippocampus	Impaired	Decreased	Decreased density and elongated spine necks	decreased	(Moretti et al., 2006; Belichenko et al., 2009)
cKO *Tsc1*-deletion in CA1 neurons	Hippocampus	Impaired	ND	Normal	ND	(Bateup et al., 2011)
Nlgn3 KO	Cerebellum	Impaired	ND	Normal	ND	(Baudouin et al., 2012; Zhang et al., 2015)

1.5. mGluR interacting proteins in ASD

mGluRs are central to several neuronal pathophysiological events in ASD and ID. Altered signaling downstream mGluR5 plays a major role as the signature disruption in models of FXS, TSC, Angelman or Phelan-McDermid syndrome. Additionally, several of the affected genes, *SHANK2*, *SHANK3* or *HOMER* for example, are known to direct link to the mGluR5 signaling pathway (Gai et al., 2011; Verpelli et al., 2011). Interestingly, genetic and pharmacological manipulation of mGluRs was shown to ameliorate behavioral abnormalities in both *Fmr1* (Dölen et al., 2007; Michalon et al., 2012) and *Shank2* (Won et al., 2012) mutant mice.

Like most GPCRs, mGluRs interact with receptor-selective partners that mediate GPCR signaling and trafficking to specific cellular locations (Ritter and Hall, 2009). For instance, it has been shown that β-arrestin2 is required for mGluR-dependent synaptic plasticity in the hippocampus (Eng et al., 2016) and genetic heterozygosity of β-arrestin in *Fmr1*$^{-}$/^{y} corrected abnormal mGluR-LTD (Stoppel et al., 2017). Nevertheless, besides the well-known partners, HOMER and β-arrestin, other direct mGluR interacting partners have been identified, albeit less well studied.

An important regulatory partner includes the G protein-coupled receptor associated sorting proteins (GPRASPs) which regulate trafficking of diverse GPCRs, such as the delta opioid receptor, oxytocin, as well as mGluR1 and mGluR5 receptors (Abu-Helo and Simonin, 2010). From this family, *GPRASP2* has recently been linked to autism and neurodevelopmental disorders (Piton et al., 2011; Zhou et al., 2014; Butler et al., 2015). However, the exact role of *GPRASP2* in normal nervous system function and the consequences of its dysregulation remain unknown.

1.5.1. *GPRASP2* a susceptibility gene for ASD and schizophrenia

Whole-genome sequencing coupled with computational approaches integrating protein interaction networks has led to hypothesis concerning molecular pathways and processes that are likely to underpin neuropsychiatric disorders (Cristino et al., 2014). Particularly, it has been shown that rare variants on the X chromosome are involved in the etiology of ASD and ID and contribute to the sex-ratio disequilibrium affecting predominatly males at at 4 to 1 rate when compared to females (Skuse, 2005). A recent study sequenced 111 X-linked synaptic genes in individuals with ASD (n = 142; 122 males and 20 females) or schizophrenia (n = 143;

95 males and 48 females). The authors identified > 200 non-synonymous variants, with an excess of rare damaging variants in ASD suggesting the presence of disease-causing mutations. Several promising non-synonymous rare variants were identified in genes encoding proteins involved in regulation of neurite outgrowth and other various synaptic functions including *MECP2*, *TM4SF2/TSPAN7*, *PPP1R3F*, *PSMD10*, *MCF2*, *SLITRK2*, *OPHN1* and *GPRASP2* (Piton et al., 2011).

Other studies based on association roles and interaction networks, proposed *GPRASP2* as an ASD susceptibility gene (Basu et al., 2009; Gong et al., 2012a). Importantly, whole exome sequencing revealed non-syndromic mutation in *GPRASP2* associated with ASD (Butler et al., 2015), while Zhou *et al.* in 2014 pointed to a large 1.1 Mb region of chromosome Xq22 covering *GPRASP2* and several other genes, which proved lethal in homozygosity male mice and led to cleft palate, epilepsy and ID in heterozygous females. Collectively, these reports point towards the implication of *GPRASP2* in neurodevelopmental disorders.

1.5.2. Molecular characterization of GPRASPs

The GPRASP2 gene belongs to a family of 10 members (GPRASP1–GPRASP10) which have been shown to display a broad spectrum of interactions with GPCRs. GPRASP family share a conserved C-terminal domain of 250 amino acids (Simonin et al., 2004). This region displays 20 to 77% sequence identity in pairwise comparisons between GPRASP1 and other GPRASPs. In addition, sequence homology performed with the SPTrEMBL database demonstrated a highly conserved and repeated motif of fifteen amino acids that is present near the conserved C-terminal domain in several GPRASPs (Simonin et al., 2004) (Fig 3). Accordingly, GPRASPs are divided into two subfamilies, subfamily 1 (including GPRASP1 to -5) and subfamily 2 (including -6 to-10). GPRASP1-5 are the only family members that share this conserved motif of 15 amino acids (Abu-Helo and Simonin, 2010). With the exception of GPRASP8, GPRASP genes contain a single coding-exon and form two clusters on human chromosome loci Xq22.1-q22.2, suggesting that they arose from a common ancestral gene (Winter and Ponting, 2005; Abu-Helo and Simonin, 2010).

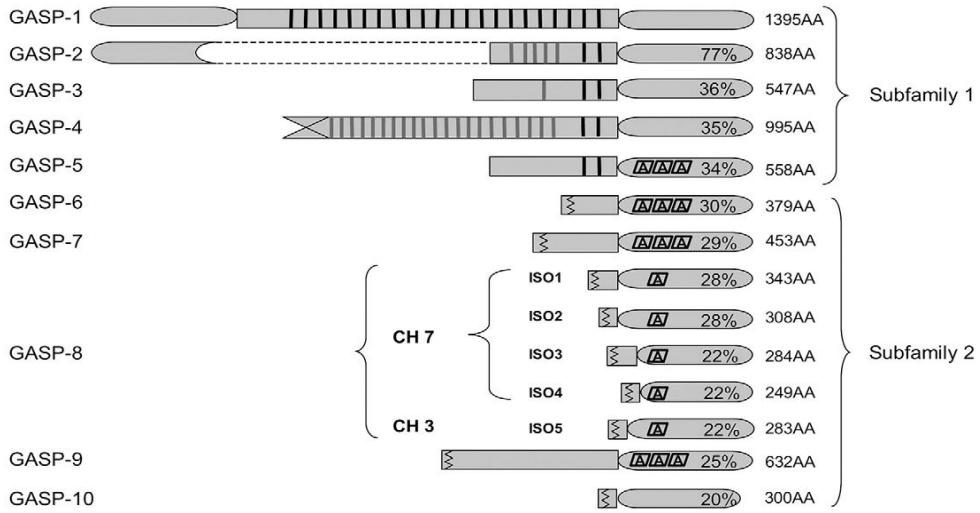

Figure 3 | Sequence homologies between GASP 1 and other family members. Adapted from (Abu-Helo and Simonin, 2010).

Most GPRASP family members are preferentially expressed in the central nervous system (CNS), suggesting that they might act in a cell type-specific manner to control the post-endocytic fate (recycling versus degradation) of certain CNS-enriched GPCRs. Interestingly, GPRASP genes are localized in a region of chromosome X that is unique to placental mammals and that may have evolved in tandem with of the development of the neocortex (Winter and Ponting, 2005).

Mechanistically, upon internalization GPCRs can be recycled back to the membrane or degraded. Although the mechanisms that govern the post-endocytic fate of GPCRs are not fully understood, several proteins have been implicated in the postendocytic sorting of GPCRs, by binding to the C-terminal tail of these receptors (Heydorn et al., 2004; Simonin et al., 2004). The functional relevance of this interaction for post-endocytic lysosomal sorting has been established for GPRASP1 (Fig.4) (Martini et al., 2010).

GPRASP1 has been shown to regulate delta opioid receptor (Whistler et al., 2002), bradykinin B1 (Enquist and Skro, 2007) and dopamine D2 receptor (D2R) (Bartlett et al., 2005) It was also hypothesized that downregulation of D2Rs in response to cocaine could arise from a GPRASP-mediated postendocytic degradation of D2Rs (Thompson et al., 2010). However, Boeuf and colleagues reported that disruption of *Gprasp1 in vivo* was associated with behavioral alteration in responses to cocaine and the authors point towards involvement of GPRASP1 in receptor recycling, rather than degradation (Boeuf et al., 2009). In addition to their postulated role in the modulation of the post-endocytic sorting of these receptors, recent data indicate that

several GPRASPs may modulate the transcriptional activity of the cell through their interaction with transcription factors (Zastrow and Hanyaloglu, 2008).

GPRASP2 which is closest in homology to GPRASP1 (Simonin et al., 2004) has been shown to interact with several GPCRs, including beta-1 and beta-2 adrenergic, calcitonin and D2R (Simonin et al., 2004; Thompson et al., 2007). As such, and because of its homology to GPRASP1 it is possible that it shares some of the same targets, including mGluRs, oxytocin, dopamine receptors. Additionally and according to the protein-protein interaction database STRING, GPRASP2 is also proposed to interact with several proteins implicated either in ASD and schizophrenia. These include Disc-1, a prominent target gene for susceptibility to schizophrenia; the muscarinic cholinergic receptor 1 (CHRM1) gene which is also altered in schizophrenia; HTR7 the serotonin neurotransmitter involved in autistic disorder and other neuropsychiatric disorders (Helsmoortel et al., 2016). Finally, GPRASP2 interacts with BTRC, a substrate recognition component of a SCF (SKP1-CUL1-F- box protein) E3 ubiquitin-protein ligase complex which mediates the ubiquitination of CTNNB1 and PSD-95.

Moreover, GPRASP2 was identified in large two-hybrid screens conducted with huntingtin (htt) fragments as bait (Goehler et al., 2004). The interaction between GPRASP2 and huntingtin may have an adverse effect on GPCR sorting leading to aberrant signaling and disease. This interaction has been shown to occur in mammalian cells both by co-immunoprecipitation and co-localization experiments, raising the possibility that GPRASP2 interacts with htt under physiological conditions (Horn et al., 2006).

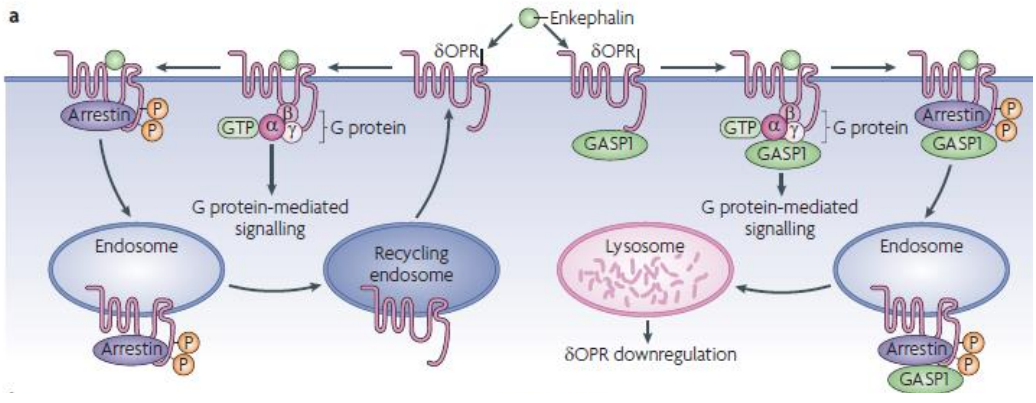

Figure 4 | GPCR-interacting proteins can regulate the post-endocytic trafficking of GPCRs. Following agonist-induced receptor endocytosis, some GPCRs are targeted for proteolytic and/or lysosomal degradation, whereas other GPCRs rapidly recycle back to the plasma membrane. The interaction between GPRASP1 (GASP1) and opioid receptor (δOPR) promotes the endocytic targeting of agonist-internalized δOPR to lysosomes, where the receptors are degraded. However, when GPRASP1 is absent, δOPR are rapidly recycled back to the plasma membrane. Adapted from (Ritter and Hall, 2009).

Besides the implication of *GPRASP2* in ASD, there are few reports of other *GPRASPs* involvement in other brain disorders. Most of these findings are based on transcriptomic studies showing alteration of mRNA levels of different GPRASPs. Two reports stand out, one showing that GPRASP3 mRNA level is decreased in the brain of Alzheimer's disease patients (Heese et al., 2004), and a second study that places GPRASP4 in a list of 892 highly dysregulated "priority genes" in the brain of Parkinson's disease patients (Moran and Graeber, 2008).

GPRASP1 was identified as a cytoplasmic protein that selectively interacts and targets delta opioid receptors for lysosomal degradation (Whistler et al., 2002). Besides these, Heydorn and colleagues reported that other GPCRs interact with GPRASPs through their cytoplasmic tails (Heydorn et al., 2004). Among the positive candidates for GPRASPs were the tails from dopamine, oxytocin and mGluR receptors, which are known to be involved in regulation of distinct types of behaviors including social behavior and ASD-like behavior (Staal et al., 2012; Hadley et al., 2014; LoParo and Waldman, 2015) (Fig.5). Although the mechanism underlying the trafficking of dopamine (Whistler et al., 2002) and oxytocin receptors (Gimpl and Fahrenholz, 2001) have been identified, little is known about the endocytic fate of mGluRs

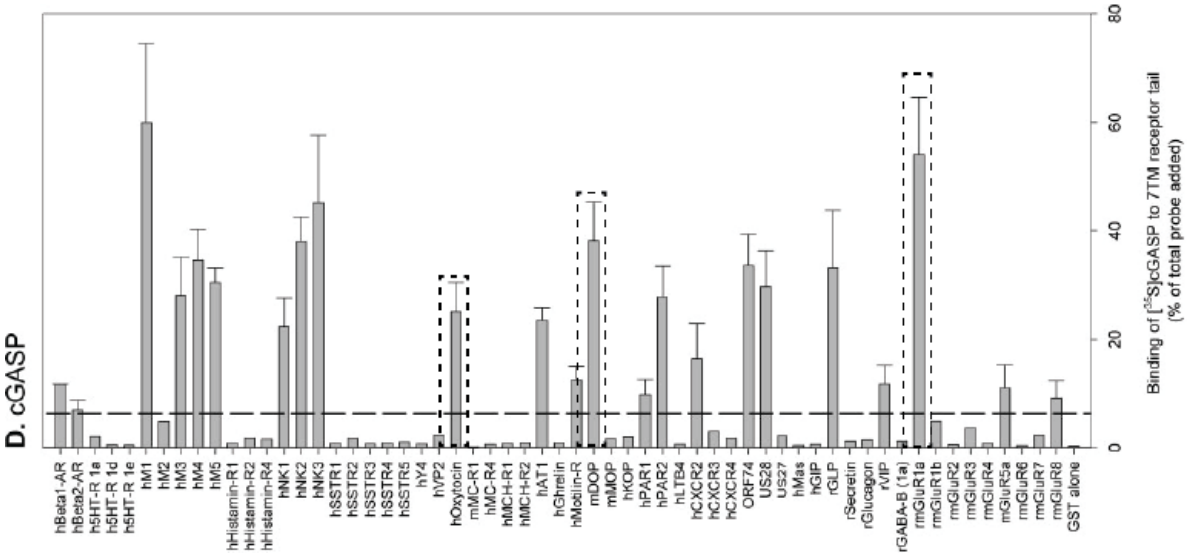

Figure 5 | 7TM receptor tail interactions with GPRASPs. The relative binding of receptor tails to GPRASPs in GST pull-down experiments. Adapted from (Heydorn et al., 2004).

GPRASP2 is clearly involved in the modulation of GPCR activity and could modulate transcription. Considering these two functions, upon activation of GPCRs (and possibly other receptor types), GPRASP2 could be involved in their sorting toward degradation or recycling and concomitantly in the receptor-induced modulation of the transcriptional activity of the cell.

Further studies are now required to better understand the precise molecular function of these proteins and to evaluate whether they are involved in disease mechanism and simultaneously if they could represent interesting targets for pharmacological intervention. Also interesting is the possibility of discrete GPRASPs playing a specific role at the synapse. In this regard, a synapse proteomics database, has identified GPRASP2 as the only GPRASP member that is detected in the PSD (Collins et al., 2006).

Taken together, and despite the clear involvement of mGluRs in neuropsychiatric disorders, the underlying molecular and cellular pathways regulating these receptors under disease conditions are poorly understood. The clinical implication of *GPRASP2* in neurodevelopmental disorders along with its function as a post-endocytic sorting protein of GPCRs, makes GPRASP2 an interesting target for further detailed analysis.

Objectives and Thesis Outline

The overall objective of this work is to i) characterize the developmental expression of GPRASP2 in the mammalian brain ii) understand the synaptic function of GPRASP2, iii) characterize its role in ASD and ID, iv) identify if GPRASP2 plays a role in mGluRs regulation.

Therefore, we pursued the following specific aims:

a. We performed a detailed characterization on the expression profile of GPRASP2 in the mouse brain at different stages of development.
b. We investigated the function of GPRASP2 in hippocampal neurons in glutamatergic excitatory synapse using gain of function and loss of function studies.
c. We investigated whether GPRASP2 is involved in regulation of spine and dendritic morphology.
d. We generated and characterized a novel *Gprasp2* KO mouse model to dissect the behavioral and *in vivo* synaptic physiological consequences of eliminating GPRASP2
e. We examined the consequences of changing levels of GPRASP2 on mGluR5 and on mGluR dependent-LTD.

Chapter 2 | Materials and Methods

2.1. Solutions

50X TAE (Tris-Acetate EDTA)

Final composition	Stock	1L
2M Tris	FW= 121.1	242.2 g
Glacial acetic acid	concentrated	57.1 mL
0.05M EDTA (PH 8.0)	0.5M	100 mL
Initial dH_2O		0.8 L (fill to 1L)

10X PBS

Final composition	Stock	1 L
1.5M NaCl	FW= 58.4	87.6 g
0.121M $Na_2HPO_4 \cdot 7H_2O$	FW= 268.07	32.5 g
0.029M KH_2PO_4	FW= 136.09	4.0 g
Initial dH_2O		0.8L (fill to 1 L)

No need to adjust pH. When diluted to 1x, the pH should be 7.5

10X TBS

Final composition	Stock	1 L
0.1M Tris	FW= 121.1	12.1 g
1.5M NaCl	FW= 85.4	87.4 g
Initial dH_2O		0.8 L (fill to 1 L)

Adjust pH to 7.4 with HCl

6x DNA Loading Buffer

Final composition	Stock	250 mL
0.25% Bromophenol Blue	FW= 669.96	0.625 g
40% sucrose	FW= 342	100 g

Bring to 250 mL volume with dH_2O

Alkaline Lysis buffer for Hotshot Digestion (for PCR genotyping)

Final composition	Stock	50 mL
25mM NaOH	10N	125 µl
0.2mM EDTA	0.5M	20 µl

Bring to 50mL volume with milliQ H_2O

pH will be close to 12

Neutralization Buffer for Hotshot Digestion (for PCR genotyping)

Final composition	Stock	50mL
40mM Tris-HCl	FW= 157.56	315 mg

Bring to 50mL volume with milliQ H_2O

pH will be close to 5

Blocking buffer

Final conc.	Stock	for 15 mL
10% normal sheep serum	100%	1.5 mL
0.2% blocking reagent	10X	0.3 mL
TBST buffer	1X	13.2 mL

Hybridization solution

Final conc.	Stock	for 10 mL
50% Formamide	100%	5 mL
5X SSC	20 X	2.5 mL
5X Denhart's solution	50 X	1 mL
250 μg/mL yeast tRNA	10 mg/mL	250 μL
500 μg/mL salmon sperm DNA	10 mg/mL	500 μL
50 μg/mL heparin	10 mg/mL	50 μL
DEPC-dH_2O up to 50mL		

Detection Buffer (for *in situ* hybridization protocol)

Final concentration	Stock	300 mL
0.1M Tris-HCl, pH 9.5	1M	30 mL
0.1M NaCl	5M	6 mL
50mM MgCl2	1M	15 mL
0.24 mg/mL levamisole	powder	72 mg
Bring to 300mL volume with milliQ H_2O		

NBT/BCIP Solution

Final conc.	Stock	for 10 mL
0.35 mg/mL NBT	100 mg/mL	35 μL
0.175 mg/mL BCIP	50 mg/mL	35 μL
Use filtered Detection Buffer and to make up 10 mL		

20X SSC

Final composition	Stock	1L
3.0M NaCl	FW= 58.4	175.3 g
0.3M Na citrate	FW= 294.01	88.2 g
Adjust pH 7.0 fill with dH_2O to 1L		

4% PFA/PBS

Preheat 425 mL DEPC H_2O to 65°C

Add 20 g PFA, stir (in fume hood)

Add 1-2 drop(s) NaOH 10N, stir ~ 10' until clear

Add 50 mL 10X PBS (from the RNA bench)

Add DEPC-H_2O to 500 mL

Cool on ice, adjust to pH 7.4, filter

DEPC-H_2O

DEPC was added to dH_2O at a ratio of 1:1000 and left stirring overnight. Next, the water was subjected to autoclave to degrade DEPC. All the RNA solutions are prepared in the same manner (treating regular solutions with DEPC, stir overnight and autoclave).

Western blot solutions:

5x Running buffer

Final composition	Stock	2L
0.125M Tris Base	FW= 121.1	30.3 g
1M Glycine	FW= 75.07	150 g
5% SDS		10 g
Initial dH_2O		1.8 L (fill to 2L)

5x Transfer Buffer

Final composition	Stock	2L
0.125M Tris Base	FW= 121.1	30.3 g
0.96M Glycine	FW= 75.07	144 g
Initial dH_2O		1.8 L (fill to 2L)

10% APS (Ammonium persulfate)

Final composition	Stock	10mL
10% APS	FW= 228.2	1 g

Fill to 10 mL with dH_2O (aliquote and use for 4-6weeks)

SDS Gel Percentage

Running Gel Percentage (8%)	2 Gels	4 Gels
H_2O	10.6	20.8 mL
40% acrylamide mix	4 mL	8 mL
Tris-HCl (1.5 M. pH 8.8)	5 mL	10 mL
10% SDS	0.2 mL	0.4 mL
10% APS	0.2 mL	0.4 mL
TEMED	8 µl	16µl

Stacking Gel Percentage (4%)	2 Gels	4Gels
H_2O	7.55 mL	15.1 mL
40% acrylamide mix	1 mL	2 mL
Tris-HCl (1.5 M. pH 8.8)	1.25 mL	2.5 mL
10% SDS	0.1 mL	0.2 mL
10% APS	0.1 mL	0.2 mL
TEMED	10 µl	20µl

Table 2 | Composition of MEF medium

Composition	Volume
DMEM	450 mL
FBS Hyclone	50 mL
Penicillin/Gentamicin (1000x stock)	500 µl

Table 3 | Composition of ES medium (*for selection)

Composition	1xGeneticin (400ml)	2xGeneticin (100mL)
DMEM	313 mL	77.8 mL
FBS hyclone	80 mL	20 mL
β-Mercaptoethanol (BME)	4 mL	1 mL
Penicillin/Gentamicin(1000x stock)	400 µl	100 µl
LIF ($1x10^7$)	60 µl	15 µl
*Geneticin	2.4 mL	1.2 mL

Penicillin/Gentamicin-1000x stock

0.59% penicillin (w/v) 0.059 g

8% Gentamicin (w/v) 0.8 g add H_2O to 10 mL

Filter and stored in aliquots at -20°C

Table 4 | Composition of hippocampal culture medium

Composition	Source
Minimum Essential Medium (MEM)	GIBCO, Invitrogen, Barcelona, Spain
Horse serum	GIBCO, Invitrogen, Barcelona, Spain
Neurobasal medium	GIBCO, Invitrogen, Barcelona, Spain
B27 supplement	GIBCO, Invitrogen, Barcelona, Spain
Gentamycin	GIBCO, Invitrogen, Barcelona, Spain

Table 5 | MEF and ES culture reagents

DPBS, no calcium, no magnesium	GIBCO, Invitrogen, Barcelona, Spain
1x Trypsin-EDTA, phenol red	GIBCO, Invitrogen, Barcelona, Spain
Penicillin/Gentamicin	Fisher Scientific, GA, USA
β- Mercaptoethanol (100X)	Merck Millipore, USA
ESGRO LIF 10 million units/1 mL	Merck Millipore, USA
Primary Mouse Embryo Fibroblasts, Strain FVB, passage 1	Merck Millipore, USA
EmbryoMax 0.1% Gelatin Solution	Merck Millipore, USA
ES Screened Fetal Bovine Serum, hyclone	Fisher Scientific, Swanee, GA, USA
DMEM, high glucose	GIBCO, Invitrogen, Barcelona, Spain
Dimethyl sulfoxide	Sigma-Aldrich
Geneticin Selective Antibiotic (50 mg/mL)	GIBCO, Invitrogen, Barcelona, Spain

Table 6 | In situ hybridization reagents

Item	**Source**
10% Normal sheep serum	Rockland Immunochemicals
Blocking solution	Roche, Indianapolis, IN, USA
Diethyl pyrocarbonate, 97%	Acros Organics, New Jersey, USA
CSPD	Roche, Indianapolis, IN, USA
BCIP	Roche, Indianapolis, IN, USA
NBT	Roche, Indianapolis, IN, USA
Levamisole	Sigma Aldrich, USA
Heparin	Sigma Aldrich, USA
Salmon sperm DNA	Invitrogen, USA
Yeast tRNA	Sigma Aldrich, USA
Denhart's solution	Invitrogen, USA
Formamide	Acros Organics, New Jersey, USA
PAP Pen for IHC and ISH	Rockland Immunochemical
O.C.T. Compound	TissueTek, Torrance, CA, USA)
Adhesive superfrost plus slide	Fisher Scientific, Swanee, GA, USA

Table 7 | Kits

NucleoBond Xtra Midi Plus	Macherey-Nagel, Germany
NucleoBond Xtra Maxi Plus	Macherey-Nagel, Germany
NZYMiniprep	Nzytech, Portugal
NucleoSpin Gel and PCR Clean-up	Macherey-Nagel, Germany
TAKARA PrimeSTAR GXL DNA Polymerase	Clontech, USA
Supreme NZYTaq 2x Green Master Mix	Nzytech, Portugal
Lipofectamine LTX with Plus Reagent	Thermo scientific, USA
T4 DNA ligase ligation kit	NEB Biolabs, USA
Maxi script T7/T3 Kit	Ambion, Austin, TX, USA
DIG-labeled Control RNA	Roche, Indianapolis, IN, USA
Pierce BCA Protein Assay Kit	Thermo scientific, USA
Pierce ECL western blot substrate	Thermo scientific, USA

2.2. Antibodies

Table 8 | Primary antibodies used in this study

Name	Dilution	Source
Anti-Digoxigenin-APFab fragments	ISH (1:2000)	Roche, Indianapolis (IN, USA)
PSD-95	ICC (1:750)	Cell Signalling Technologies, USA
vGlut1	ICC (1:5000)	Millipore (Madrid, Spain)
α-Tubulin	WB (1:10000)	Sigma-Aldrich (Sintra, Portugal)
Neuroligin-3	WB (1:500)	NeuroMab (UC Davis, USA)
GluN2B	WB (1:1000)	Allomone labs, (Jerusalem, Israel)
GluA1	WB (1:1000)	Millipore (Madrid, Spain)
NR1	WB (1:1000)	NeuroMab (UC Davis, USA)
mGluR1	WB (1:500)	BD Biosciences, USA
mGluR5	WB (1:1000)	St John's Laboratory, UK
Homer 1b/c	WB (1:500)	Synaptic systems, Germany
β-actin	WB (1:500)	Sigma-Aldrich (Sintra, Portugal)
αCamKII	WB (1:1000)	Sigma-Aldrich (Sintra, Portugal)
SAPAP3	WB (1:1000)	Abcam (Cambridge, UK)
GPRASP2	WB (1:100)	Abcam (Cambridge, UK)
Synaptophysin	WB (1:20000	Abcam (Cambridge, UK)
MAP2	WB (1:5000)	Abcam (Cambridge, UK)
mGluR5N terminus	WB (1:100)	Allomone labs, Jerusalem, Israel
GFP	WB (1:500)	MBL International (Woburn, USA)

Table 9 | Secondary antibodies used in this study

Name	Application (Dilution)	Source
Alexa488-conjugate	ICC (1:500)	Molecular Probes (Netherlands)
Alexa568-conjugated	ICC (1:500)	Molecular Probes (Netherlands)
Alexa594-conjugated	ICC (1:500)	Molecular Probes (Netherlands)
Alexa647-conjugated	ICC (1:500)	Molecular Probes (Netherlands)
Alexa 47-conjugated	ICC (1:500)	Molecular Probes (Netherlands)
AMCA-conjugated	ICC (1:500)	Molecular Probes (Netherlands)
Horseradish peroxidase conjugated donkey	WB (1:10000)	Jackson ImmunoResearch Europe
Horseradish peroxidase conjugated donkey	WB (1:10000	Jackson ImmunoResearch Europe

WB: Western blot

ISC: *in situ* hybridization

ICC: Immunocytochemistry

2.3. Biological materials

Bacterial strains:

Chemically competent Escherichia coli strain DH5α (XL10-Gold Competent Cells, Agilent technologies) were used for plasmid amplification and transformation. Electro-competent Escherichia coli strains SW102, SW105, and SW106 from the were used for BAC recombineering experiments (kindly provided by The Frederick National Laboratory for Cancer Research)

Culture medium:

LB medium Lysogeny broth (BERTANI, 1951)

LB-agar Lysogeny broth (BERTANI, 1951)

Table 10 | Antibiotics

	Stock solution	**Source**
Carbenicillin	100mg/mL dissolved in dH_2O	Fisher Scientific (Swanee, USA)
Kanamycin	30 mg/mL dissolved in dH_2O	Fisher Scientific (Swanee,USA)
Chloramphenicol	34 mg/mL dissolved in EtOH	Fisher Scientific (Swanee,USA)
Tetracycline	34 mg/mL dissolved in dH_2O	Fisher Scientific (Swanee,USA)

Table 11 | Plasmids and bacterial artificial chromosome (BAC)

Plasmid	**Source**
pNAAP (sub-cloning vector for LHA retrieval)	Guoping Feng Lab (MIT)
pFLN-DTA targeting vector	Guoping Feng Lab (MIT)
pBluescript II SK+	Stratagene(CA, USA)
pEGFP-C1	Clontech, USA
Lamp1-RFP	Addgene, Cambridge, USA
mRFP-Rab5	Addgene, Cambridge, USA
mRFP-Rab7	Addgene, Cambridge, USA
mRFP-Clc	Addgene, Cambridge, USA
ER-mRFP	Addgene, Cambridge, USA
pmRFP-LC3	Addgene, Cambridge, USA
mCherry-Golgi-7	Addgene, Cambridge, USA
GPRASP2 shRNA plasmids	Qiagen, USA
BAC DNA clones (RP23-160E, RP23-250G)	Children's Hospital Oakland Research Institute, USA

Nucleic acids:

Table 12 | Sequence of oligonucleotides used for all PCR cloning. (F) refers to forward primer and (R) refers to reverse primer.

Name	Direction	Sequence 5'-3'	Restriction site
SA cloning primers	F1	GCGGCGGCCGCCAGGTACATTATACACATTCAAAAATA	NotI
	R1	GCGGCGATCGCCCTACAACTAGAGTCACTGGATG	AsiSI
MA cloning primers	F2	GCGCGTACGATAACTTCGTATAGCATACATTATACGAAGTTAT* CTTTGTAAGTTTCTCCAGGAGGC	BsiWI
	R2	GCGGTCGACCGCCTGAGTTTTAAAGTGAAGAAG	SalI
Retrieval of long homology arm			
LHA retrieval	F3	GGATTTTCTCATGGCTGAGCTCTTCCCCTCAGCATTACGCACCAGCGTCT CGTACGATCCGAGTCGACCGGTTAATTAAGGGC	SalI
	R3	TCCACTTAGGGCTCAGGAAACCTCTCAGTAGATAAGACAA AAAGATCGTAGGCGCGCCGGTACCGCG	ASCI
GFP-GPRASP2	F4	GCCCTCGAGCGACTGGGGCAGAAGTTGAGACC	XhoI
	R4	GCCGGTACCTTACTGTCCCTCCTCGGGATCAT	KpnI

*insertion of loxP sequence not present in plasmid

Table 13 | Sequence of oligonucleotides used for all PCR cloning. (F) refers to forward primer and (R) refers to reverse primer

Name	Direction	Sequence 5'-3'
SA screening	F5	GCAGTTAGGTGTAGATTTTGTTTC
	R5	GCCTTCTAGTTGCCAGCCATC
MA screening	F6	CCAATTACGTGTCTGGGTTTCTC
	R6(FRTR2)	GGTTCTTTCCGCCTCAGG
LA screening	F7(m4668.2)	CAGGAAACAGCTATGACCATG
	R7	CTTGAGGAAATGCCTCCGTG
LHA retrieval screening	F8	GAGTTTGGACAAACCACAACTAG
	R8	GGCCTCTGCATCAGCTCCTG
Homologues recombination screening (screening for positive embryonic stem cells)		
ES cells positive	F9	GAAAGTATAGGAACTTCACCGGTT
	R9	TTAATTGCTTATAGGAACACCCCC
	R9*	ACAGCCTAATACAAAGTTAGCAATC
Genotyping Primers		
Exon -7 deletion	F10	GAGCTCTTCCCCTCAGCATTAC
	R10	GTGCCCAGTCATAGCCGAATAG
	R10*	GCCCGAGAGGAAGATTTAGTTTC

Table 14 |Sequence of oligonucleotides used for sequencing the final targeting construct and GFP-GPRASP2

Name	Direction	Sequence 5'-3'
Final targeting construct	F11 (m4668.2)	CAGGAAACAGCTATGACCATG
	F12	GGATATTAAGAATATTGAGGTAG
	F13	CCGAGGAGGGACAGTAAAGTTAG
	F14	CCAGGGCTGGCACTCTGTCGATA
	R14	GCCTCAGTCTCAATGACAGGTC
	R14	GGTTCTTTCCGCCTCAGG
GFP-GPRASP2	F15	CATGGTCCTGCTGGAGTTCGTG
	F16	GCCAGTAACCCATTCTGCTTTTG
	F17	CGCGATTCGGGTGTTGTCTCAC
	F18	GTAACAACTCCGCCCCATTGAC
	R15	GAAATTTGTGATGCTATTGC
	R16	CGAATGAAATCCCGGGTAAACTG
	R17	GTCTTATTAGGCTCTTCCTTGTC
	R17	CGTCGCCGTCCAGCTCGACCAG
	R19	CGAATGAAATCCCGGGTAAACTG
	R20	GTCTTATTAGGCTCTTCCTTGTC
	R21	CCAACATTGACTGGTGGCCATG

Restriction endonucleases and markers:

Endonuclease restriction enzymes used in the present study are listed below. The enzymes were used in combination with appropriate buffer according to the instruction of manufacture.

Table 15 | Restriction endonucleases

Name	Buffer	Source
AscI	Cutsmart buffer	NEB Biolabs, Ipswich, USA
AsiSI	Cutsmart buffer	NEB Biolabs, Ipswich, USA
BsiWI	NEBuffer 3.1	NEB Biolabs, Ipswich, USA
NotI-HF	Cutsmart buffer	NEB Biolabs, Ipswich, USA
SalI-HF	Cutsmart buffer	NEB Biolabs, Ipswich, USA

NZYDNA ladder III (200-10,000bp) was obtained from Nzytech, Portugal, restriction enzymes from NEB, Germany.

2.4. Methods

2.4.1. Cloning and targeting:

Polymerase chain reaction

PCR primers were designed to amplify the desired fragment. Restriction sites were added to the PCR primers so that both 5' end and 3' end are in frame with the vector sequence.

PCR for cloning was done by Prime STAR GXL DNA Polymerase (a high-fidelity polymerase from Takara that provides efficient PCR amplification)

Table 16 | Example PCR reaction cylces

Initial denaturation	30 Sec at 98°C
Cyclic denaturation	10 Sec at 98 °C
Primer annealing	15 Secs* * 5°C lower than the melting temperature of the primers
Elongation	68 °C* *time depended on the length of the fragment (1 min/Kb)
Final elongation	10 min at 68 °C

30 cycles

Table 17 | Example of PCR mixture

10 X PCR buffer	10 µL
dNTP (10 mM)	4 µL
Forward primer (10 µM)	1 µL
Reverse primer (10 µM)	1 µL
cDNA template (10 ng/µL)	1 µL
High Fidelity Taq (5 U/µL)	1 µL
dH_2O	32 µL

In order to check the PCR product, 5 µl was run on a 1% agarose gel. For the next cloning step 1ul proteinase K (10mg/mL) was added to the PCR product and the mixture digested for 30 min at 55˚C. Clean up the PCR product was done using NucleoSpin gel and PCR clean-up from (Zymed, USA). The product was eluted with 10µl dH_2O and digested with the appropriate restriction enzymes.

Table 18 | Digestion of the PCR product

DNA	10 µL
10x buffer	5 µL
10 X (1 mg/mL) BSA	5 µL
restriction Enzyme(s)	1-2 µL
dH_2O	28-29 µL

The mixture was incubated at 37°C for 2 hours then the digested product was run on 1% melting agarose gel. The PCR product was purified using NucleoSpin Gel and PCR Clean-up then eluted in dH_2O and saved for ligation.

Table 19 | Vector digestion

DNA (µg)	1 **µL**
10x buffer	3 µL
10 X (1 mg/mL) BSA	3 µL
restriction Enzyme(s)	1-2 µL
dH_2O	21-22 µl

The mixture Incubated at 37°C for 2 hours. Next, the mixture incubated at 75˚C for enzyme inactivation (or other appropriate temperature, depend on enzyme specifications).

Vector dephosphorylation:

To avoid vector recirculation the mixture was incubated with 1 µL CIAP enzyme at 37 °C for 1-2h. The digested vector was purified using NucleoSpin Gel and PCR Clean-up then eluted in dH_2O and saved for ligation.

DNA ligation:

Ligation was performed with T4 DNA ligase using a ratio of 1:3 vector to insert v/v.

Table 20 | DNA ligation reaction

Component	20µl Reaction
T4 DNA ligase buffer (10x)	2 µL
Vector DNA	50 ng
Insert DNA	37.5 ng
Nuclease free water	To 20µL
T4 DNA ligase	1 µL

The mixture was gently mixed by pipetting and incubated at 16º C overnight. The next day the mixture kept for 2 hours at room temperature and 10 µl of the ligated product was used for transformation into DH5α cells. Colony PCR screening, , restriction digestion and Sanger sequencing were used to confirm positive clones.

Colony PCR

Screening positive colonies by colony PCR was used for rapid detection of successful transformation using appropriate primers that determine correct ligation products by size. PCR screening was done using Supreme NZYTaq DNA polymerase and the DNA template was a single living *E.coli* colony. Using a sterile toothpick a single colony was picked and gently placed in a labelled LB plate with the appropriate antibiotic then, the toothpick dabbed into the PCR reaction mix. Extended denaturation time was set to 2 minutes to perform complete lysis of the bacterial cells. The PCR was carried out with following condition

Table 21 | Colony PCR setup

Initial denaturation	2 min at 95°C	
Cyclic denaturation	15 sec at 95 °C	
Primer annealing	15 secs* * 5°C lower than the melting temperature of the primers	30 cycles
Elongation	72 °C* *time depended on the length of the fragment (1 min/Kb)	
Final elongation	10 min at 72 °C	

Agarose gel electrophoresis:

Gel electrophoresis was used for separation of DNA fragments. The size of the fragment determines the percentage of the agarose gel:

Table 22 | Percentage of agarose DNA fragment

% of agarose	DNA fragment
0.3 %	5-60 kb
0.6 %	1-20 kb
0.7 %	0.8-10 kb
0.9 %	0.5-7 kb
1.2 %	0.4-6 kb
1.5 %	0.2-4 kb
2.0 %	0.1-3 kb

Briefly, agarose was melted in TAE-buffer then, Ethidium bromide (0.5% v/v) was added and mixed well. After the gel solidifies, 5µl of the DNA ladder were loaded beside the samples. A constant electric field (100V) was applied. The separation of the fragments was observed under UV-light.

DNA purification from agarose gel and after PCR:

NucleoSpin Gel and PCR Clean-up kit was used for DNA extraction from agarose gel. All steps were done according to the instruction of the manufacturer.

Bacterial transformation:

Transformation by heat shock using competent *E.coli* :

The bacteria were thawed on ice. 100 ng of plasmid DNA or 3 µl of ligated DNA were added to 30 µl of bacteria and kept on ice for 30 min. Heat shock was applied by 90 sec incubation at 42°C, followed by 2 min incubation on ice. 500 µl of LB medium without antibiotic were added to the bacteria and incubated for 1hr at 37°C, 350 rpm in a thermomixer. 100 µl of the transformed bacteria was plated on a LB-agar plate containing the appropriate antibiotic and incubated overnight at 37°C.

Plasmid preparation:

Mini preparation:

High pure NZY Mini Prep kit were used to extract DNA. All steps were done according to the instruction of the manufacturer.

Maxi preparation:

To amplify large scale of plasmid DNA, NucleoBond Xtra Midi, Maxi Plus kits were used to extract DNA. All steps were done according to the instruction of the manufacturer.

Plasmid construction:

The full-length mouse coding sequence for GPRASP2 (aa 584-919) was PCR amplified from BAC DNA clones and cloned into either pEGFP-C1 using restriction enzymes (XhoI, KpnI), latter the cloning was confirmed by restriction digestion analysis and sequencing using at least 4 different primers.

DNA sequencing: done by GATC Biotech, Konstanz, Germany

Hotshot (quick and dirty) method for genomic DNA isolation:

Mouse ear biopsies (1-2mm) were incubated with 200µl alkaline lysis buffer for 30 minutes at 100°C. After cooling down, 100µl neutralization buffer was added.

2.4.2. In situ hybridization

Preparation of DIG-RNA probe:

Preparation of DNA template:

GPRASP2 probe was amplified by polymerase chain reaction (PCR) from BAC DNA as previously described and cloned into pBluescript II SK+ using restriction enzymes (NotI or XhoI) that generate 5' overhang end. Successful cloning was confirmed done by both restriction digestion and sequencing. Briefly, the plasmid was linearized by either NotI or XhoI to generate Sense (T7/XhoI) or antisense (T3/NotI) probes, the digested DNA was purified by Nucleospin clean up kit and eluted in DEPC-dH_2O.

In vitro transcription-labeling the probe with DIG:

The transcription reactions and Digoxigenin (DIG)-labeling of RNA probes were performed using the MAXIscript in vitro RNA synthesis kit. For GPRASP2, the sense strands were generated by T7 RNA polymerase and the antisense strands by T3 RNA polymerase.

Table 23 | 2.5X DIG-NTP mix

4.5 µL	10mM ATP (Ambion kit)
4.5 µL	10mM CTP (Ambion kit)
4.5 ul	10mM GTP (Ambion kit)
2.9 ul	10mM UTP (Ambion kit)
1.6 ul	10mM DIG-UTP (Roche)

Table 24 | In vitro transcription reaction

2 µg DNA template in DEPC-dH_2O	8 µL
10X transcription buffer	2 µL
2.5X DIG-NTP	8 µL
RNA polymerase (T3 and T7)	2 µL

The mixture then incubated for 4 hours at 37 C followed by incubation with 1µl DNase I for 30 minutes. DEPC-dH_2O was added to make adjust the total volume to 60 ul, then the probe was purified using Ambion NucAway spin columns. The final RNA probe was eluted in DEPC-dH_2O.

Quantification of DIG-labeled probes was done by dot blotting and probing with alkaline phosphatase-conjugated anti-DIG antibody, using a DIG-RNA standard. The standard (100ng/μL) and the probe were diluted with DNA according to the following table.

Table 25 | DIG-RNA standard

Tube #	Standard or probe	dH_2O	Dilution fold	Concentration of standard
1	2 μL	198	1:100	1 ng/μL
2	5 μL from tube #1	45 μL	1:10	100 pg/μL
3	15 μL from tube #2	35 μL	1:3.3	30 pg/μL
4	15 μL from tube #3	30 μL	1:3	10 pg/μL
5	15 μL from tube #4	35 μL	1:3.3	3 pg/μL
6	15 μL from tube #5	30 μL	1:3	1 pg/μL

One μL from tubes #1-6 were spotted on to a nylon membrane (Nytran). After drying, RNA was UV crosslinked the to the membrane using a Stratalinker UV (Stratagene). Then the membrane was washed with TBS for 5 mins and incubated with 30 min in 10 mL 1X Blocking Solution followed by incubating 30 min with anti-DIG antibody in 1X Blocking Solution (1:10,000). Next, the membrane was washed 3 times with Washing Buffer (TBS+ 0.3% Tween-20) and incubated with detection buffer for 5 minutes. Then, enough amount of CSPD was used to cover the whole membrane and left incubated for 5 minutes. The membrane then exposed on film for 6 hrs. GPRASP2 probe concentration was calculated based of the standard serial dilutions. The probes were stored at -80°C until used

.

Tissue preparation and sectioning

Male C57 mice (P5, P10, P15, P20, P60) were deeply anesthetized with isofluorane, and perfused with PBS (DEPC treated). Brains were dissected, embedded in OCT compound and frozen in ethanol/dry ice slush. Blocks were mounted for coronal, sagittal and horizontal planes and 15-20 μm thick sections were cut on a Leica CM1850 cryostat (Leica Microsystems, Richmond Hill, Ontario, Canada). Brain sections were collected onto Superfrost Plus slides then air dried at room temperature for 30-60 min before long term storage at -80 in a box containing Anhydrous Calcium Sulfate (DryRight).

Slide processing

Before slide processing, the sections were circled with PAP pen (to provide a thin hydrophobic barrier) and then fixed in 4% (PFA) in PBS for 10 minutes at RT, washed 3 times with PBS for 3 minutes each, acetylated for 10 minutes at RT in TEA buffer (4 mL triethanolamine and 0.525 mL 12.1 M HCl were added to 295 mL H_2O and stirred; 0.75 mL acetic anhydride was added just before sections were immersed) and again washed 3 times with PBS for 3 minutes each.

Hybridization

For prehybridization, sections were incubated with hybridization buffer (50% formamide, 5X SSC [750 mM NaCl, 75 mM Na-Citrate], 5X Denhardt's solution, 250 μg/mL yeast tRNA, 500 μg/mL salmon sperm DNA, 50 μg/mL heparin in DEPC-dH_2O for 1 hour at RT. DIG-labeled RNA probes were diluted in hybridization solution to a working concentration of 1000 ng/mL, heated at 70°C for 10 minutes and rapidly chilled on ice. The prehybridization solution was removed and hybridization mixture was added to the sections. The sections were covered with parafilm. The hybridization was done overnight at 68°C in a humidified chamber containing 50% formamide/2XSSC.

Washing

After hybridization, the parafilm was removed by dipping the sections in 2x SSC at RT. Sections were washed 4 times in 0.2x SSC at 68°C for 3 hours, then adjusted to RT in 0.2x SSC for 5 minutes and washed 2x 5 minutes with TBS (150 mM NaCl, 10 mM Tris-HCl, pH 7.4).

Color development by NBT/BCIP:

For detection, sections were incubated with blocking buffer (10% normal sheep serum, 0.2% blocking reagent) for 1 hour at RT, followed by incubation with alkaline phosphatase-conjugated anti-DIG antibody (1:2000 in blocking buffer) overnight at 4°C. Sections were washed 4x 10 minutes with TBS and incubated with color detection buffer (100 mM NaCl, 50 mM MgCl2, 0,24 mg/mL levamisole, 100 mM Tris-HCl, pH 9.5) for 5 minutes. The color reaction was performed in the presence of nitroblue tetrazolium (NBT; 0.35 mg/mL) and 5-

bromo-4-chloro-3-indolyl-phosphate (BCIP; 0.175 mg/mL) in detection buffer at RT in the dark. Incubation depended on how quickly signal from the antisense probe appears versus background signal in the sense probe. Sections were then washed in TBS, water and then mounted with 90% glycerol/H_2O. Images were collected on a Zeiss Axioskop 2 Plus (Carl Zeiss, Thornwood, NY, USA) with 5X objective using a Zeiss Axiocam digital camera (Carl Zeiss).

2.4.3. Hippocampal primary culture

Primary cultures of rat hippocampal neurons were prepared from the hippocampi of E18-E19 Wistar rat embryos, after treatment with trypsin [0.06% (w/v), 15 min, 37°C] in Ca^{2+}- and Mg^{2+}-free Hanks' balanced salt solution [5.36 mM KCl, 0.44 mM KH2PO4, 137 mM NaCl, 4.16 mM NaHCO3, 0.34 mM Na2HPO4·2H_2O, 5 mM glucose, 1 mM sodium pyruvate, 10 mM HEPES and 0.001% (w/v) phenol red]. Hippocampal cells were washed with Hanks' balanced salt solution six times. The cells were mechanically dissociated and then plated at a final density of 3 x 10^5 cells/dish on poly-D-lysine-coated coverslips in 60 mm culture dishes for imaging purposes. The cells were plated in neuronal plating medium Minimum Essential Medium (MEM) supplemented with 10% (v/v) horse serum, 0.6% (w/v) glucose, and 1 mM pyruvic acid]. Once neurons attached to the substrate, after 2–4 h, in case of high density cultures the neuronal plating medium was replaced by neuronal culture medium containing neurobasal medium supplemented with B27 supplement (1:50 dilution), 25 μM glutamate, 0.5 mM glutamine, and 0.12 mg/mL gentamycin. The coverslips were flipped over an astroglial feeder layer in 60 mm culture dishes containing neuronal culture medium. These neurons grew face-down over the feeder layer but were kept separate from the glia by wax dots on the neuronal side of the coverslips. To prevent the overgrowth of glia, neuron cultures were treated with 5 μM cytosine arabinoside after 3 days *in vitro* (DIV). Cultures were maintained in a humidified incubator of 5% CO2/95% air at 37°C, feeding the cells once per week by replacing one-third of the medium per dish, using neuronal culture medium without glutamate. Cultures were used after 7,15, 16, 19 or 21 DIV.

Neuronal transfection:

Constructs were recombinantly expressed in primary cultures of hippocampal neurons using the calcium phosphate transfection protocol [adapted from (Jiang et al., 2004)]. Briefly, a

$CaCl_2$ solution (2.5 M in 10 mM HEPES) was added, drop-wise, to 2 μg of plasmid DNA to a final concentration of 250 mM CaCl2. This was then added to an equivalent volume of HEPES-buffered transfection solution (274 mM NaCl, 10 mM KCl, 1.4 mM Na2HPO4, 11 mM dextrose, and 42 mM HEPES, pH 7.2). The mixture was vortexed gently and incubated at room temperature for 30 min for the precipitates to develop. The precipitated DNA was added drop-wise to the coverslips, previously transferred into a 12-well plate containing conditioned medium, and the cultures were incubated for 1.5 h in the presence of kynurenic acid (2 mM). To remove DNA precipitates, each coverslip was transferred to a fresh well of the 12-well plate containing 1 mL of culture medium with kynurenic acid (2 mM), slightly acidified with HCl (~5 mM final concentration), and the plate was incubated at 37°C in 5% CO2 for 15 min. Coverslips were then transferred back into the original astroglial plate to allow expression of the transfected construct.

Immunocytochemistry:

Neurons were fixed for 15 min in 4% sucrose and 4% paraformaldehyde in phosphate buffered saline (PBS: 137 mM NaCl, 2.7 mM KCl, 1.8 mM KH_2PO_4 and 10 mM $Na_2HPO_4 \cdot 2H_2O$, pH 7.4) at room temperature, and permeabilized with PBS + 0.25% (v/v) Triton X-100 for 5 min, at 4ºC. Neurons were then incubated in 10% (w/v) BSA in PBS for 30 min at 37ºC to block nonspecific staining, and incubated in appropriate primary antibody diluted in 3% (w/v) BSA in PBS (2 h, 37ºC or overnight, 4ºC). After washing 6 times in PBS, cells were incubated with the secondary antibody diluted in 3% (w/v) BSA in PBS (45 min, 37ºC). The coverslips were mounted using fluorescent mounting medium (DAKO or Vecta Shield). For labeling surface mGluR5 receptors, non-transfected and/or transfected coverslips with EGFP, EFGP-C1, Scramble, shRNA#1 were stimulated with 100μM DHPG or vehicle (dH_2O) for 15 mins at 37ºC then washed and returned to the incubator for one hour to allow receptor internalization. Afterwards, neurons were fixed and incubated overnight with the mGluR5 intracellular N-terminus antibody (1:100). Next, as indicated above, each cover clip was washed and permeabilized, then incubated in 10% (w/v) BSA in PBS for 30 min at 37ºC to block nonspecific staining and completed as indicated above.

Quantitative imaging analysis

Imaging was performed on a Zeiss Axiovert 200M microscope or Zeiss LSM 710 confocal microscopes using a 63 X 1.4 numerical aperture oil objective. Images were quantified using image analysis software (ImageJ). For quantification, sets of cells were cultured and stained simultaneously, and imaged using identical settings. The region of interest was randomly selected avoiding primary dendrites, and dendritic length was measured using MAP2 staining. Measurements were performed in 2–5 independent preparations, and at least 7 cells per condition were analyzed for each preparation. Spine quantification performed using NeuronStudio software from Mount Sinai School of Medicine (see supplementary figure 1).

HEK cell transfection:

HEK cells were transfected using either lipofectamine transfection or Calcium phosphate method. Briefly, 2 μg of plasmid DNA is first mixed with water followed by addition of $CaCl_2$ solution drop-wise. Next, the mixture is added to an equivalent volume of HBS-buffered transfection solution (pH 7.05). The mixture was vortexed gently and incubated at room temperature for 30 min for the precipitates to develop. The precipitated DNA was added drop-wise to the coverslips or multiwell then left incubating at 37°C for 4-6 hours. After this incubation, the transfection solution is aspirated and the coverslips or multiwell are washed with HEK medium and incubated with HEK medium at 37°C for 24 or 48 hours.

SDS-PAGE:

Protein samples were mixed with 4x Laemmli Sample Buffer and denaturated at 95°C for 5 minutes. The gel caster components, including glass plates with 1.5 mm spacer and short glass plates were set up according to the manufacturer's instructions (Bio-Rad). The SDS-PAGE running chamber was filled with 1X running buffer and the gel was placed inside. Next, the samples were loaded into the gel and the protein were separated with a running speed of 100 V. The run was stopped when the loading dye left the bottom of the gel. The gel was segregated from the unit and prepared for transfer. Meanwhile, the PVDF membrane was activated in 100% methanol then incubated in 1X transfer buffer. A Wet/Tank blotting system was used to transfer proteins from the gel to the PVDF membrane. The blotting sandwich was packed in a way that the gel faced to the negative pole and the membrane faced to the positive pole. Then the blotting sandwich package was placed in the chamber filled with transfer buffer.

An ice box was used to cool the system down. An electrical current was applied at constant 100 V for 2 hours.

After the transfer, the membrane was blocked for one hour in TBS-T milk 5% at room temperature and incubated with primary antibody in TBST-milk 5% overnight at 4° C. The next day the membrane was washed 3 times with TBS-T, 10 min each time and incubated with the antibody solution containing the secondary antibody for 1hr at room temperature. Afterward the membrane was washed 3 times with TBS-T, 10 min each time.

2.4.4. Mouse molecular genetics

Gene targeting is defined as the introduction of site-specific modifications into the genome by homologous recombination. The strategy depends on using mouse ES cells which are derived from the pluripotent, uncommitted cells of the inner cell mass of pre-implantation primordial embryo. Selected targeted mutations can be introduced in ES cells using a suitable targeting vector, normally containing large regions of homology (1-8 Kb), and a positive selection cassette located inside the homology regions (antibiotic resistance) and a negative selection cassette (Diphtheria toxin subunit A) located outside the homology regions.

Gene targeting strategy involves 4 major steps:

- Construction of the targeting vector
- Electroporation of ES cells with the targeting vector
- Blastocyst injection of positive ES cells to generate chimeras
- Confirmation of germline transmission from chimeric mice

Construction of the targeting vector:

Retrieval of DNA from the BAC:

Purification of BAC DNA (quick& dirty method):

The BAC DNA clones obtained as LB agar stab culture format. From this, the original culture is streaked on a plate a single bacterial colony was inoculated overnight in 5 mL medium supplemented with chloramphenicol. Next the cells were pelleted at 5000x g for 5 minutes, the supernatant was removed and the pellet suspended in 250 µL buffer P1 (miniprep kit, Qiagen) and transferred to an Eppendorf tube. An aliquot of 250 µl P2 buffer was added and mixed by

inversion. Following an incubation for <5 min at room temperature, 250 µl N3 buffer was added followed by mixing and incubation on ice for 5 min. DNA was precipitated by adding 750 µL isopropanol, mixing and incubating on ice for 10 min. Next the a centrifugation was performed 10 min at 16.000g. The pellet was washed once in 70% ethanol, then air dried. The pellet was then dissolved in 50µl milliQ H_2O and 1 µL was used for electroporation (see below). Successful BAC DNA purification was tested by PCR screening using cloning primers for the short homology arm (SHA) F1, R1.

Electroporation of BAC DNA into recombinogenic bacterial strain (SW102):

SW102 bacteria is a recombinogenic bacteria that has been transformed by the defective λ prophage to promote homologous recombination. The expression of these genes is temperature inducible. When this strain is grown at 32°C, no recombination proteins are produced. However, briefly culturing the bacteria at 42°C induces expression of all the recombination proteins, which readily promotes the modification of targeted DNA sequences via homologous recombination.

SW102 cells was grown from a glycerol stock in 5mL LB low salt medium (Lennox LB) with Tetracycline (1:2000). On the following day, upon reaching OD_{600}= 1.2 cells were collected by centrifugation at 2000g for 5 minutes at 4 °C. Starting from this step on, all steps were performed at 4ºC. The pellet was suspended in 1mL ice cold water and transferred to 1.5mL tubes, then centrifuged at the maximum speed for 10 s at 4 °C. The supernatant was aspirated then the cells were resuspended in ice cold dH_2O and centrifuged at least 3 times as described before. At the last wash, the pellet was resuspended in 50µl ice cold dH_2O and mixed with 1µl BAC DNA (from "quick and dirty" method above). The mixture was then transferred to chilled 0.2 cm cuvettes and electroporation was performed using the following conditions: 1.75kV, 25µF and 200Ω resistance, the time constant was between 4-8 ms. Cells were recovered by adding 1mL LB medium and incubated at 30° C for 1 hour, then pelleted and transferred to LB plates with chloramphenicol (resistance granted by the BAC construct).

Preparation of the PCR vector for retrieval.

The primers for long-homology arm region (LHA) are designed to recover an 8Kb section of DNA via homologous recombination in bacteria, using an intermediate cloning vector (pNAPP). Retrieval primers were designed using 50bp homology to the BAC sequence

and a priming site on the pNAPP sub-cloning vector. The forward primer was modified by adding a restriction site for BsiWI enzyme in order to clone the middle arm (containing the exon 7 of GPRASP2 and a loxP sites). The DNA template for the PCR (pNAAp) was purified with a final concentration 0.1 ng/µl. To removed remaining plasmid template (pNAPP), the PCR product was digested with DpnI for 1 hour at 37° C then gel purified using the Zymoclean gel purification kit. The DNA is eluted in 20ul water and the concentration was measured using a Nanodrop.

Retrieval of LHA into PNAPP from BAC clone via recombineering:

SW102 cells contain BAC DNA were grown overnight at 30°C in low salt LB medium with tetracycline and chloramphenicol. The following day, 1mL of the overnight culture (OD_{600}=2) was transferred to 50mL falcon contain 20 mL of LB with tetracycline then returned to the incubator at 30°C shaking. When the bacteria containing the target plasmid/BAC reached an OD_{600} of 0.6, 10 mL was transferred to a 50 mL Erlenmeyer flask and agitated slowly in a water bath at 42°C for 15 min. The other 10 mL were kept at 30°C as a negative control. After 15 minutes, both 50 mL Erlenmeyer flask and the 50mL falcon were kept on ice 5 minutes. Next, the cells were transferred to pre-cooled test tubes, centrifuged at 2000 g for 5 minutes at 4°C. Both cells (induced or non-induced) were resuspended and washed in ice cold water three times as described above. Following the last wash, the cells were resuspended in 50 µl ice cold water and 25µl of the freshly prepared electrocompetent cells were mixed with 300 ng of PNAPP amplified via PCR. The electroporation was performed as described previously. The bacteria were recovered and screening for positive colonies was done first by PCR using primers F7 and R7, then confirmed by restriction digestion using SalI-HF and AscI. Before cloning the homology arms, the targeting vector pLFN-DTA was modified in order to clone the short homology arm (1kB). Two restriction sites (AsiSI and FseI) were inserted using standard linker ligation protocol (see Supplementary fig. 2a and Figure 9 in Chapter 3).

Cloning the homology arm in the targeting construct:

Cloning the long homology arm (LHA):

The LHA (6096 bp) was retrieved from the subcloning vector (pNAAP) by digestion with SalI-HF and AscI-HF (Supplementary fig. 2b). The product was purified and inserted in the final cloning vector (pLFN-DTA) using the same set of enzymes. The ligated product plated

on ampicillin selection plates. Screening for positive colonies done first by PCR using primers F6, R6 then confirmed by restriction digestion (Supplementary fig. 2c).

Cloning the middle homology arm (MHA) in the targeting construct:

F2, R2 Primers were used to amplify the MA from the BAC DNA. The PCR product (3153 bp) was purified and digested with BsiWI, SalI-HF. The ligated product plated on ampicillin selection plates. Screening for positive colonies done first by PCR using F5, R5 then confirmed by restriction digestion (Supplementary fig. 2d).

Cloning the short homology arm(SHA) in the targeting construct:

F1, R1 Primers were used to amplify the SA from the BAC DNA. The PCR product (882 bp) was purified and digested with NotI-HF and AsiSI. The ligated product plated on ampicillin selection plates. Screening for positive colonies done first by PCR using F4, R4, then confirmed by restriction digestion. The final targeting vector was confirmed by digestion using NotI-HF, AscI and AsiSI (Supplementary fig. 2 e, f) followed sequencing using primers F10, F11, F12, F13, R10, R11.

Electroporation of ES cells with the targeting construct:

Culturing MEF cells:

Expanding and passage of MEF cells:

Development and maintenance of pluripotent stem cells in culture require mitotically inactivated fibroblast as a feeder layer. Initially, mouse embryonic fibroblast (MEF) are cultivated to help ES cells adherence and also to provide differentiation inhibitory signals.

For preparation of feeder cell layer, one vial P1 MEF cells is pre-warmed in a 37 °C water bath. Cells are resuspended by adding 5 mL MEF medium, then centrifuged at 600g for 3 minutes and the pellet resuspended in 15 mL MEF medium. Flasks coated with 0.1% gelatin are prepared in advance and cells are plated and grown to 90% confluence. When the flask reached confluency, splitting was performed at a ratio of 1:5 for 4 additional rounds (P5) before proceeding to mitotic inactivation.

Inactivation of MEF cells by γ irradiation:

MEF cells were trypsinized, collected in MEF media and kept at 4º C. Gamma irradiation was performed with dose of 3000 RADs using a facility in the *Instituto Português Oncologia de Coimbra Francisco Gentil E. P. E.* (Coimbra, Portugal). Cells where then collected by centrifugation and resuspended in MEF freezing medium (MEF medium+20% DMSO). Irradiated MEF (γ-MEF) cells were aliquoted in 1 mL per cryotube at a rate of 5 million per tube, frozen at -80°C and then transferred to liquid nitrogen. These γ-MEF cells are the feeder cells that are plated on gelatinized plates for ES cell growth. Feeder cells can be plated 24-48h before ES cells are added to the culture.

Preparations of ES cells:

Murine R1 ES cells were a kind gift from Andreas Nagy. Culture conditions included using gelatinized plates with a MEF feeder layer cultured using ES medium. Cell splitting was performed with total ES colony growth reached 60% confluency. Media was changed daily.

Homologous recombination in ES cells:

Preparation of DNA for electroporation:

A large-scale purification of DNA targeting vector was performed using Macherey-Nagel endotoxin free kit. Briefly, 80 μg of DNA vector was linearized by digestion with 25 μl of AscI enzyme overnight. Purification of DNA repeated and enzymatic digestion was confirmed by running 200ng of digested DNA on 1% agarose gel.

Validation of the targeting construct and Cre-mediated recombination

To validate the conditional knockout strategy (Cre-lox mediated deletion) and the functionality of the targeting vector, HEK cells were transfected with the targeting construct with or without a co-transfection with a Cre expressing vector. Co-transfection with RFP plasmid was used to test for overall transfection efficiency. Triple transfection and controls were performed using lipofectamine LTX. HEK cell DNA was extracted using a Zymo DNA kit. A PCR reaction was used to assess if exon-7 deletion in the targeting vector was achieved in Cre-transfected conditions (using F9, R9 and R9*primers).

Preparation of ES cells for electroporation:

For ES cells for electroporation, at least four 10-cm plates were maintained and cultured to 70-80% confluence. At this stage cells are carefully dissociated to single cell suspension, pelleted, and resuspended in 10 mL PBS. Next, cell concentration was adjusted to $2x10^7$ cells/mL with PBS.

Electroporation of ES cells:

For each electroporation, 800 μL of ES cells ($2x10^7$ cells/mL) and 25μg of linearized targeting vector DNA (in 100 μL) are mixed and transferred to pre-cold 4mm gap electroporation cuvette. The electroporation was carried out with a single 225 V, 500 μF pulse to each cuvette (ECM 630 – low-voltage mode, resistance= 0). The cuvette kept on ice for 10min before recovery of the cells. Cells are then divided across six plates and 24 hours later ES cells medium was replaced by ES medium+2×Geneticin (1:83.5 dilution of Geneticin). After 48 hours, the medium was changed to ES medium + 1× Geneticin for the remainder of the culture time.

Picking the ES colonies:

Three days after selection, widespread cell death appeared due to gradual loss of neomycin resistance antibiotic. After 8-9 days, individual drug resistant colonies appeared on the surface of MEF cell plates and become visible for picking and sub-cloning. Using a dissection microscope, drug resistant colonies are maked with a circular shape (to avoid re-picking the same colony). Each colony was then transferred to a 96 well plate for trypsinization of individual colonies and re-plating on 24-well plate coated with MEF. Cells are then grown for 3-5 days.

Harvesting colonies:

From the 24-well plates containing ES cells, colonies reaching 70-80% confluency were selected for harvesting. In this step, trypsinization is stopped by adding pure FBS to each well, half the total volume being used for PCR screening and the remaining volume is mixed with

DMSO (to 10%) for storage at -80°C. Tubes allocated for PCR screening were centrifuged at maximum speed for 2 min in a bench-top centrifuge and the pellets stored at −80°C.

Screening for positive ES colonies:

The harvested ES colony pellets were resuspended in 50µl of digestion buffer and incubated at 55°C overnight. Next day, digestion by proteinase K was performed, followed by boiling for 10 min and centrifugation. For PCR screening, 2µl of each digested colony was used. In order to screen for homologous recombination, PCR primers were designed so one primer is outside the shorter homologous sequence arm in the native mouse genomic sequence and one primer inside the NEO cassette (see Figure 9 in Chapter 3).

Up to five positive ES cells were grown and stored at -80 °C using standard procedures.

Test for Cre mediated recombination in ES cells:

The lox-P positive targeted ES cells clone was analyzed for their functionality by in vitro recombinase-mediated deletion. 3 positive colonies (colonies 2,38,45) were selected to test Cre mediated deletion. The cryotubes were thawed out then plated, cultured, passaged as described before. When the cells reached confluency, the cells were electroporated with 25ug of both (Cre, RFP) plasmids using the same condition of electroporation mentioned before. After electroporation, the cells were maintained in Geneticin free medium. After two days, when the colonies were established, the cells were washed with PBS, trypsinized and genomic DNA extraction was made as described before for PCR (Supplementary fig. 2 g, h).

Blastocyst injection of positive ES cells

Homologous recombinant ES cells clone 45 was microinjected into the fluid-filled blastocoele cavity of 3.5-day-old embryos at the blastocyst stage (performed with the assistance of the MIT transgenic core). Blastocysts were obtained from a C57BL/6 mouse (black coat color) and microinjected with our targeted R1 ES cells (129 genetic background: agouti coat color). The injected embryos were then surgically implanted in the uterus of pseudopregnant females. The resulting brown pubs were screened for homologous recombination by PCR and the F1 mice were established at CNC.

β-actin Cre germline deletion

After PCR confirmation, two positive females were crossed with β-actin Cre mouse line for germline deletion of exon-7. The resulting heterozygous female mice *Gprasp2*$^{+}$/$^{-}$ are then mated with male WT C57 to generate F2 offspring which are either *Gprasp2* $^{-}$/^{y}, *Gprasp2* $^{+}$/^{y}, *Gprasp2* $^{+}$/$^{+}$ or *Gprasp2*$^{+}$/$^{-}$. GPRASP2 mice were viable and born at the expected Mendelian ratio (Table 26), indicating no embryonic lethality of this genotype as reported when there is a 0.35 Mb deletion in Xq22.1 region (containing five genes including *Gprasp2*) (Zhou et al., 2014).

Table 26 | Mendelian ratio

	♂		♀	
WT♂ x (-/+) ♀	WT	(-/y)	WT	(-/+)
Total (animals)	21	19	18	15
Percentage	52	47	54	45
Expected (%)	50	50	50	50

2.4.5. Electrophysiology

Acute hippocampal slices were prepared from P15-P20 WT and *Gprasp2* KO littermates to perform both field recording experiments. The osmolarity of all solutions was adjusted to 300-310 mOsm. The pH of all solutions was adjusted to 7.4 with HCl.

Before brain dissection, mice were anesthetized with isofluorane and perfused with a sucrose-enriched buffer (SB) containing (in mM): sucrose 198.86, KCl 2.55, $NaHCO_3$ 25, $NaH_2PO_4.2H_2O$ 1.09, Glucose 25.03, $MgSO_4$ 2.5 and $CaCl_2$ 0.5. The brain was quickly removed and glued to a vibratome support filled with ice-cold, oxygenated SB (saturated with 95% O2/5% CO2). Sagittal hippocampal slices were obtained with the following vibratome settings: speed 0,12 mm/s, amplitude 0,45 mm and thickness 300 μm and immediately placed in recovery at 32°C for 30 min in artificial cerebral spinal fluid (aCSF) containing (in mM): NaCl 130.9, KCl 2.55, $NaHCO_3$ 24.05, $NaH_2PO_4.2H_2O$ 1.09, Glucose 12.49, $MgSO_4$ 0.5 and $CaCl_2$ 2.

Following recovery for 1h at RT in aCSF, hippocampal slices were placed in a submersion chamber perfused with oxygenated aCSF (2 to 3 mL/min) at 25°C and fEPSP were recorded in CA1 stratum radiatum with a borosilicate glass recording electrode filled with aCSF (2-4 MΩ) as previously described (Auerbach et al., 2011), the electrode was placed at the depth

in the slice that gave the largest signal amplitude with a stable signal for at least 10 min. Evoked responses were obtained by stimulating the Schaffer collaterals at 0.05 Hz with a concentric bipolar stimulating electrode (0.2 ms stimulus). The current applied was calculated as 50% of the maximal response of an input-output curve starting at 20 μA with 10 μA increments. The LTD protocol consisted in: a stable baseline for 20 min followed by application of 50 μM (S)-3,5-DHPG (Tocris) for 5 min and continuous recording for another 55 min. Field potential recordings were filtered at 0.1 Hz to 1 kHz, digitized at 10 kHz and analyzed using Clampfit 10.7 software (Axon Instruments). Each fEPSP point corresponds to the average of 3 slopes (1 slope every 20 s), normalized to the mean of the 20-min baseline and presented as mean ± s.e.m. Significance was determined by two-way. All experiments were performed blind to the genotype.

Before the LTD protocol, basal synaptic transmission was assessed by input-output curves and paired-pulse ratio (PPR) protocol. Briefly, PPR was assessed by applying to consecutive pulses separated by 20, 30, 50, 100, 200, 300 and 500 ms inter-stimulus intervals and plotting the ratio of the fEPSP slope of stimulus 2 to stimulus 1. PPR was assessed in all slices used for the LTD protocol.

2.4.6. Behavior tests

Mouse cages were maintained at a constant temperature (22ºC) and humidity (60%), under a cycle of 12 hours / light (lights on from 7 a.m. to 7 p.m.) in an individual cage ventilation system in the CNC vivarium. Animals were allowed access to water and food ad libitum. Mice were transferred from the animal house one day before the experiment to acclimatize to the behavioral room; tests were conducted from ~09:00 Am until ~17:00 PM and afterward the animals were returned to the animal house. The maintenance and treatment of the animals were performed according to the Animals Use and Care Guidelines issued by FELASA. All experiments with mice were carried out according to the protocols approved by ORBEA (Local agency responsible for Animal Welfare of the University of Coimbra/CNC), DGAV (Portuguese Regulatory Agency) and European Directives on Animal Welfare. All behavioral tests and quantifications were performed by trained experimentalists blinded to genotype.

Rotarod performance:

Motor coordination was assessed in an accelerating rotarod test (4–40 r.p.m.). Briefly, animals were introduced in the apparatus (Med Associates) and the latency to fall was determined. Animals were given three successive trials in a single day for three days with an inter-trial interval of 10 min.

Forced swimming test:

To assess depressive-like behavior in *Gprasp2* KO mice, the forced swimming test was performed. Briefly, a 2 L glass beaker was filled with 1.5 L of water at 24 ± 1°C. Animals were introduced into the water and their behavior videotaped for 10 min. Afterwards, the mice were removed and allowed to dry in a clean dry cage before returning to their home cage. The water was changed and the beaker cleaned between each subject. Only the last 6 min of the test were scored for latency to the first immobility and total time spent immobile. The immobility was defined as the lack of motion of the whole body, except for small movements necessary to keep the animal's head above the water.

Sucrose splash test:

Animals were first isolated in their home cages for 24 hrs. A 10% sucrose solution was squirted on the dorsal coat; the latency to initiate grooming behavior as well as the frequency and the duration of grooming was recorded during five minutes after the vaporization of sucrose solution using.

Dyadic social interaction test

Mice were tested for reciprocal social interaction as previously described (Peça et al., 2011). Males C57BL/6 mice unfamiliar with the test mice were used as stimulator partner and their paws were marked one week before the experiment. To reduce reactivity and promote social investigation, partners were handled a week before testing. Twenty-four hours prior the test, test mice were trained to the test chamber interacting with an unfamiliar C57BL/6 mice (not included in our study) for 20 min. The experiment was performed in a non-transparent acrylic open arena (40x40x30cm) filled with fresh bedding. Illumination on the arena floor was

kept at 100 lx during the test. The open arena was cleaned with 70% ethanol then wiped with paper towels in between trials. The target mouse is removed from the home cage and placed on one side of the test chamber and is separated by a solid partition from the age-sex-weight matched partner. After the 10-min acclimatization period, the barrier was removed and social interactions are recorded for 30 min. Social interactions were defined as time spent in reciprocated or non-reciprocated interaction. The total time spent in reciprocated interaction, consisting of one mouse either WT or KO engaging the stimulus and the stimulus reciprocating the social behavior; and total time spent in non-reciprocated interaction, wherein the GPRASP2 mouse's responses were not reciprocated by stimulus. Trials involved animals engaged in fighting (sustained for more than 30 s without interruption) were terminated and excluded from analysis. Quantification of those behaviors were scored manually by observers blinded to the genotype of the animals using the Observer XT 9 software (Noldus, Netherland).

Three-chamber social interaction test

WT and *Gprasp2* KO mice were tested for voluntary social interaction as previously described (Peça et al., 2011). The assay consisted of three sessions, a first session began with a 20-min habituation where the subject mouse could freely explore all three chambers. Next, the mouse was confined to the center chamber while an empty wire cage (Empty) and a caged unfamiliar mouse (Stranger 1) were introduced to the side-chambers. The subject mouse was then allowed to freely explore all three chambers for 20 min. Following the 10-min session, the animal remains in the chamber for an extra 10 min (post-test) to better acquire the identification cues from Stranger 1 animal. Before the last session, the subject mouse was again gently guided to the center chamber while the empty wire cage was replaced with a caged wild-type mouse (Stranger 2). The subject mouse again freely explored all three chambers for 10 min. All stranger mice were males at the same age and previously habituated to the plastic cage during the previous days. The positions of empty cage and Stranger 1 were alternated between tests. No position bias was observed. Time spent in each chamber, time spent in close proximity and heat maps were calculated using the automated software Ethovison (Noldus, Netherland).

Marble burying test

Marble burying was measured as previously described. Each mouse was placed in a clean empty home cage (20×26×13 cm) with 24 marbles evenly spaced apart in a 4x6

arrangement on 5-cm-thick fresh bedding. The number of marbles buried to the 2/3 depth of their height were counted. Mice were placed facing the cage corner and left for free exploration for 30min. All trials were videotaped and the number of marbles buried were scored manually by observers blinded to the genotyping.

Nest building

Subjects were individually housed in a new standard home cage (20×26×13 cm) with corn bedding without environmental enrichment like cardboard houses and tunnels. In each cage, a nestlet was added at 17:00. Nest quality was scored 16 hours later, following a 5-point rating scale by different observers blind to the experimental conditions, as described elsewhere (Deacon, 2006). A still image of nestle was taken above the cage before animal removal and nest area were measured by image J software.

Open field test

Open field was a non-transparent acrylic open arena (40x40x30cm) and mice were automatically tracked using Ethovision (Noldus, Netherlands). Mice were placed at the corner of the apparatus and locomotor behaviors was recorded for 1 h. Indirect and homogenous illumination of the room was provided by white LED lamps at 100 lx. Time spent in the center zone (15 cm x 15 cm) and distance travelled in the center was evaluated. The test box was cleaned with 70% ethanol between each test.

Elevated plus maze

This maze was built in-house according to the dimensions and materials specified (Gerfen, 2006). The maze was built from semi-opaque reflecting acrylic (0.5 cm thickness). A rim of 0.5 cm in height was built around the open arms to prevent excessive falling of the animals. The illumination was provided from white LED lamps positioned over the maze and the surface of the maze illuminated at ~100 lx. Tracking was performed using Ethovision (Noldus, Netherlands). The mouse was placed in the center of the maze facing towards one of the closed arms and then released into the closed arm. Animals were tested individually for 5 min, and the maze was cleaned with 70% ethanol and wiped with paper towels between trials to remove residue or odors. Movement of the mice was video-recorded for 10min and the

number of entries into the open and closed arms, the time spent in each arm, and the total distance moved was measured and analyzed using Ethovision (Noldus, Netherlands).

Novel object recognition test

The experimental arena consisted was of non-transparent acrylic material (40x40x30cm). Habituation was done by exposing the animal to the experimental apparatus for 10 min. The next day, for the training session, mice were placed in the experimental apparatus in the presence of two identical objects for 10 min. After a retention interval of 6 h, mice were again introduced in the arena; with one familiar and one novel object. Mice were also allowed to explore for 10 min. The objects chosen for this experiment included a 25-mL tissue culture flask and a plastic Lego, both approximately the same height and weight. The durations of time mice spent exploring each object (familiar object; novel object) was recorded by a trained observer, blind to the genotype, using Observer XT 9 (Noldus, Netherlands).

Dark-light emergence test

The maze consisted of an open-field arena divided into two chambers, with an opening between the two parts. Mice were placed into the dark side of a two-chambered apparatus and given 10 min to freely explore the arena whie the illuminated side was kept under 400 lux intensity.. Mice were filmed with a camera positioned overhead and the time spent on light versus the dark part of the maze, the number of transitions and latency to first enter the light were analyzed manually using the Observer XT 9 (Noldus, Netherlands).

Table 27 | List of cohorts used in different behavior test.

Cohort 1	Cohort 2	Cohort 3	Cohort 4	Cohort 5	Cohort 6
n= 3 WT n= 2 KO	n= 7 WT n= 7 KO	n= 3 WT n= 3 KO	n= 4 WT n= 5 KO	n= 4 WT n= 3 KO	n= 4 WT n= 4 KO
Open field test	Open field test	Open field test	Three chamber test	Three chamber test	Three chamber test
Elevated plus maze	Elevated plus maze	Elevated plus maze	Social dyadic test	Social dyadic test	Social dyadic test
Marble Burying test	Marble Burying test	Marble Burying test	Open field test	Elevated plus maze	Elevated plus maze
Rotarod	Rotarod	Rotarod	Elevated plus maze	Novel Object Recognition	Splash test
Novel Object Recognition	Novel Object Recognition	Novel Object Recognition	Novel Object Recognition	Splash test	
Light/dark box	Light/dark box	Light/dark box	Splash test	Forced swimming test	
Nesting behavior	Nesting behavior	Nesting behavior	Forced swimming test		
Home cage recording	Home cage recording	Home cage recording			
Splash test	Splash test	Forced swimming test			
Forced swimming test	Forced swimming test	Sacrifice			
Sacrifice	Sacrifice				

Statistical analysis

All graphs represent average values ± s.e.m. Statistical differences were performed using unpaired student t-test, one-way or two-way ANOVA analysis followed by either Bonferroni or Tukey posthoc test: n.s. non-significant, ***$p<0.001$, **$p<0.01$, *$p<0.05$.

2.4.7. Supplementary figures

a

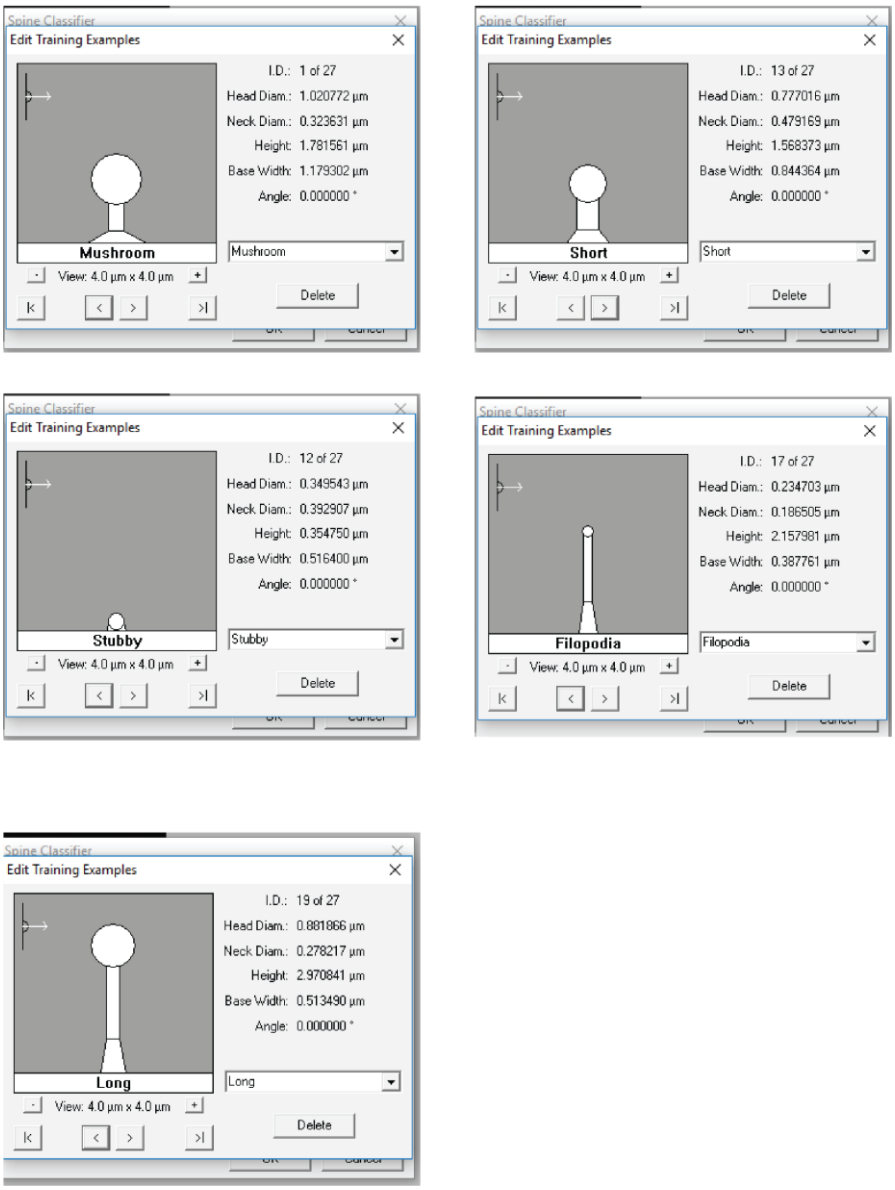

Supplementary figure 1 | Representative examples for spine categories used in spine analysis. Extracted from Neuron studio software

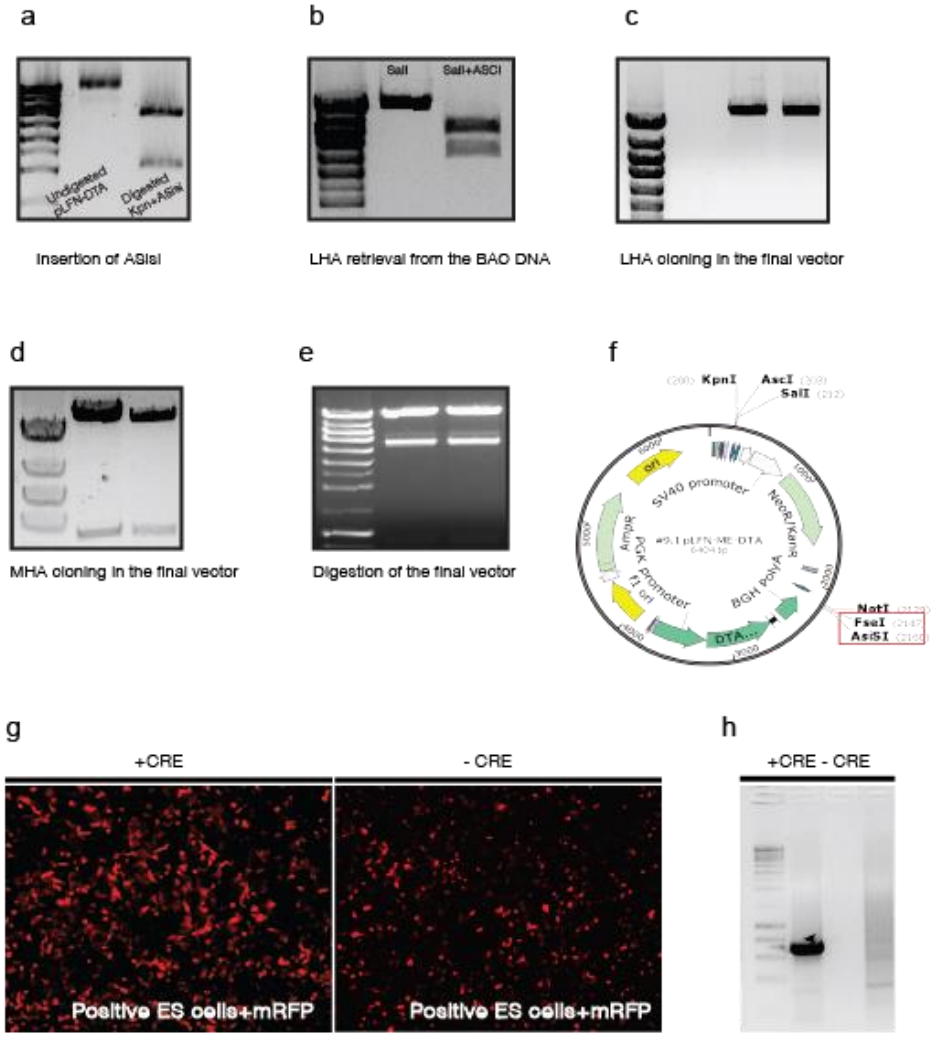

Supplementary figure 2 | Construction of targeted vector for *Gprasp2* KO mice. The targeting vector pLFN-DTA was modified for the purpose of generating conditional-knockout targeting vector. Two restriction sites (AsiSI and FseI) were inserted using standard linker ligation protocol. The long homology arm (LHA) was cloned through retrieval of DNA from a BAC, while the short homology arm (SHA) was cloned using PCR. To introduce the second loxP site into PLFN-DTA plasmid, the middle arm (MA) was cloned using a forward primer that includes loxp sequence. (a-e) Cloning the homology arms in the targeted vector. (a) DNA electrophoresis confirming insertion of AsiSI restriction sites in the final vector using AsiSI enzyme. (b) DNA electrophoresis confirming LHA retrieval, first lane digestion with SalI only, second lane digestion with SalI+ AscI. (c) DNA electrophoresis confirming cloning LHA in the final targeted vector, digestion with SalI results in 12500bp (LHA+PLFN-DTA) (d) DNA electrophoresis confirming cloning MA in the final targeted vector, digestion with NotI and AscI results in 2 fragments 12500bp (LHA+PLFN-DTA) and 4400 for the MA. (e) DNA electrophoresis confirming cloning all the homology arms (LHA, MA, SHA) in the final vector. (f) Representative image for the targeted construct, red rectangle highlighting insertion of (AsiSI and FseI). (g-h) Test for Cre mediated recombination in ES cells. (g) Positive ES cells (have loxp sites) electroporated with both Cre and mRFP (left) or mRFP only (Right). (h) PCR screening for Exon 7 deletion, in the first lane a band of (700bp) show up refers to successful Cre mediated deletion, but not in the second lane, since absence of deletion is incompatible with PCR amplification.

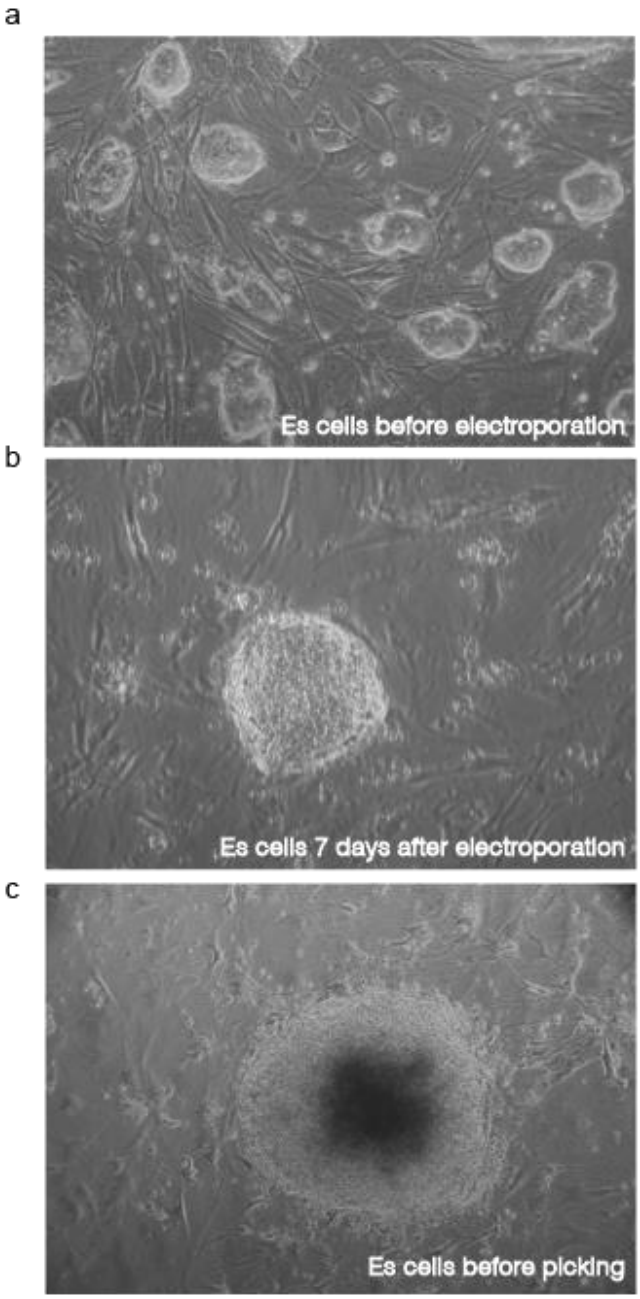

Supplementary figure 3 | ES cell morphology and confluence throughout homologous recombination protocol. (a) Healthy R1 ES cells after 4 days in culture plated on gamma irradiated fibroblasts (10× magnification). (b) ES cells 7 days after electroporation of the targeted construct and (c) ES cells before individual colony picking for dispersal and clonal growth.

Chapter 3 | GPRASP2 in ASD and ID

This chapter is under preparation for submission as a research article.

Edfawy M., et al and Peça, J. Gprasp2 deletion causes synaptic and behavioral aberrations associated with autism and intellectual disability (in preparation)

The electrophysiological experiments shown in Figure 13 were performed by Joana Guedes.

Gprasp2 deletion causes synaptic and behavioral aberrations associated with autism and intellectual disability

3.1. Abstract

Metabotropic glutamate receptors (mGluR) dysfunction has been implicated in the pathophysiology of autism spectrum disorder (ASD) and intellectual disability (ID). However, the role of mGluR regulating proteins in this process remains largely unknown. Previous studies have shown that G Protein-Coupled Receptor Associated Sorting Proteins (GPRASPs) regulate mGluRs and that GPRASP2 is particular is involved in ASD. To further study the role of this gene we created a novel *Gprasp2* knockout mouse line. We observe that mutant animals exhibit social abnormalities, abnormal anxiety, cognitive impairments and exaggerated hippocampal mGluR-LTD in the hippocampus. Concomitant with this dysfunction in synaptic plasticity, we observe that mGluR5 endocytosis is significantly enhanced when GPRASP2 is acutely overexpressed in neuronal cultures. We found that changing the levels of GPRASP2 bidirectionally affects both dendritic spine density and neuronal complexity. Broadly, our findings strongly suggest a role for GPRASP2 in neuronal development, implicate the protein in the modulation of mGluRs and highlight the role of GPRASP2 in ASD and ID associated dysfunction.

3.2. Introduction

Autism spectrum disorder (ASD) is an early onset neurodevelopmental condition characterized by persistent problems in social interaction and communication, as well as by the presence of stereotypies, restricted interests and repetitive behaviors (American Psychiatric Association, 2013a). A recent epidemiological survey conducted by the Center for Disease Control estimates that the prevalence of ASD may be as high as 1.47% (Baio, 2014). Additionally, not only are ASD and intellectual disability (ID) often co-morbid, there is high degree of pleiotropism with ID and ASD candidate genes (Huguet et al., 2013; Volk et al., 2015). Currently, key molecular focal points for these neurodevelopmental conditions have been identified to include: i) synaptic proteins involved in scaffolding, and signaling at the postsynaptic density and ii) proteins in the mTOR signaling pathway involved in cellular growth, transcription and mRNA translation. Together, both molecular complexes share as a key feature the regulation of mGluR signaling (Peça and Feng, 2012; O'Connor et al., 2014; Bourgeron, 2015).

Abnormal mGluR5 signaling is a hallmark dysfunction in *Fmr1* (Huber et al., 2002b), *Tsc1* (Bateup et al., 2011), *Tsc2* (Auerbach et al., 2011), *Pten* (Takeuchi et al., 2013) and *SHANK3* mutant mice (Verpelli et al., 2011). Moreover, the genetic and pharmacological manipulation of mGluRs has been shown to ameliorate behavioral abnormalities in *Fmr1* and *Shank2* mutant mice (Dölen et al., 2007; Michalon et al., 2012; Won et al., 2012). More recently, partial genetic ablation of β-arrestin in *Fmr1* animals was shown to correct the aberrant mGluR-LTD in this model (Stoppel et al., 2017). However, with the exception of β-arrestin and Homer, little is known on the intracellular proteins that regulate mGluR surface expression and trafficking. Nevertheless, like most GPCRs, mGluRs interact with receptor-selective partners that mediate GPCR signaling and trafficking to specific cellular locations (Ritter & Hall, 2009). GPRASPs are important partners in these processes and are known to interact and regulate the delta opioid, oxytocin, mGluR1 or mGluR5 receptors (Heydorn et al., 2004; Abu-Helo and Simonin, 2010), from this family, mutation in *GPRASP2* gene have been identified in patients afflicted with ASD (Piton et al., 2011; Butler et al., 2015).

Here we explore the potential role of GPRASP2 in regulation of mGluR and its involvement in ASD and ID. Towards this, we developed a novel knockout mouse model of GPRASP2 and demonstrate that *Gprasp2* mutat mice display several phenotypes reminiscent of ASD and ID including social abnormalities, abnormal anxiety and enhanced mGluR-LTD. We present a detailed characterization of the expression of GPRASP2 in the mouse brain as well

as the electrophysiology, biochemistry and behavioral alterations present in these mice. We show that GPRASP2 is expressed in several brain regions including hippocampus, thalamus and hypothalamus which are areas linked with cognition, locomotor activity, anxiety and obesity. Additionally, we found that changing the expression levels of GPRASP2 bidirectionally affects dendritic spine morphology, neuronal complexity and interfere with mGluR5 trafficking in neuronal culture. Our data suggest that *Gprasp2* mutations contribute to the pathogenesis of neurodevelopmental disorders, affecting dendritic and spine morphology via disruption of mGluR5 trafficking.

3.3. Results

3.3.1. GPRASP2 is highly expressed in ASD-relevant brain regions

Multiple lines of evidence from human studies and mice models have converged to suggest that cortico-striatal circuit dysfunction is intimately associated with the etiology and pathophysiology of ASD as it pertains to repetitive behaviors and stereotypies (Peça et al., 2011; Langen et al., 2014), Still, the full extent of neural circuits impacted by ASD and ID are not well understood in the context of social and cognitive function.

We first examined the developmental expression pattern of GPRASP2 in mouse brain and found that GPRASP2 expression can be detected at the embryonic stage (E18) and steadily increased during postnatal development reaching a peak expression at P15 (Fig. 1a). Our results show that GPRASP2 can be detected in synaptic fractions that include PSD, synaptosome plasma membrane and (SPM) brain lysate (Fig.1b).

To provide additional details regarding GPRASP2 expression, we performed mRNA *in situ* hybridization and found that GPRASP2 is expressed in adult mouse brain, particularly in hippocampus, cerebellum, cortex and thalamus (Fig.1d). Moreover, western blot analysis of microdissected adult brain tissue confirmed strong expression of GPRASP2 in distinct nuclei (Fig.1e).

Next, we assessed the developmental expression of GPRASP2 mRNA in parasagittal mouse brain across three developmental time-points P5, P15 and adult mice (P60) (Fig.1c). In P5 animal, we found strong expression in the striatum along with a moderate level of expression in the hippocampus, olfactory bulb and cerebellum. In P15 sections GPRASP2 mRNA was strongly detected in the hypothalamus, hippocampus, thalamus and a sparse expression pattern was observed in the cerebellum (Fig.1c). GPRASP2 expression in the striatum was restricted to

early post-natal period (P5). The expression profile in the hippocampus and hypothalamus was strongly detected across all ages.

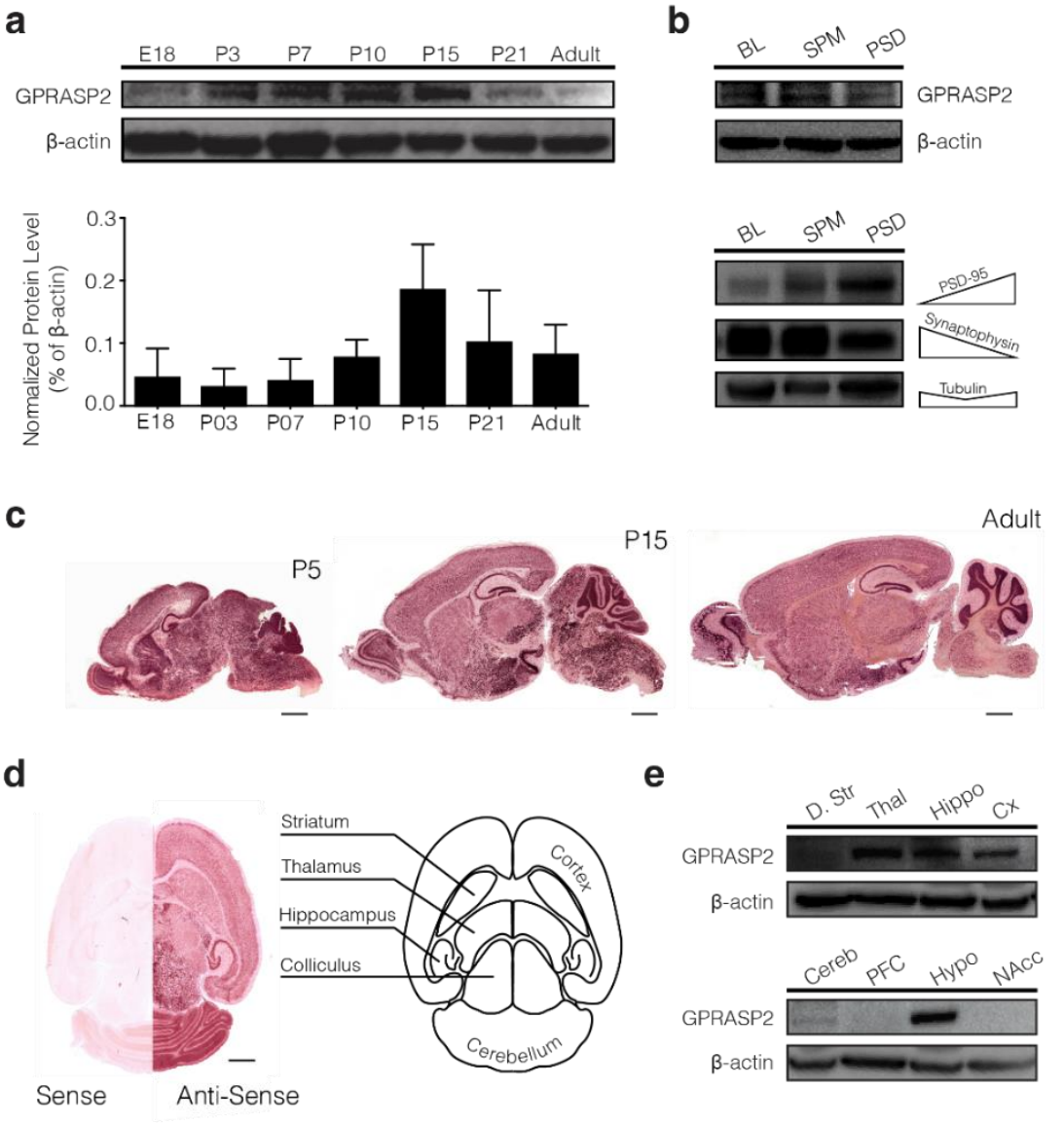

Figure 1 |Developmental and region-specific expression profile of GPRASP2 in the mouse brain. (a) Expression patterns of GPRASP2 in brain lysates of C57BL/6 mice from embryonic stage (E18) to adult ages analyzed by western blot. Data represents as mean ± s.e.m. n = 3 mice. (b) GPRASP2 is detected as a single band in brain lysate, synaptosomal plasma membrane (SPM) and twice Triton X-100-washed (PSD-2T) fraction purified from whole mouse brain. Quality control for PSD isolation shows increase in PSD-95 signal and decrease in synaptophysin signal. (c) Dig-labeled *in situ* hybridization analysis of GPRASP2 mRNA expression across development using parasagittal mouse brain sections (from P5 to adult), scale bar, 2 mm. (d) GPRASP2 mRNA levels in horizontal adult mouse brain with sense probe (left) and anti-sense probe (right), scale bar, 2 mm. (e) Adult mouse brain was dissected into subregions, and lysates were subjected to immunoblot analysis using anti-GPRASP2 antibody. "D. Str" – dorsal striatum; "Thal" – thalamus; "Hippo" – hippocampus; "Cx" – cortex; "Cereb" – cerebellum; "PFC" – prefrontal cortex; "Hypo" – hypothalamus; "NAcc" – nucleus accumbens.

Since GPRASP2 expression levels were highly abundant at P15, we performed a detailed *in situ* mRNA analysis across coronal sections to determine its expression in discrete brain nuclei (Fig.2a). We found that GPRASP2 is broadly expressed in medial prefrontal cortex (mPFC) (Fig.2b), lateral septal nucleus (LSr) (Fig.2c), thalamus (Fig.2d), medial habenula (Fig.2f), amygdala (Fig.2h). The strongest labelling was in discrete regions within the hypothalamus, such as paraventricular, ventromedial and arcuate nucleus suggesting that GPRASP2 may play a role in hypothalamic function (Fig.2k). GPRASP2 mRNA was also strongly expressed present in all areas of the hippocampus and showed particularly high expression in especially the dentate gyrus (Fig.2j) (Supplementary table.1).

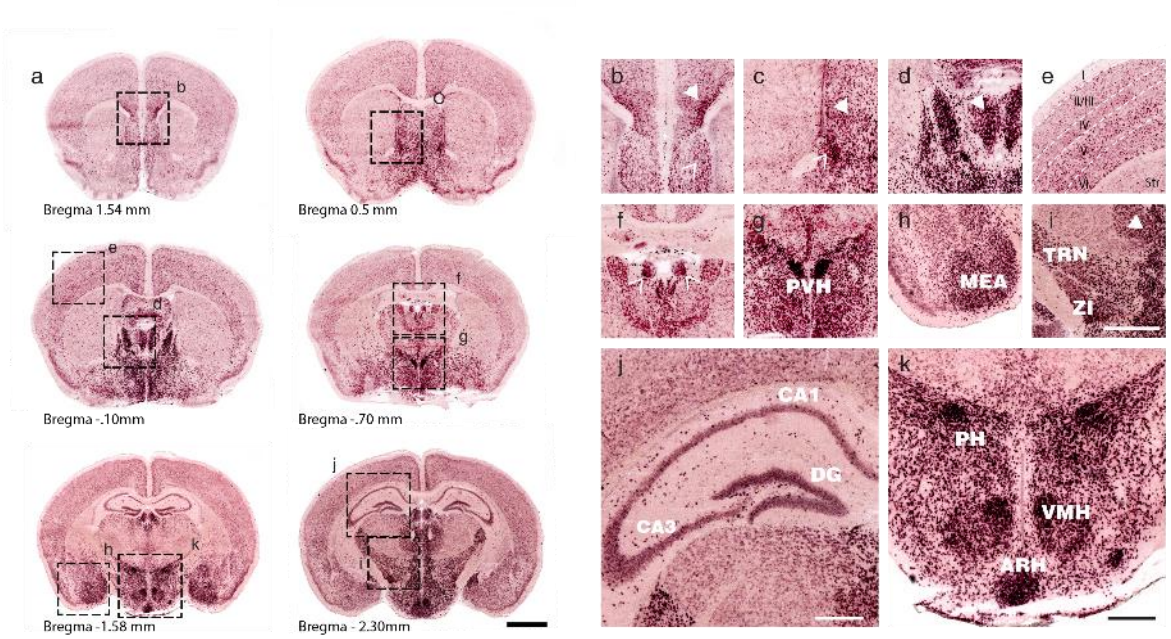

Figure 2 | *In situ* mRNA labelling of GPRASP2 in juvenile mouse brain. (a) Coronal sections of P15 mice hybridized with GPRASP2 antisense probe. (b) Expression of GPRASP2 mRNA in the medial prefrontal cortex, solid arrow head points to prelimbic (PL) and arrow head points to infralimbic (IL) regions.(c) GPRASP2 transcripts are detected in the lateral septal nucleus (LSr) (solid arrow head) and strong labelling was found in the bed nucleus of the stria terminalis (BNST) (arrow head).(d) The thalamus displays strong GPRASP2 labelling, solid arrow head refers to paraventricular nucleus of the thalamus (PVT). (e) GPRASP2 transcript is lightly expressed in cortical layers I-VI. (f) Arrow head refers to GPRASP2 mRNA labelling in the medial habenula (MH). (g) Strong expression of GPRASP2 mRNA in the paraventricular nucleus of the hypothalamus (PVH). (h) Strong labelling is detected in medial amygdalar nucleus (MEA). (i) GPRASP2 transcript is highly expressed in thalamic reticular nucleus(TRN) and zona incerta (ZI) of the hypothalamus, solid arrow head pointed to parafascicular nucleus of the thalamus(PF). (j) Strong expression of GPRASP2 transcripts is present in several regions of the hippocampus, including CA1, CA3 and dentate. (k) The hypothalamus presents a dense labelling for GPRASP2 in the posterior hypothalamic nucleus (PH), ventromedial nucleus of the hypothalamus (VMH) and arcuate nucleus of the hypothalamus (ARH.) High magnified images of the squared region in the left panels (scale bar, 2 mm) are shown in the adjacent right panels (scale bar, 500 μm).

3.3.2. GPRASP2 regulates spine morphology and enhances neuronal complexity

In neurodevelopmental disorders, neuronal deficiencies in spine morphology and neuronal complexity have been correlated with the behavioral and intellectual deficits (Auerbach et al., 2011; Durand et al., 2012; Valnegri et al., 2012). Additionally, dysregulation of mGluR1/5 signaling is also a consistent observation found in mouse models of ASD and ID where there is prominent spine abnormality (Irwin et al., 2001; Santini et al., 2013).

To test whether overexpression of GPRASP2 contributes to synapse formation and/or maturation, we transfected hippocampal neurons at DIV 7 with GFP-GPRASP2 or GFP alone and stained transfected neurons for excitatory synaptic markers PSD-95 and VGLUT1 (Fig.3a). We found that GPRASP2 overexpression induces remarkable increase in the number of PSD-95 (19.43±6.171%) and VGLUT1 puncta (23.9±9.921%) without any significant changes in area and intensity (Fig.3b,c). These results suggest that overexpression of GPRASP2 in hippocampal neurons promotes the formation of excitatory synapses.

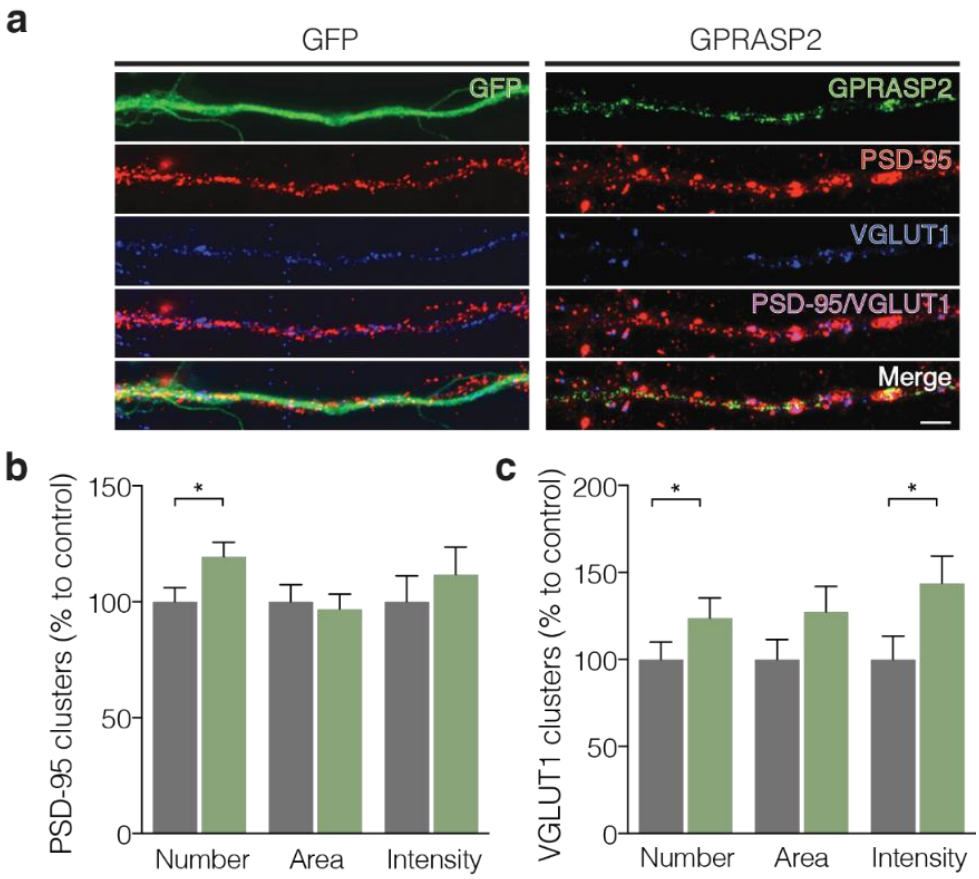

Figure 3 |Overexpression of GPRASP2 in cultured neurons increases excitatory synaptic markers. (a) Cultured hippocampal neurons were transfected with GFP alone or GFP- GPRASP2 at DIV 7 and immunostained for PSD-95 and VGLUT1 at DIV15. Neurons were analyzed for the PSD-95 and VGLUT1 clusters number, area and fluorescence intensity. (b, c) Results are expressed as % of control cells; n=31 for GFP, n=32 for GPRASP2 from three independent experiments. The statistical comparisons in (b, c) were performed using the Mann-Whitney test (*p<0.05, **p<0.01, ***p<0.001). Data are presented as means ± SEM. Scale bars 2 μm

Considering the high expression levels of GPRASP2 in the hippocampus, we decided to examine the functional consequences of gain and loss of function in hippocampal neuronal culture and neuronal morphology. Overexpression of GPRASP2 or control GFP vectors were performed alongside with mRFP vector to better visualize cellular morphology in transfected neurons. MAP2 staining was used to visualize the dendritic structure and spines were categorized into 5 different groups based on shape and size as indicated at the table below (see Supplementary fig. 1).

Table 1 | Spine categories

Protrusion	Description
Stubby	No neck
Mushroom	Neck ≤0.5μm, head >0.5μm
Short	head+ neck <2μm in length
Long	head+ neck ≥2μm in length
Filopodia	headless protrusion

We found that neurons overexpressing GPRASP2 displayed a 20 ± 6.17% increase in the total spine density compared to controls (Fig. 4a-b). When analyzed by spine categories, we found that GPRASP2 overexpression induced significant decrease in filopodia and a marked increase in stubby, short, long and mushroom spines (Fig. 4e). This suggests that GPRASP2 influence spine maturation by altering the ratio of mature versus immature spines in neurons. Consistent with these morphological changes, the head of spines were wider and longer in neurons overexpressing GPRASP2 (Fig. 4c, d). These observations suggest GPRASP2 contributes to the regulation of dendritic spine maturation.

Dendritic morphogenesis and synaptogenesis play an important role in the development and maintenance of functional neuronal networks (Jan and Jan, 2010). Hence, disruption in any of these processes leads to deficits in neuronal connectivity and may help explain why changes in spine morphology, dendritic complexity and plasticity are associated with several neuropsychiatric including schizophrenia, ASD and ID (Penzes et al., 2011).

In light of the role of GPRASP2 in spine maturation, we sought to determine whether GPRASP2 could also play a role in dendritic arborization. Surprisingly, overexpression of GPRASP2 induces an increase in dendritic complexity as measured with Sholl analyses, i.e. the number of dendritic intersections when concentric rings are drawn outward from the cell body (Fig. 5a). In addition, total dendritic length and area (Fig. 5b, c) were also markedly increased in neurons overexpressing GPRASP2. These results indicate that enhancing GPRASP2 expression levels above baseline enhances dendritic complexity and might have a potential effect in changing network activity.

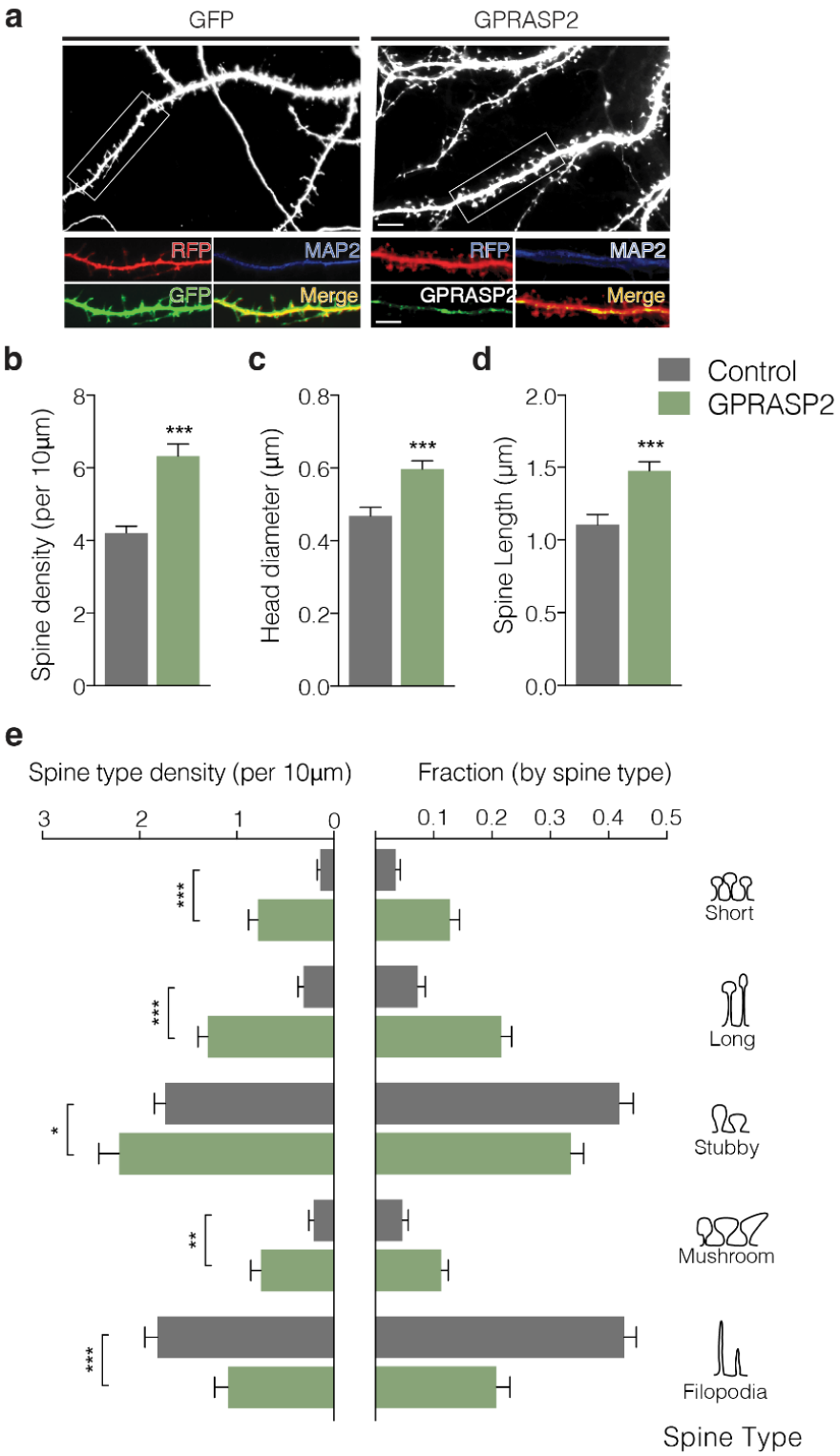

Figure 4 |Overexpression of GPRASP2 alters spine morphology. (a) Cultured hippocampal neurons were transfected with GFP alone or GFP-GPRASP2 at DIV 11 and analysed at DIV 17. (b) Analysis of spine density per 10 µm, (c) head diameter and (d) spine length in GPRASP2 overexpressing and control neurons. (e) Dendritic spines were classified into five groups: short, long, stubby, mushroom, filopodia; spine density (per µm) and spine fractions were determined for both conditions. n=31 for GFP, n=28 for GPRASP2 from three independent experiments. Statistical analysis was performed using the Mann-Whitney test (*p<0.05, **p<0.01, ***p<0.001). Data are presented as means ± SEM. Scale bars 2 µm.

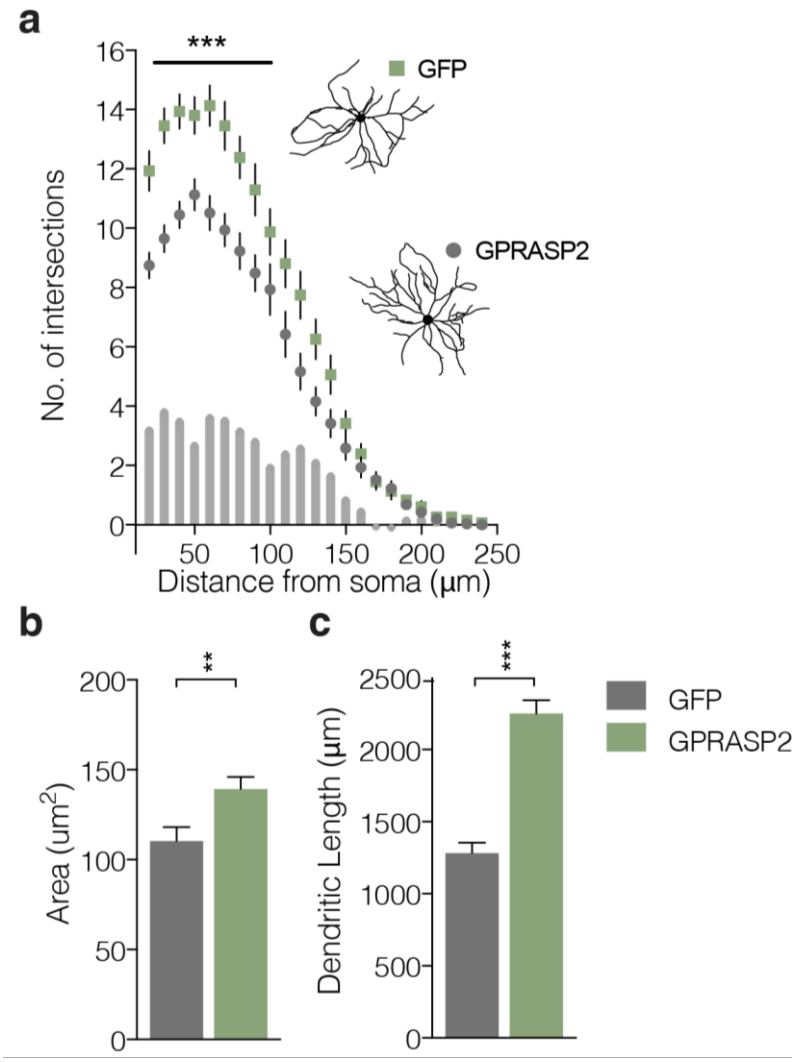

Figure 5 | GPRASP2 overexpression promotes increased dendritic complexity and total dendritic length. Cultured hippocampal neurons were transfected with GFP alone or GFP-GPRASP2 at DIV11 and analyzed at DIV17. (a) Sholl analysis quantification measured neuronal complexity as number of intersections from the soma in 20 µm radius increments. Effect of GPRASP2 overexpression on (b) total dendritic area and (c) total dendritic length when compared with GFP control; n=31 for GFP, n=32 for GPRASP2 from three independent experiments. The statistical significance for Sholl analysis was calculated using Two-way repeated measures ANOVA followed by Bonferroni's multiple comparison test (***P < 0.001). The statistical comparisons were performed using the Mann-Whitney test (*p<0.05, **p<0.01, ***p<0.001). Data are presented as means ± SEM.

3.3.3. Knockdown of GPRASP2 reduces spine density and dendritic complexity

To further assess if endogenous GPRASP2 is required for excitatory synapse formation we used RNA interference (shRNA) against GPRASP2 to knockdown expression of GPRASP2 in rat hippocampal neurons. Suppression of GPRASP2 expression by shRNA-GPRASP2 (shRNA), but not by scrambled shRNA-GPRASP2 (scramble), was confirmed by immunofluorescence staining against GPRASP2. shRNA#1 construct reduced the expression of endogenous expression of GPRASP2 by 43±3.33% in hippocampal neurons (Supplementary Fig.1b,c).

Knockdown of GPRASP2 significantly reduced the number, area, and intensity of PSD-95 and VGLUT-1 clusters indicating that GPRASP2 contributes to excitatory synapse formation (Fig. 6 b, c).

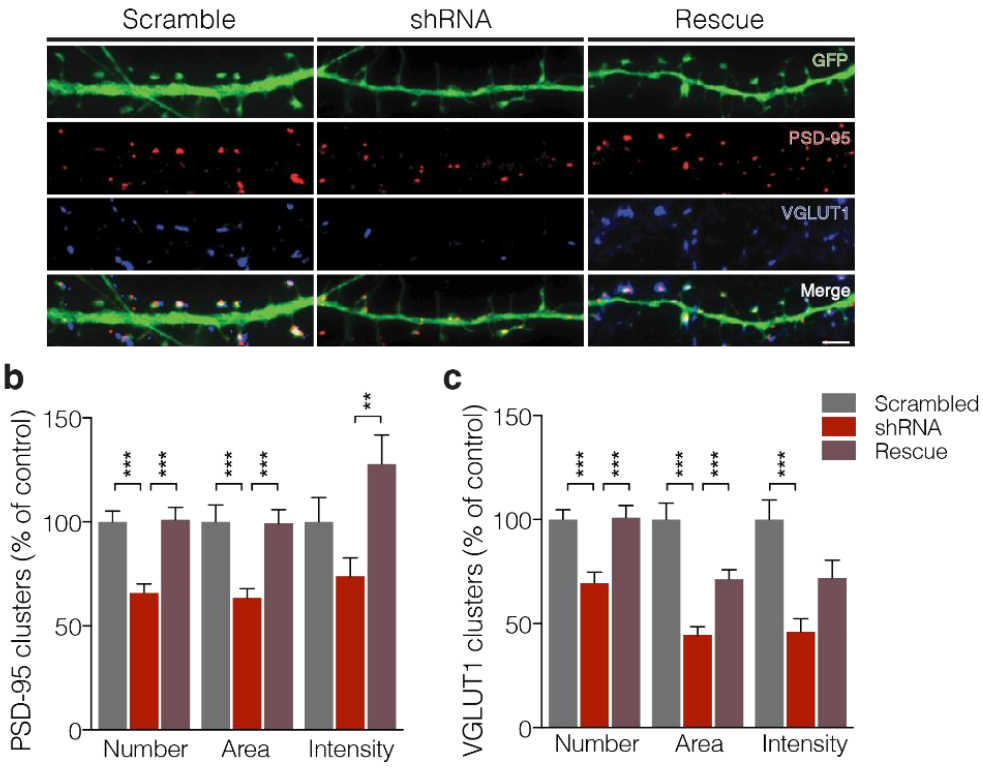

Figure 6 | Knockdown of GPRASP2 in cultured neurons reduces excitatory synaptic markers. (a) Cultured hippocampal neurons were transfected with scramble shRNA (Scramble), shRNA GPRASP2 (shRNA) or GFP-GPRASP2+shRNA (Rescue) at DIV10 and immunostained for PSD-95 and VGLUT1 at DIV15. Neurons were analyzed for PSD-95 and VGLUT1 clusters number, area and fluorescence intensity. (b,c) Results are expressed as % of scramble cells ; (n=26 for scramble, n= 32 for shRNA and n=27 for rescue) from three independent experiments. The statistical comparisons in were performed using One- way ANOVA test (*p<0.05, **p<0.01, ***p<0.001) followed by Tukey's multiple comparisons test. Data are presented as means ± SEM. Scale bars 2 μm.

Similarly, when endogenous GPRASP2 was knocked down, the overall spine density was significantly decreased (Fig. 7b), but no significant effect was found in spine head diameter (Fig. 7c) or spine length (Fig. 7d). Also, diminished GPRASP2 expression resulted in a global decrease in all spine categories; short, long, stubby, mushroom and filopodia-shaped spines (Fig. 7e) suggesting that GPRASP2 is crucial to maintain normal spine density but does not affect spine maturation. The effect of knocking-down GPRASP2 was successfully rescued by molecular replacement with an shRNA-insensitive GFP-GPRASP2 construct. Specifically, shRNA was directed against endogenous rat GPRASP2 mRNA, while our GFP-GPRASP2 construct was cloned from a mouse cDNA library that displays a different sequence for the shRNA targeted locus.

In contrast to overexpression, GPRASP2 knockdown decreased neuronal complexity (Fig. 8a), area (Fig. 8b) and total dendritic length (Fig. 8c). Again, these effects were largely rescued by co-expression of shRNA-GPRASP2 and GFP-GPRASP2. Collectively, these results corroborate the view that gain-of-function and loss-of-function of GPRASP2 display opposite effects on dendritic spine density. and neuronal complexity.

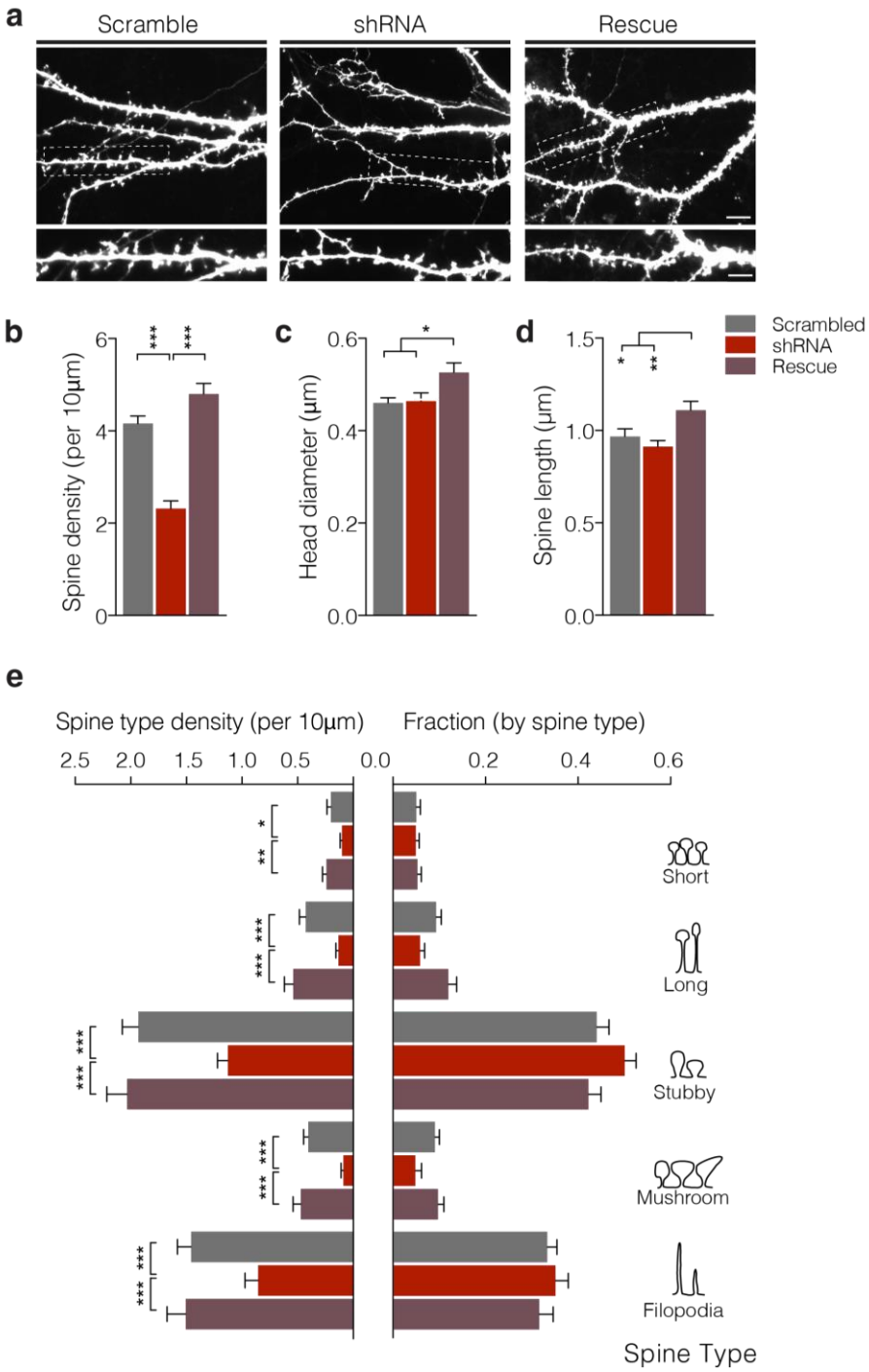

Figure 7 | GPRASP2 knockdown in cultured neurons decreases dendritic spine density. (a) Cultured hippocampal neurons were transfected with scramble shRNA (Scramble), shRNA GPRASP2 (shRNA) or GFP-GPRASP2+shRNA (Rescue) at DIV10 and analyzed at DIV15. (b) Quantification of spine density per 10 µm, (c) spine head diameter and (d) spine length in scramble, shRNA and rescue condition. (e) Dendritic spines were classified in five groups (short, long, stubby, mushroom, filopodia) based on shape. Spine density (per µm) and spine fractions were determined for all experimental conditions; (n=28 for scramble, n= 30 for shRNA and n=25 for rescue) from three independent preparations. The statistical comparisons in (b,c) were performed using One-way ANOVA test followed by Tukey's multiple comparisons test (*p<0.05, **p<0.01, ***p<0.001). Data are presented as means ± SEM. Scale bars represent 2 µm.

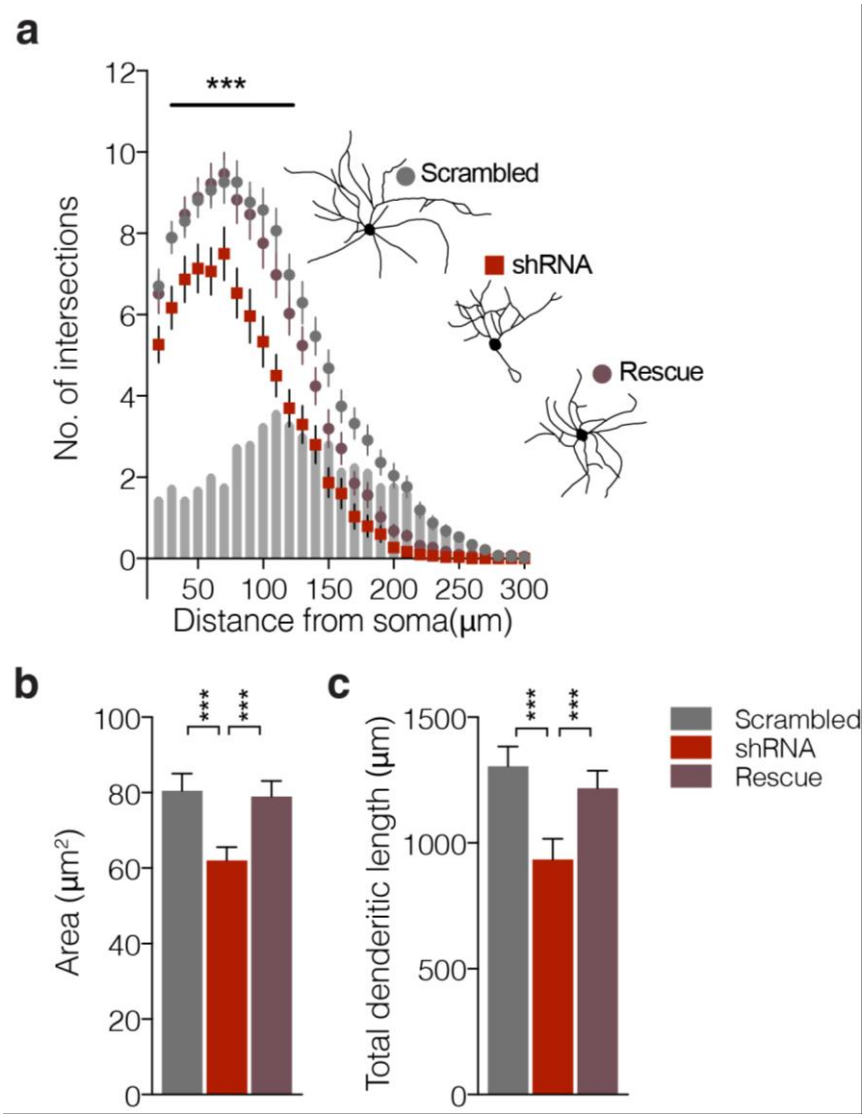

Figure 8 | Knockdown of GPRASP2 in cultured neurons decreases dendritic complexity and reduces total dendritic length. Cultured hippocampal neurons were transfected with scramble shRNA (Scramble), shRNA GPRASP2 (shRNA) or GFP-GPRASP2+shRNA (Rescue) at DIV10 and fixed at DIV15. (a) Sholl analysis quantification measured as number of intersections across the soma with 20µm radius in scramble, shRNA and rescue experiment. Effect of GPRASP2 knockdown on (b) total dendritic area and (c) total dendritic compared with scramble and rescue expressing neurons; (n=38 for scramble, n= 30 for shRNA and n=37 for rescue) from three independent preparations. The statistical significance for Sholl analysis was calculated using Two-way repeated measures ANOVA followed by Bonferroni's multiple comparison test (***P < 0.001). The statistical comparisons in (b, c) were performed using One way ANOVA test followed by Tukey's multiple comparisons test (*p<0.05, **p<0.01, ***p<0.001). Data are presented as means ± SEM.

3.3.4. *Gprasp2* null mice are viable and do not display gross anatomical defects

There is accumulating genetic evidence for the involvement of GPRASP2 in the etiology of ASD and other psychiatric disorders (Piton et al., 2011; Zhou et al., 2014; Butler et al., 2015). To investigate the function of GPRASP2 *in vivo* and to understand if *GPRASP2* deletion might contribute towards cognitive and social behavior dysfunction we generated a knockout mouse by deleting exon 7 of *Gprasp2* using the Cre/lox system. The targeting vector was introduced via homologous recombination in ES cells as described in (Heyer and Feng, 2010; Peça et al., 2011) (Fig. 9a). We confirmed our genetic manipulation by PCR (Fig. 9c), western blot (Fig 9b) and through in situ hybridization in brain slices from WT and *Gprasp2* mice (Fig. 9d).

Because X-linked ASD and ID affect males at a higher rate than females, in this study we focused on *Gprasp2* hemizygous male knockouts (*Gprasp2* $^{-/y}$ or *Gprasp2* KO). Our initial analysis revealed *Gprasp2* KO mice were born in expected Mendelian frequency (Supplementary Fig 2a). Anatomical examination of young *Gprasp2* KO mice did not show any gross abnormalities. However, at approximately 5 months of age, *Gprasp2* KO exhibited increased body weight (Supplementary Fig.2b). This phenotype did not interfere with downstream behavior tests since these were performed in juvenile, 6-8 weeks old mice.

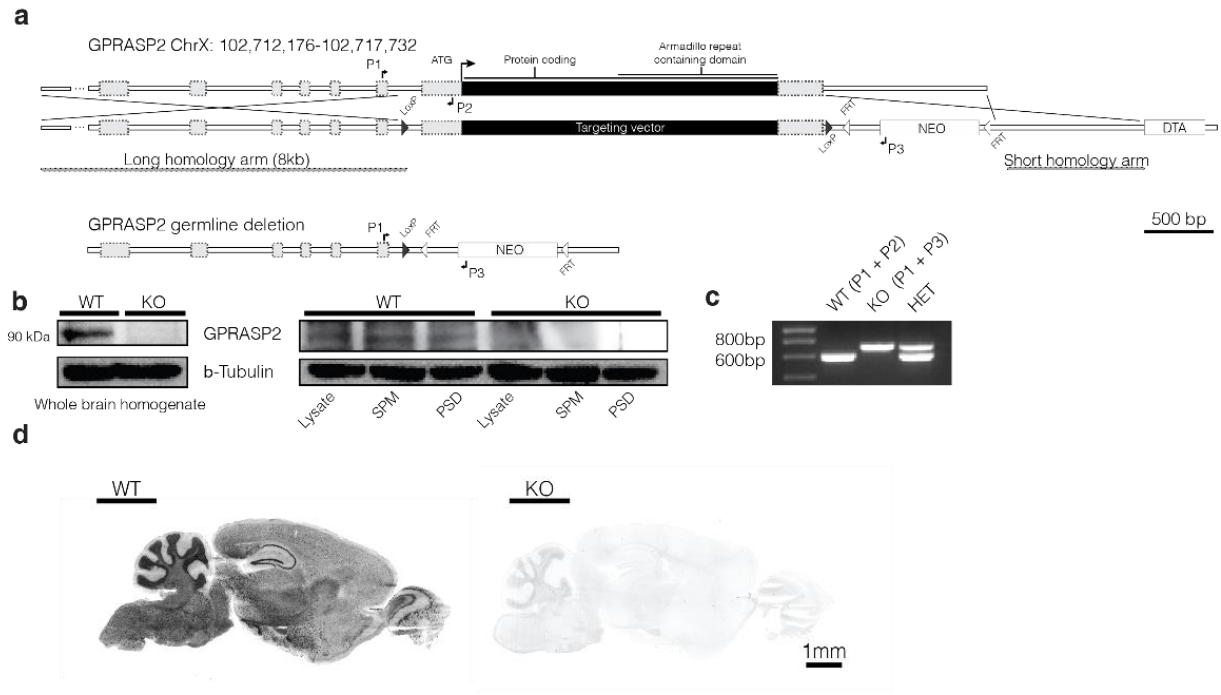

Figure 9 | Generation of GPRASP2 knockout mice. (a) Schematic describing *Gprasp2* gene structure, functional domain and strategy to create *Gprasp2*-knockout mouse. Exon 7 was flanked by 2 loxp sites (floxed) for Cre recombinase mediated excision. After the generation of chimeric mice, the loxp flanked exon 7 was removed in the germline by intercrossing with β-actin:Cre mouse strain. (b) (left) GPRASP2 antibody staining in whole brain homogenate in WT and *Gprasp2* KO mice. (right) Western blot showing GPRASP2 antibody staining in brain lysate (lysate), synaptosomal plasma membrane (SPM) and Triton X-100-washed PSD fraction in wildtype (WT), and *Gprasp2* KO mice. (c) PCR genotyping confirms deletion of exon 7 from genome of male knockout mice. (d) *In situ* hybridization probe targeting exon 7 confirm successful genetic ablation of GPRASP2 mRNA (scale bar, 1 mm).

3.3.5. *Gprasp2* KO mice display reduced anxiety-like behavior and normal emotional response in forced swimming test

First, we recorded the spontaneous locomotor activity of *Gprasp2* KO and WT mice in an open field test. *Gprasp2* KO mice did not show significant difference in locomotor activity or in distance traveled when compared to WT mice (Fig.10 a, b). However, *Gprasp2* KO showed a marked increase in the time spent in the center of the open field compared to WT mice (Fig.10 c). Next, we conducted an elevated plus maze test to confirm the reduced anxiety behavior in these mice. In the elevated plus-maze test, *Gprasp2* KO mice spent longer times in the open arms of the maze (Fig.10e), showed reduced latency to enter the open arms (Fig.10f) and entered the open arms more frequently than WT mice (Supplementary Fig.2b), no significant differences in locomotor activity were found (Supplementary Fig.2c). However, in the dark-

light box emergence test, we did not observe any significance difference between genotypes (Supplementary Fig.2d). To determine if the reduced anxiety of *Gprasp2* KO mice was accompanied by changes in depressive-like behaviors we performed the Porsolt forced swim test. In this paradigm, *Gprasp2* KO mice did not show significance change in the time spent immobile but displayed a reduction in the number of struggling bouts when compared to WT (Supplementary Fig.3a). Together, these results indicate that *Gprasp2* KO mice show reduced anxiety but normal depressive-like behavior.

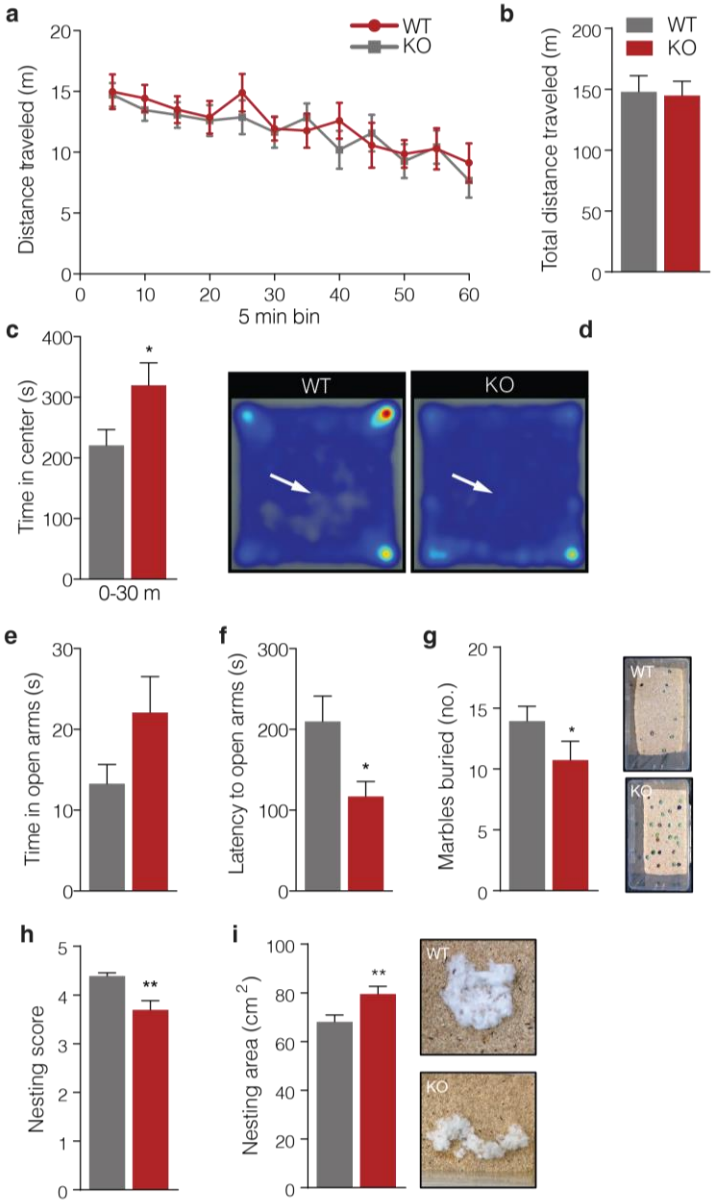

Figure 10| *Gprasp2* KO display anxiety-like behavior, impaired marble burying and abnormal nest building behavior. (a-d) Novelty-induced locomotor activity in the open field during the 60-min observation period *Gprasp2* KO mice compared with WT littermate controls, WT, n = 16; *Gprasp2* KO n = 15. Data binned 5 min intervals. (a) Distance travelled during the 60-min observation period. (b) Cumulative distance plot for data shown in (a). (c) Time spent in the center of the center of the open field. (d) Heatmaps of animals in the open field test, arrows refer to crossing activity in the center of the open field. (e, f) Anxiety levels was determined using the elevated plus-maze (e) Time spent and (f) latency to enter the open arms of the elevated plus-maze; WT n = 25; *Gprasp2* KO, n = 23. (g) Number of marble buried by *Gprasp2* KO mice compared to wild type in the marble burying test. (right) representative images from the test for both genotypes; WT n = 13; *Gprasp2* KO n = 12. (h- I) The quality of the nest built by each genotype was assessed after 12 h. (h) Nest building was scored on a scale of 1–5. (i) Nesting area performed by *Gprasp2* KO compared to WT from one nestlet. (right) representative images from the test for both genotypes; WT n = 13; *Gprasp2* KO n = 12. All values represent as mean ± SEM, for (a) Two-way repeated measures ANOVA followed by Bonferroni's test; (b-i) Mann-Whitney's U–test; *p<0.05, **p<0.01 and ***p<0.001.

3.3.6. *Gprasp2* KO exhibit impaired nesting and reduced marble burying

Nest building and marble burying are spontaneous behavior that measures home cage activity related to social behavior and a good performance in these behaviors is an indication of well-being in mice (Decon, 2006). Recently those behaviors have been shown to assess behavioral domains associated with neuropsychiatric dysfunction (Jirkof, 2014). In the marble-burying test, *Gprasp2* KO mice buried significantly fewer marbles (13.92 ±1.22) compared with WT mice(Fig.10g).

To further assess the behavioral consequences of *Gprasp2* deletion, we measured nest building for 12 hours after introduction of an intact nestlet. We found that the quality score of the nest was significantly reduced in *Gprasp2* mice when compared to WT littermates, a phenotype which may suggest impaired social behavior (Moretti et al., 2005; Blundell et al., 2010)(Fig 10 h, i). *Gprasp2* KO mice displayed normal motor coordination and balance in accelerating rotarod (Supplementary Fig.3c) suggesting that the impairment in nesting building and marble burying were not related to motor abnormalities.

3.3.7. *Gprasp2* KO exhibit social abnormalities and hyper-locomotion activity

Impairments in social interaction skills are a key behavioral defect displayed by individuals with ASD (American Psychiatric Association, 2013b). To address whether *Gprasp2* KO mice display social interaction deficits, we first examined social interaction in the three-chamber test. When a stranger mouse was placed in one wired cage (stranger–empty session), *Gprasp2* KO showed a lower preference for the stranger-containing cage than the empty one when compared to controls (Fig.11c, d), suggesting there is a clear trend for low sociability. When the empty wire cage was replaced by a second stranger mouse, *Gprasp2* KO spent less time interacting with the second stranger mouse when compared to WT littermates (Fig.11f, g), suggesting that social recognition may also be impaired in *Gprasp2* KO mice. Interestingly, KO mice traveled significantly longer distances than wild-type mice in both sociability (Fig.11e) and social novelty session (Fig.11h).

To further validate the social abnormalities in *Gprasp2* mice, we next performed a reciprocal social interaction test, where a mouse can freely interact with a novel stranger with the same age. We found that *Gprasp2* KO mice engaged in longer non-reciprocated behaviors. When *Gprasp2* KO mice initiate a social approach, the C57 partner do not reciprocate and

withdraw by either ignoring or turning away (Fig.11i). Moreover, *Gprasp2* KO mice showed a decrease in the time spent in reciprocal interaction compared to WT animals (Fig.11j). Whenever WT mice initiate a social contact, the stranger mice engage and reciprocated for longer time than *Gprasp2* KO mice. Taken together, our result suggests that genetic ablation of *Gprasp2* leads to abnormal social behavior.

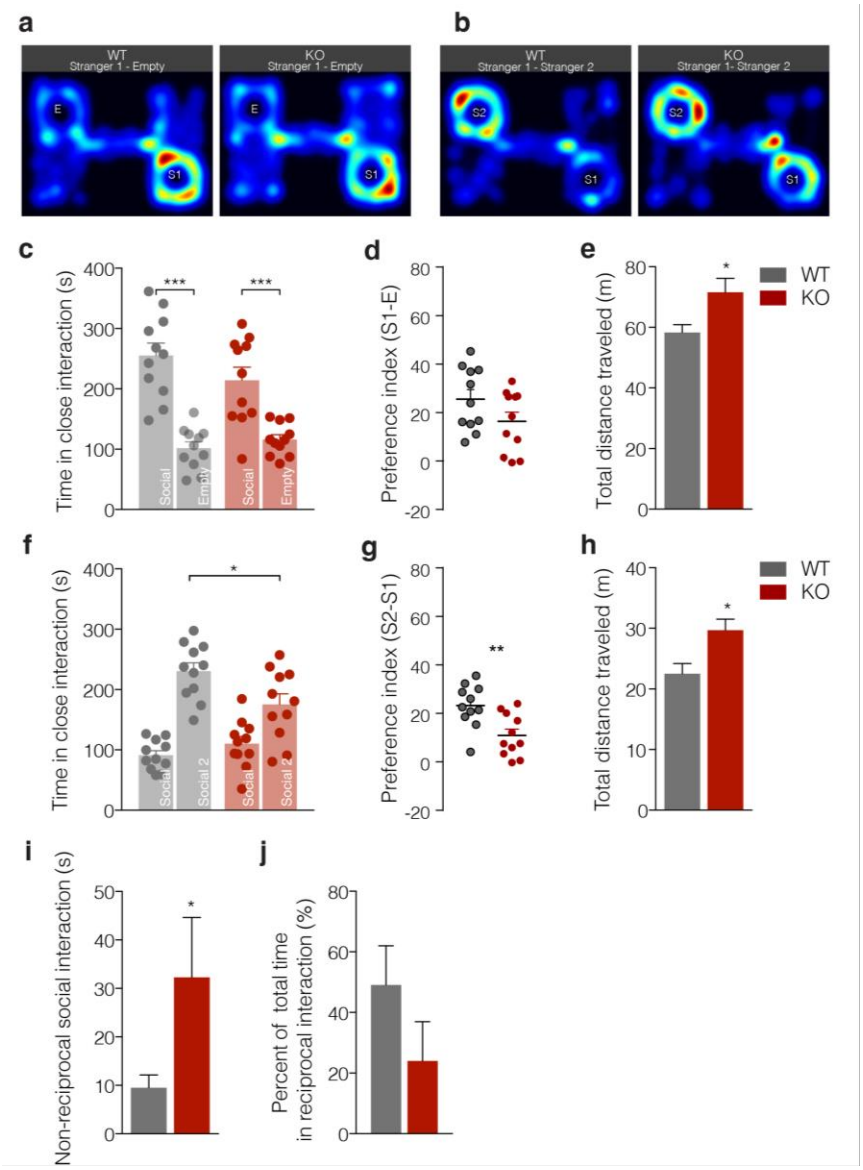

Figure 11| Altered social interaction behavior and hyperactivity in *Gprasp2* KO mice. (a-h) Three-chamber social interaction test. (a-b) Representative heatmap images from 'Stranger1–Empty' and 'Stranger1–Stranger2' trials from *Gprasp2* KO mice and controls. (c-e) Quantification of the results in (a), as shown by the amount of (c) time spent in close interaction with novel mouse versus an empty cage (e) or the preference index derived from the numerical difference between the time in close interaction with S1 and E divided by total time spent × 100 or (e) total distance travelled; WT, n = 11; *Gprasp2* KO, n = 11. (f–h) Three-chamber social novelty preference test. Quantification of the results in (b), as shown by the amount of time spent in (f) close interaction with novel social mouse versus familiar mouse or (g) the preference index derived from the numerical difference between the time in close interaction with S2 and S1 divided by total time spent × 100, and (h) total distance travelled; WT, n = 11; *Gprasp2* KO, n = 11. (i, j) Responses in a free interaction social dyadic test. (i) Time spent in non-reciprocated interaction in both genotypes. (j) Time spent in reciprocal interaction (% of total time) in *Gprasp2* KO mice compared with WT ;(WT, n = 11; *Gprasp2* KO, n = 10). All values represent as mean ± SEM. One-way ANOVA followed by Tukey's multiple comparison test; (c, f) statistical comparison were performed by Mann-Whitney's U–test; *p<0.05, **p<0.01 and ***p<0.001

3.3.8. *Gprasp2* KO displayed memory impairment in novel object recognition test

Intellectual disability is present in up to 70% of ASD patients (Belardinelli et al., 2016). Additionally, learning and memory deficits are a common observations in several mouse models of ASD and ID such as *Pten* (Lugo et al., 2014), *Tsc1* (Bateup et al., 2013), *Shank3* (Lee et al., 2015) and *Fmr1* (Ventura et al., 2004). Considering the high expression level of GPRASP2 mRNA in the hippocampus, we asked if there are cognitive or memory dysfunction in *Gprasp2* KO mice. In the novel object recognition test, the animals were exposed to two identical objects in the training session and after 6 hours, a new object replaces one of the two familiar objects. While WT mice showed preference to explore the novel object, *Gprasp2* KO mice failed to show preference to the new object, (Fig.12 a,b), suggesting that genetic perturbation of *Gprasp2* results in memory impairment.

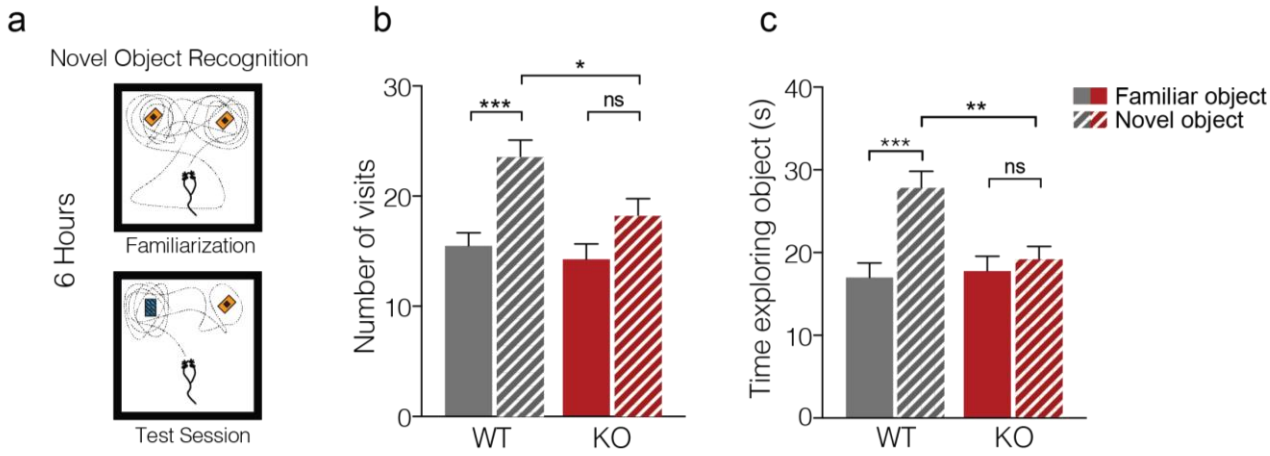

Figure 12 | *Gprasp2* KO mice display memory impairment in novel object recognition test. (a) Schematic diagram of the novel object recognition task. Familiarization phase (top), animals are exposed to two identical objects. Test phase (bottom), animals are exposed to a novel object and a familiar one. Time spent in exploration (b) and frequency of exploration (c) of the novel and the familiar objects was measured during the test session for both genotypes; WT n = 19; *Gprasp2* KO n = 19. All values represent as mean ± SEM. One-way ANOVA followed by Tukey's multiple comparison test (b-c); *p<0.05, **p<0.01 and ***p<0.001.

3.3.9. *Gprasp2* KO mice display exaggerated mGluR-dependent LTD

In addition to memory impairment, dysregulation of long-term depression (LTD) in the hippocampus has also been observed in several mouse models of autism and ID (Huber et al., 2002b; Santini et al., 2013; Barnes et al., 2015). In order to test whether synaptic plasticity is impaired in the hippocampus of *Gprasp2* KO mice, we performed mGluR dependent LTD protocol (Fig. 13a). Interestingly, we found that DHPG-induced LTD was markedly increased in the hippocampus of *Gprasp2* KO mice compared to WT (Fig.13b-c).

To further investigate functional circuitry deficits caused by *Gprasp2* deletion, we examined electrophysiological properties of GPRASP2 mice by performing extracellular field recordings at the Schaffer collateral CA3–CA1 synapse in acute hippocampal slices. We also determined paired-pulse ratio (PPF) between WT and *Gprasp2* KO mice (Fig.13 d) and did not find alterations, suggesting that there is no overt presynaptic dysfunction in *Gprasp2* KO mice.

Taken together, we demonstrate that mice lacking GPRASP2 showed memory impairment, social deficits and dysfunction in mGluR-dependent plasticity in the hippocampus, all features present in ASD and ID.

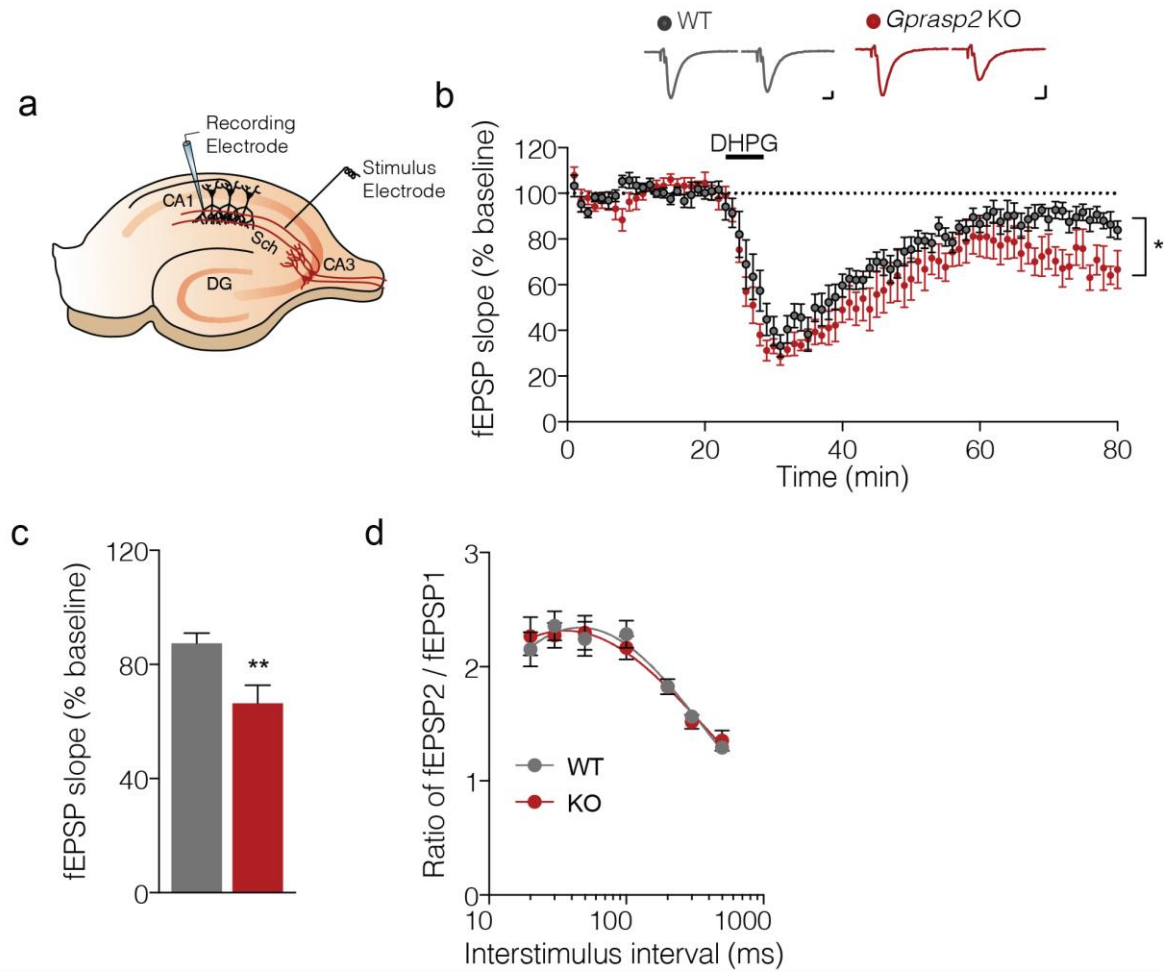

Figure 13 | *Gprasp2* KO mice exhibit enhanced mGluR-dependent LTD. (a) Schematic diagram of the mouse hippocampal slice preparation, demonstrating the CA1 and CA3 regions as well as the dentate gyrus (DG) and Schaffer collateral (SC) as well as typical electrode placements. (b) Time-course of fEPSP slope; normalized to baseline from WT (gray) or KO mice (red), and DHPG stimulation (100 μM for 5 minutes); scale bar, 0.2 mV, 20 ms. (c) Quantification of change in fEPSP slope following DHPG stimulation and showing the average responses for the last 5 minutes in control and *Gprasp2* KO mice. (d) Paired-pulse ratio across varying inter-stimulus intervals in *Gprasp2* KO mice compared with WT mice; (WT n = 11 slices, from 7 animals; *Gprasp2* KO n = 7 slices from 7 animals). All values represent as mean ± SEM. Two-way repeated measures ANOVA for (b and d), Mann-Whitney's U–test for (c), *p<0.05, **p<0.01 and ***p<0.001.

3.3.10. GPRASP2 regulates surface trafficking of mGluR5 receptors

Previous studies have shown that activation of mGluRs by DHPG lead to a significant and long-last shrinkage and eliminations of spines as a consequence of induction of mGluR-LTD (Ramiro-Cortés and Israely, 2013). Importantly, defects in dendritic spine morphology were associated with dysregulation in LTD in multiple mouse models for ASD and ID (Huber et al., 2002b; Auerbach et al., 2011; Santini et al., 2013). Our data suggests that GPRASP2 plays

a significant role in the regulation of spine and dendritic morphology, and we hypothesized that GPRASP2 might be involved in regulation of mGluRs

To further validate the role of *Gprasp2* in mGluR-dependent LTD, we evaluated the role of GPRASP2 on mGluR5 trafficking in primary cultured hippocampal neurons. We again turned to transfected neurons with GFP or GFP-GPRASP2 and introduced DHPG (100μM for 30 min) to induce internalization of the receptors (Fig. 14 a,b). In the absence of DHPG, overexpression of GPRASP2 decreased the mGluR5 fluorescent cell surface signal by (23±4.57%) compared with the GFP-expressing neurons.

Next, we asked whether manipulation of GPRASP2 expression could have a global effect on group 1 mGluRs (mGluR1&5). We found that overexpression of GPRASP2 shows similarly remarkable decrease on total mGluR1&5 puncta in the presence of DHPG only (Fig. 14e). These results could suggest that manipulation of GPRASP2 expression not only altered mGluR5 surface expression but also had an effect on total mGluR1&5 receptors levels.

Due to the potential effect of GPRASP2 on surface availability of mGluR5 and total mGluR1&5 levels, we hypothesized that the reduction of GPRASP2 levels might have an opposite effect of mGluRs trafficking. We found that knockdown of GPRASP2 increased surface mGluR5 clusters by 28±3.0%, however when DHPG was added the change compared to basal conditions was of 20%±3.51 (Fig. 14d) suggesting that in when GPRASP2 is knockdown, the agonist is no longer able to trigger receptor internalization.

At the same time, reduction in GPRASP2 levels induced a significant increase in the total mGluR1&5 receptors (Fig. 14f). Interestingly, activation of mGluRs by DHPG mediated a decrease in surface mGluR5 in control conditions (both GFP and scramble expressing cells), an effect that is consistent with agonist-mediated internalization of the receptors when GPRASP2 is present within normal basal levels (Fig. 14c&e).

Our results suggest that overexpression of GPRASP2 is sufficient to occlude DHPG mediated internalization. Conversely, endogenous GPRASP2 is necessary for this process, since knockdown of the endogenous protein prevents DHPG mediated internalization of the receptors.

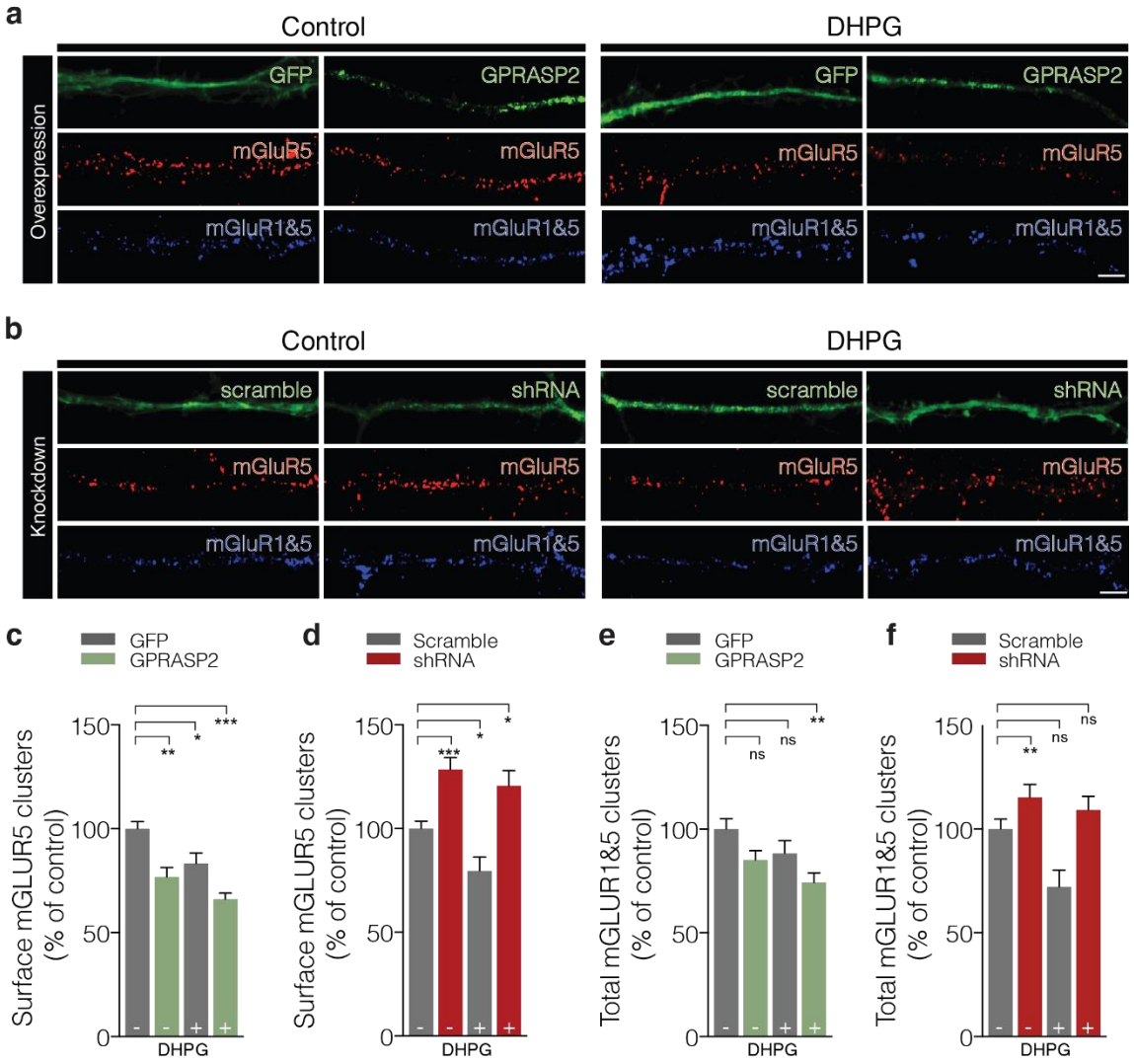

Figure 14 |GPRASP2 regulates mGluR5 surface expression in primary cultured hippocampal neurons. (a) Hippocampal neurons were transfected with either GFP or GFP-GPRASP2 in presence or absence of DHPG. (b) Hippocampal neurons were transfected with either Scramble or shRNA in presence or absence of DHPG. mGluR5 surface expression was visualized with rabbit mGluR5 N-terminus antibodies under non-permeabilizing conditions. Total mGluR1&5 expression was visualized with mouse mGluR1&5 antibodies under permeabilizing conditions. Neurons were analyzed for the surface mGluR5 cluster number (c-e) and for the mGluR1&5 synaptic cluster number (d-f) per dendritic length. Results are expressed as % of control cells for GPRASP2 overexpression versus GFP control or shRNA versus scramble; n= 21-45 per condition, from four independent experiments. The statistical comparisons performed were One-way ANOVA test followed by Tukey's multiple comparisons test. Data are presented as means ± SEM. *p<0.05, **p<0.01, ***p<0.001. Scale bar 2 μm.

3.4. Discussion

Upregulation of mGluR5 activity has been associated with ID and autism in FXS (Dölen et al., 2007; Zoghbi and Bear, 2012b). Previous studies also showed that dysregulation of LTD is a consistent observation in various mouse models of autism (Auerbach et al., 2011; Santini et al., 2013; Piochon et al., 2014; Zhang et al., 2015). Here we demonstrate that genetic deletion of *Gprasp2* promotes enhanced LTD in the CA1 region of the hippocampus, which mimics phenotype in the *Fmr1* gene. We were interested in investigating the possibility that *Fmr1* and *Gprasp2* mutations might share pathophysiology in terms of mGluR5 signaling dysfunction. First, mGluR5 and GPRASP2 are highly expressed in the hippocampus, where this receptors plays an important role in the regulation of synaptic plasticity. Second, *Gprasp2* KO mice manifested cognitive impairment in the novel object recognition test and social interaction tests, which is reminiscent to the pathophysiology of ASD and ID (Ventura et al., 2004).

Our results support the hypothesis that dysfunction in the synapse (in synapse formation and plasticity) and dendritic arborization are major contributing factors to ID and ASD. Defects in dendritic spine morphology have been consistently found in several mouse models of ID and ASD genes (Bateup et al., 2011; Peça et al., 2011; Clement et al., 2012; Williams et al., 2015). In the present work, we found that manipulation of GPRASP2 expression affected spine and dendritic morphology. GPRASP2 knockdown resulted in reduced dendritic spine density and reduced dendritic arborization, while GPRASP2 overexpression caused the opposite results (i.e. higher density of spines, more dendritic branching), suggesting that fine-tuned expression of GPRASP2 is necessary for the formation and maturation of dendritic spines during brain development. Interestingly, and in accordance with our results, GPRASP3 (p60TRP) overexpression was previously shown to increase dendritic arborization in the hippocampus and cortex (Mishra and Heese, 2011) suggesting a common role for GPRASP family in regulating neuronal morphology.

We found that changing levels of GPRASP2 in hippocampal neurons directly affects mGluR5 surface levels. Overexpression of GPRASP2 worked synergistically with DHPG stimulation to reduce surface levels of mGluR5. These results are in accordance with the subcellular localization of GPRASP2 in clathrin-coated endocytic vesicles and early endosome compartments (Supplementary fig. 4).

We characterized the expression profile of GPRASP2 by evaluating its developmental profile and differential expression in the brain. We found that the GPRASP2 is expressed from

early development, peaking at P15, then decreased gradually, which is consistent with the emerging premise that dysfunction in ASD-related mechanisms occur during early development.

At the behavioral level, we found that *Gprasp2* KO mice exhibited reduced anxiety-like behavior during exposure to the open field (OF) and elevated plus maze (EPM). Similar to our findings, decreased anxiety was also a common feature across several genetic animal models of ASD such as *Fmr1* (Peier et al., 2000; Eadie et al., 2009), *Mecp2* (Pelka et al., 2006), *Va1R* (Bielsky et al., 2005) and *IL1RAPL1* (Yasumura et al., 2014). Additionally, the decreased marble burying in *Gprasp2* KO mice could be interpreted as decreased anxiety-like behavior which is consistent with our data in OF and EPM. The high expression profile of GPRASP2 in various hypothalamic nuclei, as well as LSN, could pinpoint the role of GPRASP2 in anxiety related circuits. In addition to reduced anxiety, *Gprasp2* KO mice showed hyperlocomotion activity in three chambered test, a phenotype that was also seen in *IL1RAPL1* KO mice model for ASD (Yasumura et al., 2014).

Impairments in social interaction are a core clinical phenotype of individuals with ASD. We found that *Gprasp2* KO displayed impaired nesting, a social behavior dysfunction constantly observed in *Tsc1* (Goorden et al., 2007), *Nlgn1* (Etherton et al., 2009) and *Neuroligin1* mutant mice (Blundell et al., 2010). Additionally, the decreased preference for the novel stranger in three chambered test could highlight an impairment in social recognition in *Gprasp2* KO similar to several ASD mice models such as mutations in *Shank3* (Peça et al., 2011), *Nlgn4* (Jamain et al., 2008), *Pten* (Kwon et al., 2006) and *Mecp2* (Gemelli et al., 2006). Moreover, *Gprasp2* KO displayed increased non-reciprocal social interaction in social dyadic test demonstrating that genetic ablation of *Gprasp2* interferes with the social interaction with conspecific animals as is seen in *Shank3* mutant mice (Wang et al., 2011). Taken together, our data show that loss of function of *Gprasp2* results in abnormal social behavior, a common phenotype described in several ASD mice models such as *Mecp2*, *Shank1/2/3*, *Fmr1*, *Pten*, *Nlgn3/4*, *Oxt*, *Tsc1/2* (de la Torre-Ubieta et al., 2016). However, the circuitry dysfunctions underlying these social abnormalities remain to be elucidated.

It is reasonable to assume that multiple brain functions are affected by the mutation in this gene. However, it remains to be examined how neural circuits responsible for these mental disorders are mainly affected by *GPRASP2* mutations. Identifying the precise circuit and mechanism underlying social abnormalities in *Gprasp2* KO mice would help develop a therapeutic target for the social deficits that occur in individuals with ASD.

Collectively, the current study provides insight into the profile of GPRASP2 during brain development; demonstrates that *Gprasp2* KO recapitulate several synaptic and behavioral deficits seen in autism and ID and offers a novel mechanistic link between mGluR5 trafficking and GPRASP2 that may elucidate the molecular basis underlying various types of neurodevelopmental disorders.

3.5. Supplementary figures and tables

Supplementary table 1| Expression of GPRASP2 mRNA of coronal mouse brain sections from P15 old mice

	GPRASP2 mRNA
mPFC	+
Cortex	
▪ Layer I	+/-
▪ Layer II/III	+
▪ Layer IV	+
▪ Layer V	++
▪ Layer VI	++
Hippocampus	
▪ CA1	+++
▪ CA3	++
▪ Dentate Gyrus	++++
Cerebellum	++
Olfactory bulb	++
Hypothalamus	
▪ paraventricular nucleus	++++
▪ posterior hypothalamic nucleus	++++
▪ ventromedial nucleus of the hypothalamus	+++
▪ Arcuate nucleus of the hypothalamus	+++
▪ Zona incerta	+++
Thalamus	
▪ Thalamic reticular nucleus	++++
▪ paraventricular nucleus of the thalamus	++++
▪ parafasicular nucleus of the thalamus	+++
Medial habenula	++
Striatum	
▪ Dorsal region	+/-
▪ Ventral region	+
Lateral Septum region	++++
Amygdala	++

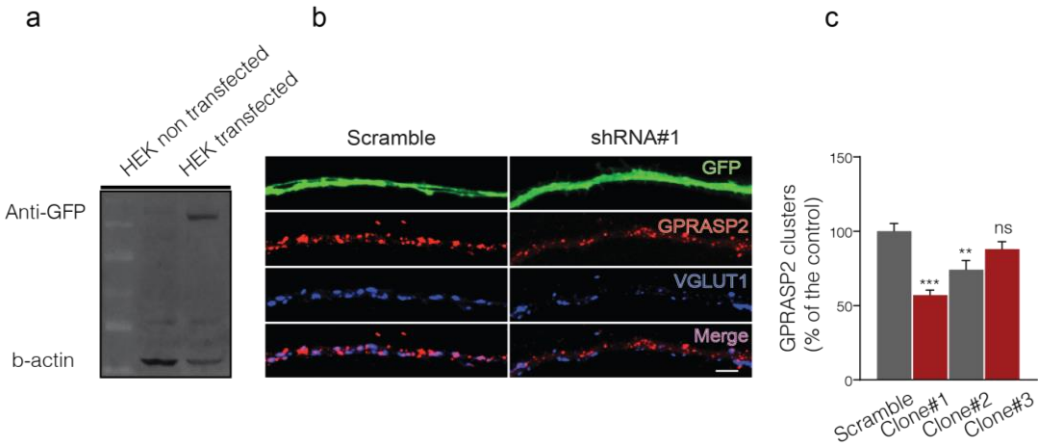

Supplementary figure 1 | Validation of GPRASP2 overexpression and knockdown constructs (a) Anti-GFP antibody detect a band around 130 KD for overexpression GPRASP2 in HEK cells. (b) Endogenous GPRASP2 knockdown in hippocampal neuronal culture using commercially available RNA interference (shRNA) for mouse GPRASP2. Cultured hippocampal neurons were transfected at P10 with scramble shRNA (Scramble) and different clones for shRNA GPRASP2, immunostained for GPRASP2, VGLUT1 and analyzed at P15. (c) Neurons were analyzed for the GPRASP2 clusters number. (b) Results are expressed as % of scramble cells; (n=20 for scramble, n= 30 for clone 1, n= 17 for clone 2 and n= 15 for clone 3) from three independent experiments. The statistical comparisons in (c) were performed using One way ANOVA test (*p<0.05, **p<0.01, ***p<0.001) followed by Tukey's multiple comparisons test. Data are presented as means ± SEM. Scale bars represent 2 μm

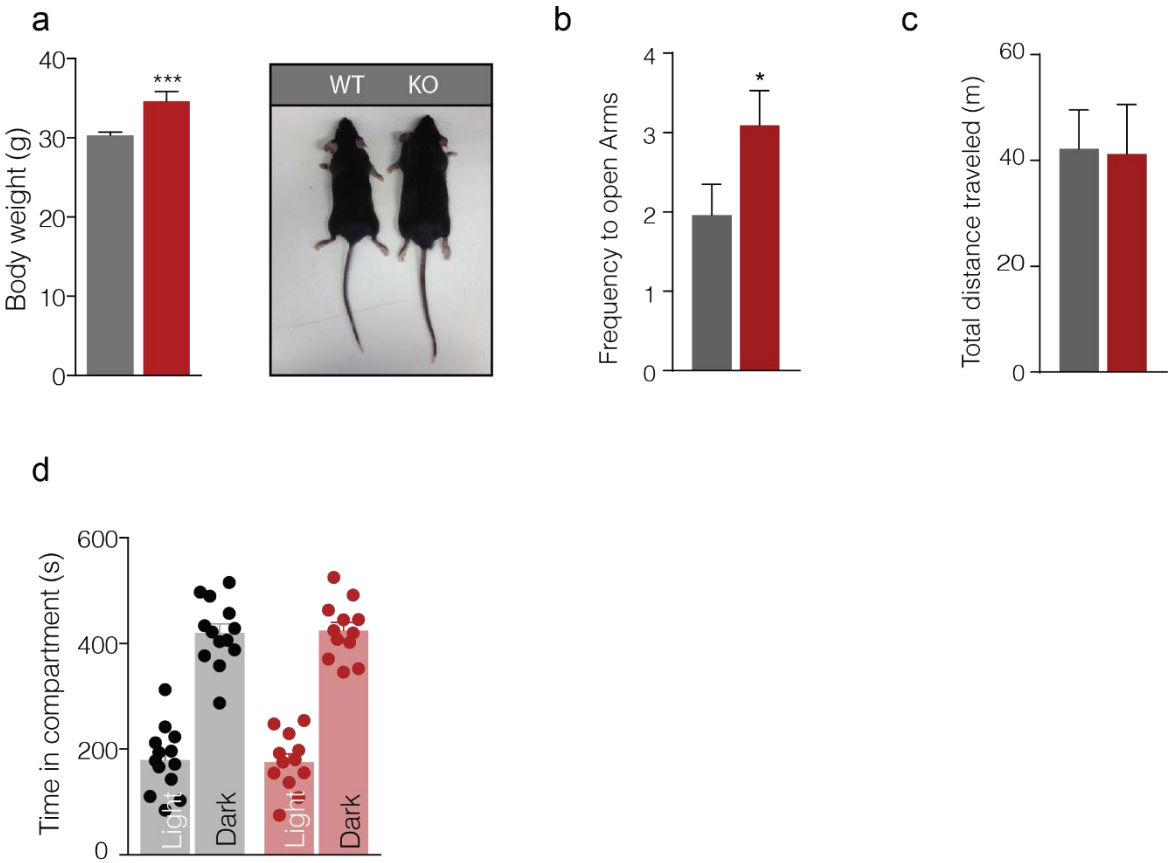

Supplementary figure 2 | Body weight and anxiety behavior in *Gprasp2* KO. (a) Left, quantification of body weight in KO compared to WT mice. Right, 5-month old male KO mouse compared with WT; WT, n = 13; *Gprasp2* KO, n = 13. (b-c) Analysis of elevated plus maze test. (b) Frequency to enter the open arm. (c) Total distance travelled during 5 minutes in the elevated plus maze; WT n = 25; *Gprasp2;* KO n = 23. (d) Anxiety assessment in dark-light box emergence test; WT n = 13; *Gprasp2* KO n = 12. Mann-Whitney test *p<0.05, **p<0.01, ***p<0.001. Data are presented as means ± SEM

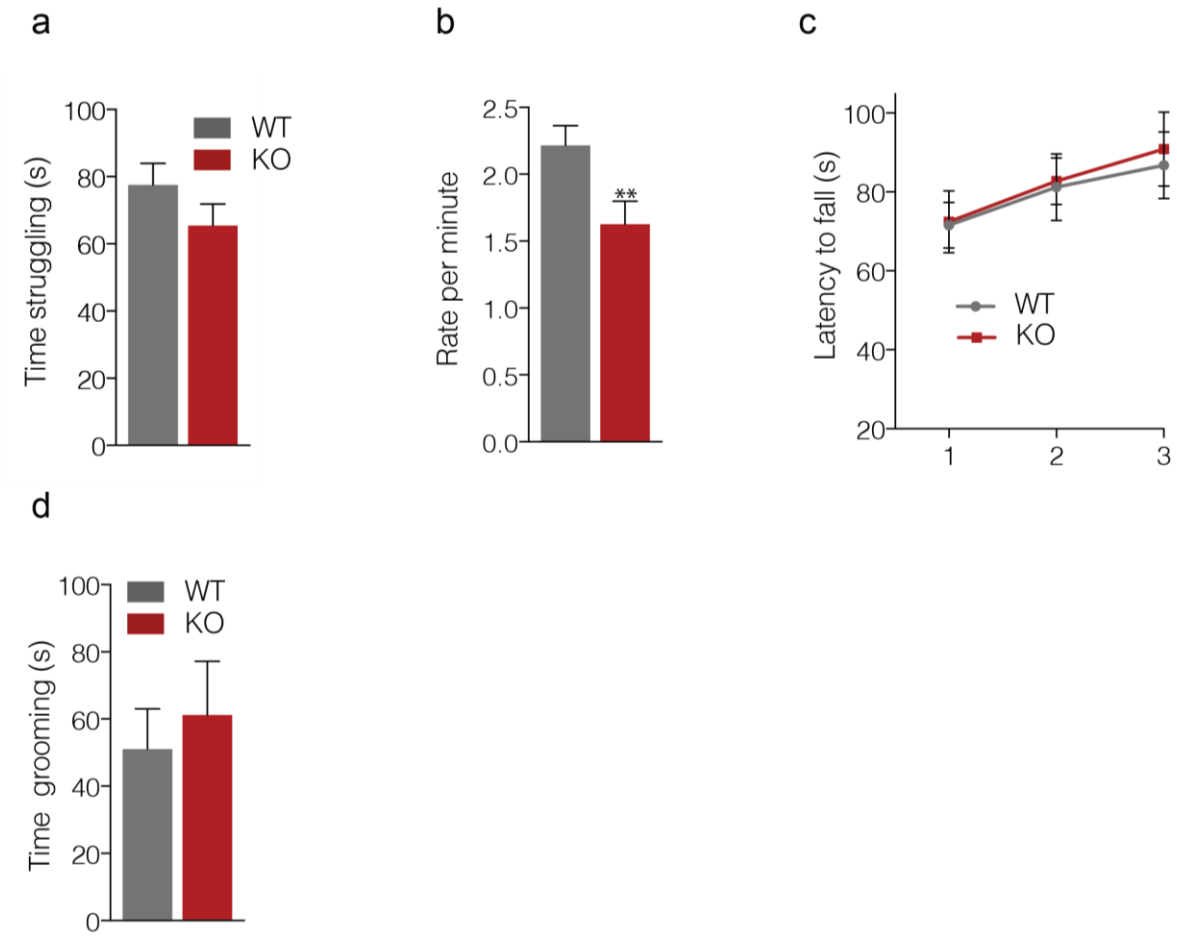

Supplementary figure 3 | Depression, grooming and motor leaning behavior in *Gprasp2* KO. (a-b) Performance of WT and KO in forced swimming test; WT n = 25; *Gprasp2* KO n = 24. (a) Time spent struggling, (b) rate per minute in the forced swimming test. (c) Performance of WT and KO in the rotarod test; (WT, n = 10; *Gprasp2* KO, n = 10). (d) Time spent grooming in sucrose splash test; WT, n = 10; *Gprasp2* KO, n = 10. Mann-Whitney test *p<0.05, **p<0.01, ***p<0.001. Data are presented as means ± SEM

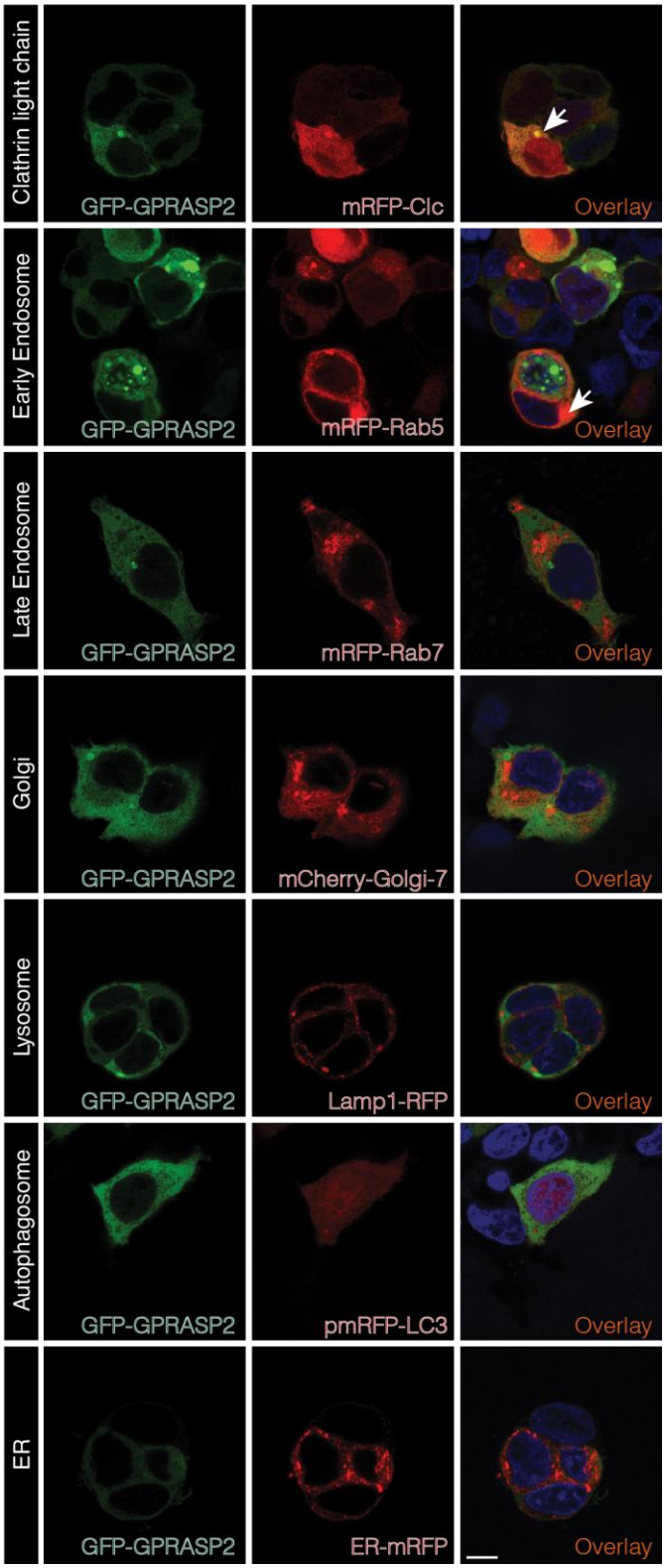

Supplementary figure 4 | Subcellular localization of GPRASP2. HEK cells were co-transfected with GFP-GPRASP2 and either (a) Clathrin light chain marker (mRFP-Clc), (b) Early endosome (mRFP-Rab5), (c) Late endosome marker (mRFP-Rab7), (d) Golgi marker (mcherry-Golgi-7), (e) Lysosome marker (Lamp1-RFP), (f) Autophagosome marker (pmRFP-LC3) or (9) ER marker (ER-mRFP). Arrow shows point of overlap with clathrin light chain and Rab5 markers. Scale bars 10 μm.

Chapter 4 | General discussion and future directions

4.1. Expression profile of GPRASP2 in the mouse brain

Recently, *GPRASP2* has been associated with the etiology of ASD (Piton et al., 2011; Zhou et al., 2014; Butler et al., 2015). However, the role of GPRASP2 in the development of proper neuronal circuitry in the mammalian CNS, and how changes in its expression can potentially contribute to neurological dysfunction remains unclear. Previous reports have shown that proteins of the GPRASP family are predominantly expressed in the CNS (Abu-Helo and Simonin, 2010), however, the expression profile of GPRASP2 is not characterized. Analyzing the expression profile of ASD-associated genes can help disclose the role of candidate genes in psychiatric disorders and understand which circuits are most likely affected by its dysfunction. Strong labeling of GPRASP2 mRNA was found in the lateral septum, a key component of the limbic system that has been connected to several behavioral traits including social behavior (Ophir et al., 2009), anxiety-related behaviors (Le Merrer et al., 2006; Singewald et al., 2011) and contextual fear conditioning (Reis et al., 2010). Both sagittal and coronal P15 sections revealed high expression of GPRASP2 at discrete thalamic nuclei including the TRN (thalamic reticular nucleus), a region enriched in GABAergic neurons and involved in several disease related functions, such as attention and arousal (Halassa et al., 2014; Lewis et al., 2015). Dysfunction of the TRN was previously associated with epilepsy (Huguenard and McCormick, 2007), schizophrenia (Ferrarelli and Tononi, 2011), attention deficits and hyperactivity (Wells et al., 2016). However, the current study lacks specific behavior assays that are relevant to thalamic function.

One interesting finding was the strong local enrichment of GPRASP2 in the hypothalamus, leading us to speculate that GPRASP2 may play an important role in several hypothalamic functions, such as control of circadian rhythms, body weight, appetite, aggression and sexual behaviors. Coronal sections of P15 mice revealed strong GPRASP2 expression in discrete nuclei, especially the ventromedial nucleus of the hypothalamus (VMH) a distinct morphological nucleus which has been linked to control of aggression during social behavior (Falkner et al., 2014). Furthermore, GPRASP2 is highly expressed in the arcuate nucleus of the hypothalamus (ARH) that controls food intake and energy through coordination between POMC and AGRP neurons (Sohn, 2015). Consistent with this, G*prasp2* KO displayed marked increased in body weight at approximately 5 months, and preliminary results from our lab showed also that KO mice exhibit dominance-like behavior in the tube test (Marta Pereira, personal communication), suggesting a potential aggressive behavior in those mice. Collectively, these findings could suggest that GPRASP2 deletion is associated with hypothalamic dysfunction.

4.2. The role of GPRASP2 in spine and dendritic morphology

Several studies have suggested that spines and dendritic branches are key regulators of neuronal function and crucial for the plasticity of neuronal circuits (Holtmaat and Svoboda, 2009; Jan and Jan, 2010). In several neurodevelopmental disorders, such as ID and ASD, neurons exhibited deficiencies in spine morphology and neuronal complexity which can correlate with behavioral and intellectual deficits (Auerbach et al., 2011; Durand et al., 2012; Valnegri et al., 2012). In this work, we showed that GPRASP2 regulates dendritic arborization and neuronal morphology. *In vitro*, overexpression of GPRASP2 in hippocampal neurons led to an increase in dendritic length and complexity whereas neurons lacking GPRASP2 showed smaller and less complex dendrites, characteristic of neuronal hypotrophy. Furthermore, our results suggest that overexpression of GPRASP2 in hippocampal neurons increases the number of excitatory synapses (manifested by global changes in PSD-95 and VGLUT1 clusters) and dendritic spines, while GPRASP2 reduction attenuated the number of excitatory synapses and spines. Importantly, GPRASP2 overexpression altered the ratio of immature-to-mature spines suggesting that GPRASP2 is important for regulation of spine maturation. Taken together, overexpression and knockdown of GPRASP2 elicited oppose mechanisms in excitatory synapses, strongly suggesting that an appropriate balance of GPRASP2 expression is crucial for synapse function. Interestingly, in accordance with our results, GPRASP3 (p60TRP) overexpression increased dendritic arborization in the hippocampus and cortex *in vivo* (Mishra and Heese, 2011) suggesting a role for GPRASP family in regulating neuronal morphology. Importantly, defects in dendritic spine morphology were consistently observed in several mouse models of ID and ASD (Belichenko et al., 2004; Peça et al., 2011; Tang et al., 2014). Considering the high expression profile of GPRASP2 in different brain regions, it would be interesting to further assess the morphological and functional consequences of GPRASP2 deletion *in vivo*. Still, an open question remains whether the genetic deletion of GPRASP2 will have a similar effect to GPRASP2 knockdown *in vitro* and, if confirmed, what is the molecular pathway through which GPRASP2 regulates spine morphology.

Previous studies have shown that activation of mGluRs by DHPG lead to a significant and long-lasting shrinkage and elimination of spines as a consequence of induction of mGluR-LTD plasticity (Ramiro-Cortés and Israely, 2013). To test this, we performed electrophysiological recordings and demonstrated that GPRASP2 KO mice exhibited increased mGluR-dependent LTD following DHPG stimulation suggesting that GPRASP2 is an essential component for mGluR-dependent LTD. Based on the above-mentioned results, we could

speculate that GPRASP2 deletion in CA1 regions of the hippocampus might lead to spine alterations based on its role in regulating mGluR-dependent LTD.

In the current study, we showed that manipulation of GPRASP2 expression in hippocampal neurons altered excitatory synapse formation manifested by global changes in PSD-95 and VGLUT1 clusters (marker for excitatory synapse), however little is known about the role of GPRASP2 in inhibitory synapses. It will be interesting to understand whether GPRASP2 function is restricted only to the excitatory synapse or it has other potential roles in maintaining excitation /inhibition balance in hippocampal circuit. Moreover, the striking effect of GPRASP2 in spine rearrangement suggests a possible crosstalk between GPRASP2 and other signaling proteins that regulate actin cytoskeleton organization, such as members of the family of small Rho GTPases (RhoA, Rac, and Cdc42), which play a major role in the structure and function of dendrites and spines (Hotulainen and Hoogenraad, 2010).

4.3. GPRASP2 regulates the surface trafficking of mGluR5 receptors

The best-characterized post-endocytic sorting of GPCRs to the lysosome, involves the ESCRT (endosomal sorting complex required for transport) machinery (Emr, 2008). Previous evidence also highlighted endosomal sorting machinery that is independent of the ESCRT pathway and instead involves GPCRs downregulation through binding of partners to cytoplasmic tails without the need for ubiquitination. GPRASPs are one example of these proteins that modulate the trafficking of several GPCRs to the lysosomes via direct interaction with the receptors (Whistler et al., 2002). GPRASP1 has been shown to regulate the lysosomal degradation of delta opioid, dopamine D2, and bradykinin 1 receptors (Moser et al., 2010).

Previous studies showed that clathrin-mediated endocytosis of postsynaptic receptors occurs in the proximity PSD (Blanpied et al., 2002; Rácz et al., 2004). Several reports have highlighted that disruption of endosomal pathways affects the morphogenesis of dendritic spines (Park et al., 2006; Jia et al., 2014). The localization of GPRASP2 in the PSD in addition to its role in the regulation of spine morphology suggests its functions in the endocytosis and sorting of postsynaptic receptors. Our data also indicate that GPRASP2 colocalize with Rab5, a protein involved in the transportation of cargo to early endosomes, demonstrating that GPRASP2 is localized in the vicinity of partners involved in endosomal trafficking. Importantly, several studies point towards the role of Rab5 in mediating the trafficking of proteins from the plasma membrane to early endosomes via clathrin-mediated endocytosis (de Hoop et al., 1994; Lakadamyali et al., 2006).

Consistent with this, our co-localization analysis of GPRASP2 in HEK cells revealed a strong overlap between GPRASP2 and clathrin light chain marker, futher suggesting a potential role of GPRASP2 in the early steps of endocytosis. Taken together, we can speculate that GPRASP2 mediates the trafficking of GPCRs to endosomes and their consequent lysosomal degradation, hence decreasing their surface expression. However, under basal condition, we did not observe strong colocalization of GPRASP2 with the lysosomal marker (LAMP1), which could suggest that mobilization of GPRASP2 occurs only after agonist-mediated activation of GPCR.

Indeed, mGluR endocytosis and intracellular trafficking are crucial to mGluR function (Collingridge et al., 2004). This process is dependent on β-arrestin-, dynamin- and clathrin-mediated endocytosis (Dhami and Ferguson, 2006). Like most GPCRs, mGluRs interact with receptor-selective partners that mediate GPCR signaling and trafficking to specific cellular locations (Ritter and Hall, 2009). Calmodulin (CaM) and Siah-1A are examples of mGluR5 binding proteins that have been identified to have a crucial role in the regulation of mGluR5 expression at the cell surface (Lee et al., 2008; Ko et al., 2012). Manipulation of Siah-1A in hippocampal neurons increased endosomal trafficking and lysosomal degradation of mGluR5 in a CaM- dependent manner (Ko et al., 2012). In line with this, disruption of Caveolin-1 (a key adaptor protein that co-localizes with mGluR1/5 receptors) binding to mGluR1, enhances mGluR1 internalization through clathrin-independent endocytosis (Francesconi et al., 2009).

Like most of the GPCRS, once mGluR5 receptors internalize they are either dephosphorylated in the endosomal compartment and rapidly recycled to the cell surface or they are sorted to the late endosomal/lysosomal pathway for degradation. *In vitro*, overexpression of GPRASP2 in hippocampal neurons decreases surface levels of mGluR5 and DHPG stimulation in these conditions accelerates receptor internalization, functioning as a synergistic mechanism. These results are in accordance with the subcellular localization of GPRASP2 in clathrin-mediated endocytic vesicles and early endosome compartments. Therefore, we propose two possible scenarios for the role of GPRASP2 in mGluR5 trafficking. First, GPRASP2 can potentially trigger the receptor for lysosomal degradation and second, the receptors can be retained in endosomal compartments to be recycled to the cell surface. The effects of knocking down endogenous GPRASP2 solidifies our hypothesis, since the loss of GPRASP2 increases the surface levels of mGluR5 both in the presence and absence of DHPG, suggesting that GPRASP2 is necessary for agonist-stimulated mGluR endocytosis.

The present study sheds light on a novel role of GPRASP2 as an endosomal sorting protein and as a regulator of mGluR5 trafficking in cultured hippocampal neurons. However, it remains unclear if GPRASP2 is also involved in the trafficking of other GPCRS. Indeed, data from Heydorn *et al.*, 2004 showed that GPRASP family bind to various GPCR cytoplasmic tails, and some of the receptors also linked to neuropsychiatric disorders such as oxytocin (Wu et al., 2005; Tost et al., 2010; LoParo and Waldman, 2015), muscarinic (Langmead et al., 2008) and dopamine receptors(Yan et al., 2017). Understanding mechanisms controlling GPCR signaling and trafficking is essential for the development of new pharmacological strategies for neurodevelopment diseases.

4.4. *Gprasp2* KO mice as an animal model for ASD and ID

Recent genetic and genomic studies have identified many candidate genes for ASDs that encode for synaptic proteins, indicating that synaptic dysfunction may play a critical role in these disorders. Using mouse molecular genetics, we generated a novel KO mouse model for *Gprasp2* to test the functional, cellular and behavioral consequences of disrupting this gene. *Gprasp2* KO mice displayed several phenotypes reminiscent of autism and ID-related behaviors, including memory impairment, hyperactivity, reduced anxiety and social abnormalities all of which can be related to brain regions where GPRASP2 is highly expressed and that can be associated with cellular and molecular modifications we identified in *Gprasp2* KO mice.

We observed that genetic deletion of *Gprasp2* altered synaptic plasticity in the hippocampus. Our results suggest enhanced mGluR5-dependent LTD in KO mice following DHPG stimulation, a common phenotype across several mouse models carrying mutations that cause human ASD and ID, including mutations in *Fmr1* (Huber et al., 2002b), *Syngap* (Barnes et al., 2015) and eIF4E (Santini et al., 2013) genes. This data is consistent with the role of GPRASP2 in mGluR5 trafficking in hippocampal neuronal cultures since the absence of GPRASP2 in presence or absence of DHPG interfered with the mGluR5 endocytosis and intracellular sorting resulting in the accumulation of receptors at the synapse which can be correlated with enhanced LTD. Importantly, our results are in agreement with the *in vivo* role of GPRASP1 in the endocytosis-dependent sorting of GPCRs (Boeuf et al., 2009).

The electrophysiological results in the current study elucidate a shared function between GPRASP2 and FMRP in terms of regulation of mGluR5 receptors that is necessary to maintain hippocampal synaptic plasticity. Impairment of long-lasting synaptic plasticity is the molecular basis underlying FXS (Bear et al., 2004). Similarly to our results, *Fmr1* KO mice showed

increased mGluR-induced LTD which led to a loss of synaptic contacts and memory impairment (Hou et al., 2006; Nosyreva and Huber, 2006). The high levels of GPRASP2 expression in the hippocampus may explain the prominent hippocampal defects found in GPRASP2 KO mice. Enhanced LTD could interfere with the establishment and maintenance of strong synapses required for normal brain function. However, it is still unclear if the enhanced mGluR LTD is due to the removal of AMPA receptors from synaptic sites, the direct elimination of spines, or a combination of both effects.

The learning and memory deficits observed in *Gprasp2* KO mice resemble features of ID and ASD related conditions such as Rett and FXS syndromes (Bakker et al., 1994). Using electrophysiology and behavioral tests, we uncovered alterations in mGluR5 mediated synaptic plasticity and hippocampus-dependent learning that are also reminiscent of observations in mouse models of syndromic autism and ID (Auerbach et al., 2011).

Another characteristic feature of *Gprasp2* KO mice is reduced anxiety. This results are in accordance with several animal models of ASD which exhibited reduced anxiety levels, including *Mecp2* null mice (Pelka et al., 2006) *, vasopressin 1 receptor* (V1aR) KO (Bielsky et al., 2004), *IL1RAPL1* KO (Yasumura *et al.*, 2014) and *FmR1* KO mice (Eadie et al., 2009).

Additionally, the reduction in marble burying in GPRASP2 KO mice could be interpreted as decreased anxiety-like behavior, since the results are in accordance to the anxiolytic behaviors in EPM and OFT. The interpretations of marble burying as reflecting anxiety-like behaviors are based on the fact that benzodiazepines, antipsychotics, and selective serotonin re-uptake inhibitors decrease marble burying (Broekkamp et al., 1986; Bruins Slot et al., 2008). Repetitive behaviors in mice could be also associated with decrease marble burying and several ASD mouse models have been shown to present decreased marble burying based on repetitive behaviors (Moy et al., 2014; Sungur et al., 2014; Wurzman et al., 2015). Taken together, we speculate that the decreased marble burying behavior in *Gprasp2* KO might be connected to anxiety rather than repetitive behavior since deletion of *Gprasp2* did not affect grooming in the sucrose splash test. Interestingly, these behavioral phenotypes resemble features of Mecp2-related Rett syndrome (Pelka et al., 2006; De Filippis et al., 2014) and indeed, previous data supported our hypothesis showing that GPRASP1 is downregulated in *Mecp2* null mice (Urdinguio et al., 2008). Considering that both genes are encoded on the X chromosome, it would be interesting to explore if there is an additional link between *Gprasp2* and *Mecp2* mice and understand if the behavioral dysfunctions in both models share similar circuitry deficits.

Impairments in social interaction are the core clinical phenotype of individuals with ASD. To address whether loss of *Gprasp2* influences social behaviors, we tested hemizygous *Gprasp2* male mice in the three-chamber test. *Gprasp2* KO mice showed a trend for reduced voluntary social interaction and a strong impairment in the social recognition test. We also conducted the social dyadic test to evaluate social behaviors in a novel environment. Interestingly, our KO mice engaged in longer non-reciprocated social behaviors. Whenever *Gprasp2*KO mice initiate a social event, the stranger mice did not reciprocate and disengaged its partner. Interestingly, this particular phenotype was reported in Shank3 ΔDe4-22$^{-/-}$ mice (Wang et al., 2016b). Our results in the tube test (data not shown here) also showed increased social dominance behavior in *Gprasp2* KO mice. Collectively, the increased non-reciprocal social interaction along with social dominance behavior in the tube test could suggest an aggressive-like behavior in *Gprasp2* KO mice.

GPRASP2 is highly expressed in the lateral septum, a brain region marked by high expression levels of oxytocin and vasopressin 1A receptor which are crucial for social recognition and related social behaviors (Curley et al., 2012), we speculate that GPRASP2 disruption is this location may underlie some of the social abnormalities we observed. Interestingly, and similar to *Gprasp2* KO, mice lacking the vasopressin 1A receptor exhibit marked decrease in anxiety and profound impairment in social recognition (Bielsky et al., 2004).

Another possible explanation for the social abnormalities in *Gprasp2* Kos is the observed hypothalamic dysfunction. GPRASP2 mRNA *in situ* hybridization showed strong labeling in distinct hypothalamic nuclei including ARH, DMH, PH, and PVN. Recently, Peñagarikano *et al* showed that the dysregulation of oxytocin system in the PVN of the hypothalamus was responsible for social deficits in *Cntnap2* knockout mice (Peñagarikano *et al.*, 2015). Taken together our data show that loss of function of *Gprasp2* results in abnormal social behavior, a common phenotype described in several ASD mice model such as *Mecp2*, *Shank1/2/3*, *Fmr1*, *Pten*, *Nlgn3/4*, *Oxt*, *Tsc1/2* (de la Torre-Ubieta et al., 2016). However, the precise circuitry dysfunctions underlying these social abnormalities remains to be elucidated.

In addition to the social abnormalities observed in the three chamber and social dyadic tests, male *Gprasp2* KO mice showed disruption of home cage behavior since they did not engage in normal nesting behavior, a phenotype correlated with impaired social behavior (Moretti et al., 2005; Blundell et al., 2010; El-Kordi et al., 2013; Lang et al., 2013) and linked to hyperactivity (Ballard et al., 2002; Fox et al., 2013) . The striking difference between *Gprasp2* KO mice and their WT littermates in nest building were also reported in multiple ASD mice

models include *neurexin1a* (Etherton et al., 2009), neuroligin-1 (Blundell et al., 2010), *Pten* (Kwon et al., 2001) and *Tsc1* (Goorden et al., 2007). In the rotarod test, *Gprasp2* KO did not show any significant difference with respect to WT mice suggesting that the reduction in nest building is due to social behavior deficits rather than motor impairments.

Although *Gprasp2* KO mice exhibited normal locomotor activity in the open field test and elevated plus maze, analysis of the three-chamber test revealed increased locomotor activity in sociability and social recognition sessions, suggesting there is hyperactivity related to social exploration. Hyperactivity in general is also seen in other animal models of ASD such as *Cntap2* $^{-/-}$ (Peñagarikano et al., 2015), *Shank2* $^{-/-}$ (Won et al., 2012) and *Fmr1* KO mice (Bakker et al., 1994). Of particular interest, *IL1RAPL1* KO mice demonstrated also a similar pattern of hyperactivity during social events (Yasumura et al., 2014). Indeed, the hyperactivity in the three-chamber test could also explain the increased non-reciprocal interaction in the social dyadic test. *Gprasp2* KO mice spent more time following and tracking the WT partner and the latter disengaged by either ignoring or escaping. We can interpret this hyperactivity as a lack of inhibition control, a unique function of the thalamus, or increase aggressive behavior. The thalamic reticular nucleus (TRN) is a bundle of GABAergic neurons that provides the major inhibitory input to thalamocortical neurons (Pinault, 2004) and dysfunction in this circuit was associated with hyperactivity and attention deficits in *Ptchd1* mice (Wells et al., 2016). Our *in situ* hybridization analysis revealed strong expression of GPRASP2 in this region, especially in the TRN. It will be interesting to understand the role of GPRASP2 in TRN using our conditional *Gprasp2* KO mouse and test this hypothesis with functional studies, including electrophysiology measurements in the brain regions involved in regulating the abnormal behaviors.

4.5. Synaptic changes in response to *Gprasp2* deletion

Recent evidence have highlighted impairments in Homer-mGluR interaction in ASD mice models (Guo et al., 2016; Wang et al., 2016b). *Shank3* ΔDe4-22$^{-/-}$ mice displayed abnormal expression of Homer1b/c and mGluR5 proteins in striatal neurons, but not neocortex and hippocampus (Wang et al., 2016b). In this context, it would be interesting to assess whether genetic perturbation of *Gprasp2 in vivo* could affect mGluR5-homer interaction. If confirmed, disruption of homer-mGlu5 scaffolds could be responsible for the cognitive and synaptic plasticity dysfunction in our model, similarly to *Fmr1*$^{-/y}$ mice (Ronesi et al., 2012).

Dysregulation of LTD in our animal model was one of the striking phenotypes that suggested impairment in hippocampal synaptic plasticity and possible dysfunctions in signaling pathways downstream of mGluR5. In this context, it would be interesting to explore the functional sequences of *Gprasp2* deletion in the PI3K/Akt/mTOR pathway, since mutations in *Pten* or *Tsc1/2* resulted in exacerbation of its activation related to ASD-related behaviors, tuberous sclerosis and macrocephaly (Kelleher and Bear, 2008; Huber et al., 2015).

4.6. *Gprasp2* mutations and obesity

Several reports have linked obesity to neuropsychiatric disorders (Curtin et al., 2005; Chouinard et al., 2016). Our preliminary results showed that after approximately 5 months, *Gprasp2* KO mice started to show an increase in body weight, however further investigation needs to elucidate whether the changes associated with GPRASP2 deletion are due peripheral metabolic impairments or with hypothalamic function. So far, the impact of *Gprasp2* on behavioral domains beyond feeding behavior has not yet been studied.

Similarly to *Gprasp2* KO mice, several genetic variants linked to ASD and schizophrenia also showed increases in body weight and obesity. Interestingly those variants coded for GPCRs such as oxytocin receptor (Nishimori et al., 2008), ADRB1 (Bachman et al., 2002) and ADRB2 (Soloveva et al., 1997). In 2004, Heydorn and colleagues (Heydorn *et al.*, 2004) observed that GPRASP family binds to the C-terminal motif of several GPCRs including the oxytocin receptor. It is worth noting that *Oxtr* KO mice showed social interaction deficits, aggression and dysfunction in body temperature control and those effects were related to hypothalamic dysfunction (Nishimori et al., 2008).

One possibility for the excessive weight of the mutant mice is that genetic ablation of *Gprasp2* could disrupt the hypothalamic hormonal balance and produce alterations in the expression of metabolic genes involved in the appetite regulating system, such as neuropeptide Y, leptin receptor, ghrelin receptor, or melanocortin receptors 3 and 4. Another interpretation is the disruption of hypothalamic circuits in the dorsomedial, ventromedial, paraventricular and arcuate hypothalamus. Since we developed a conditional mouse model, we could potentially study the role of GPRASP2 in this particular circuit by breeding Cre-expressing mouse lines that express Cre in specific hypothalamic neurons, such POMC-Cre in the arcuate nucleus (Padilla et al., 2012), or alternatively, perform local viral delivery of Cre recombinase.

4.7. Future directions

Several lines of evidence point towards the implication of mGluRs in the pathology of ASD, however, the molecular and cellular pathways regulating these receptors under disease conditions are poorly understood. Aligned with the idea of targeting downstream mediators and proteins associated with mGluRs network, we propose that altered GPRASP2 expression may provide a mechanistic tool to understand the molecular basis of ASD where mGluR dysfunction is more prominent. Understanding the GPRASP-mGluR interplay may uncover new therapeutic candidates to correct deficits in synaptic plasticity and behavior relevant for ASD due to dysregulated mGluR signaling.

Interestingly, it has been shown that postnatal rescue of *Mecp2*, *Fmr1* and *Shank3* expression can correct several of the abnormalities seen in the mouse models for these disorders (Giacometti et al., 2007; Guy et al., 2007; Zeier et al., 2009; Guo et al., 2011; Mei et al., 2016). It would be interesting to see if genetic rescue of *Gprasp2* could correct the synaptic and behavior deficits in *Gprasp2* KO mice.

Another possible rescue approach is to focus on β-arrestin signaling pathway. β-arrestin targets many GPCR for internalization after phosphorylation through GPCR Kinase (Moser et al., 2010), but more recent data suggests β -arrestin2 mediates the mGlu5-stimulated protein synthesis in the hippocampus (Stoppel et al., 2017). We can speculate that GPRASP2 might interact with β-arrestin for receptor sorting or GPRASP2 and crosstalk on receptor mediated activation of signaling cascades.. Recently, it has been shown that genetic reduction of β-arrestin in *Fmr1*$^{-/y}$ correct exaggerated mGluR-LTD (Stoppel et al., 2017). Therefore, it would be interesting to understand if a similar phenomenon could occur for *Gprasp2*.

A key question in ASD research is how different cell types contribute to the symptoms and pathology of ASD. The advent of new genetic technologies, enables a precise temporal and spatial control of gene manipulation essential for the study of gene-circuit interfaces. It will be important to use *Gprasp2* conditional mice, and maximize this tool to explore cell-type specific effects and dissect what the neuronal circuit defects linked to specific behaviors. This will allow us to better understand how neurodevelopmental disorders progress from gene mutations, to neuronal changes, circuit dysfunction and finally, abnormal behaviors and cognition.

Chapter 5 | References

Abu-Helo A, Simonin F (2010) Identification and biological significance of G protein-coupled receptor associated sorting proteins (GASPs). Pharmacol Ther 126:244–250.

Ahlsen G, Gillberg IC, Lindblom R, Gillberg C (1994) Tuberous sclerosis in Western Sweden. A population study of cases with early childhood onset. Arch Neurol 51:76–81.

Ali IU, Schriml LM, Dean M (1999) Mutational spectra of PTEN/MMAC1 gene: a tumor suppressor with lipid phosphatase activity. J Natl Cancer Inst 91:1922–1932.

American Psychiatric Association (2013a) Diagnostic and Statistical Manual of Mental Disorders, 5th Edition. Diagnostic Stat Man Ment Disord 5th Ed:280.

American Psychiatric Association (2013b) Diagnostic and Statistical Manual of Mental Disorders, 5th Edition (DSM-5). Diagnostic Stat Man Ment Disord 4th Ed TR:280.

Ango F, Prézeau L, Muller T, Tu JC, Xiao B, Worley PF, Pin JP, Bockaert J, Fagni L (2001) Agonist-independent activation of metabotropic glutamate receptors by the intracellular protein Homer. Nature 411:962–965.

Auerbach BD, Osterweil EK, Bear MF (2011) Mutations causing syndromic autism define an axis of synaptic pathophysiology. Nature 480:63–68.

Bachman SE, Dhillon H, Zhang CY, Cinti S, Bianco CA, Kobilka KB, Lowell BB (2002) βAR Signaling Required for Diet-Induced Thermogenesis and Obesity Resistance. Science (80-) 297:843–845.

Backman SA, Stambolic V, Suzuki A, Haight J, Elia A, Pretorius J, Tsao MS, Shannon P, Bolon B, Ivy GO, Mak TW (2001) Deletion of Pten in mouse brain causes seizures, ataxia and defects in soma size resembling Lhermitte-Duclos disease. Nat Genet 29:396–403.

Bailey A, Le Couteur A, Gottesman I, Bolton P, Simonoff E, Yuzda E, Rutter M (1995) Autism as a strongly genetic disorder: evidence from a British twin study. Psychol Med 25:63–77.

Baio J (2014) Prevalence of autism spectrum disorder among children aged 8 years - autism and developmental disabilities monitoring network, 11 sites, United States, 2010. CDC Morb Mortal Wkly Rep Surveil Sum 63:1–21.

Bakker C, Verheij C, Willemsen R, van der Helm R, Oerlemans F, Vermey M, Bygrave a, Hoogeveen A, Reyniers E, De Boulle K, D'Hooge R, Cras P, van Velzen D, Nagels G, Martin J, De Deyn P, Darby J, Oostra B, Willems P (1994) Fmrl Knockout M ice : A Model to Study Fragile X Mental Retardation. Cell 78:23–33.

Ballard TM, Pauly-Evers M, Higgins G a, Ouagazzal A-M, Mutel V, Borroni E, Kemp J a, Bluethmann H, Kew JNC (2002) Severe impairment of NMDA receptor function in mice carrying targeted point mutations in the glycine binding site results in drug-resistant nonhabituating hyperactivity. J Neurosci 22:6713–6723.

Banerjee A, Luong JA, Ho A, Saib AO, Ploski JE (2016) Overexpression of Homer1a in the basal and lateral amygdala impairs fear conditioning and induces an autism-like social impairment. Mol Autism 7:16.

Barnes SA, Wijetunge LS, Jackson AD, Katsanevaki D, Osterweil EK, Komiyama NH, Grant SGN,

Bear MF, Nagerl U V., Kind PC, Wyllie DJA (2015) Convergence of Hippocampal Pathophysiology in Syngap+/- and Fmr1-/y Mice. J Neurosci 35:15073–15081.

Bartlett SE, Enquist J, Hopf FW, Lee JH, Gladher F, Kharazia V, Waldhoer M, Mailliard WS, Armstrong R, Bonci A, Whistler JL (2005) Dopamine responsiveness is regulated by targeted sorting of D2 receptors. Proc Natl Acad Sci U S A 102:11521–11526.

Basu SN, Kollu R, Banerjee-Basu S (2009) AutDB: A gene reference resource for autism research. Nucleic Acids Res 37.

Bateup HS, Johnson CA, Denefrio CL, Saulnier JL, Kornacker K, Sabatini BL (2013) Excitatory/Inhibitory Synaptic Imbalance Leads to Hippocampal Hyperexcitability in Mouse Models of Tuberous Sclerosis. Neuron 78:510–522.

Bateup HS, Takasaki KT, Saulnier JL, Denefrio CL, Sabatini BL (2011) Loss of Tsc1 in vivo impairs hippocampal mGluR-LTD and increases excitatory synaptic function. J Neurosci 31:8862–8869.

Baudouin SJ, Gaudias J, Gerharz S, Hatstatt L, Zhou K, Punnakkal P, Tanaka KF, Spooren W, Hen R, De Zeeuw CI, Vogt K, Scheiffele P (2012) Shared synaptic pathophysiology in syndromic and nonsyndromic rodent models of autism. Science 338:128–132.

Bayés À, van de Lagemaat LN, Collins MO, Croning MDR, Whittle IR, Choudhary JS, Grant SGN (2011) Characterization of the proteome, diseases and evolution of the human postsynaptic density. Nat Neurosci 14:19–21.

Bear MF, Huber KM, Warren ST (2004) The mGluR theory of fragile X mental retardation. Trends Neurosci 27:370–377.

Bejjani A, O'Neill J, Kim JA, Frew AJ, Yee VW, Ly R, Kitchen C, Salamon N, McCracken JT, Toga AW, Alger JR, Levitt JG (2012) Elevated glutamatergic compounds in pregenual anterior cingulate in pediatric autism spectrum disorder demonstrated by1H MRS and 1H MRSI. PLoS One 7.

Belardinelli C, Raza M, Taneli T (2016) Comorbid Behavioral Problems and Psychiatric Disorders in Autism Spectrum Disorders. 2:1–9.

Belichenko P V., Masliah E, Kleschevnikov AM, Villar AJ, Epstein CJ, Salehi A, Mobley WC (2004) Synaptic structural abnormalities in the Ts65Dn mouse model of Down syndrome. J Comp Neurol 480:281–298.

Belichenko P V., Wright EE, Belichenko NP, Masliah E, Li HH, Mobley WC, Francke U (2009) Widespread changes in dendritic and axonal morphology in Mecp2-mutant mouse models of Rett syndrome: Evidence for disruption of neuronal networks. J Comp Neurol 514:240–258.

Berkel S, Marshall CR, Weiss B, Howe J, Roeth R, Moog U, Endris V, Roberts W, Szatmari P, Pinto D, Bonin M, Riess A, Engels H, Sprengel R, Scherer SW, Rappold GA (2010) Mutations in the SHANK2 synaptic scaffolding gene in autism spectrum disorder and mental retardation. Nat Genet 42:489–491.

Berkel S, Tang W, Trevião M, Vogt M, Obenhaus HA, Gass P, Scherer SW, Sprengel R, Schratt G, Rappold GA (2012) Inherited and de novo SHANK2 variants associated with autism spectrum

disorder impair neuronal morphogenesis and physiology. Hum Mol Genet 21:344–357.

Berry-Kravis E, Hessl D, Coffey S, Hervey C, Schneider A, Yuhas J, Hutchison J, Snape M, Tranfaglia M, Nguyen D V, Hagerman R (2009) A pilot open label, single dose trial of fenobam in adults with fragile X syndrome. J Med Genet 46:266–271.

BERTANI G (1951) Studies on lysogenesis. I. The mode of phage liberation by lysogenic Escherichia coli. J Bacteriol 62:293–300.

Betancur C (2011) Etiological heterogeneity in autism spectrum disorders: More than 100 genetic and genomic disorders and still counting. Brain Res 1380:42–77.

Bhattacharya A, Kaphzan H, Alvarez-Dieppa AC, Murphy JP, Pierre P, Klann E (2012) Genetic Removal of p70 S6 Kinase 1 Corrects Molecular, Synaptic, and Behavioral Phenotypes in Fragile X Syndrome Mice. Neuron 76:325–337.

Bielsky IF, Hu S, Szegda KL, Westphal H, Young LJ (2004) Profound impairment in social recognition and reduction in anxiety-like behavior in vasopressin V1a receptor knockout mice. Neuropsychopharmacology 29:483–493.

Bielsky IF, Hu SB, Ren X, Terwilliger EF, Young LJ (2005) The V1a vasopressin receptor is necessary and sufficient for normal social recognition: A gene replacement study. Neuron 47:503–513.

Blanpied TA, Scott DB, Ehlers MD (2002) Dynamics and regulation of clathrin coats at specialized endocytic zones of dendrites and spines. Neuron 36:435–449.

Blundell J, Blaiss CA, Etherton MR, Espinosa F, Tabuchi K, Walz C, Bolliger MF, Sudhof TC, Powell CM, Südhof TC, Powell CM (2010) Neuroligin-1 Deletion Results in Impaired Spatial Memory and Increased Repetitive Behavior. J Neurosci 30:2115–2129.

Böckers TM, Segger-Junius M, Iglauer P, Bockmann J, Gundelfinger ED, Kreutz MR, Richter D, Kindler S, Kreienkamp HJ (2004) Differential expression and dendritic transcript localization of Shank family members: Identification of a dendritic targeting element in the 3' untranslated region of Shank1 mRNA. Mol Cell Neurosci 26:182–190.

Boeckers TM, Kreutz MR, Winter C, Zuschratter W, Smalla K, Sanmarti-vila L, Wex H, Langnaese K, Bockmann J, Garner CC, Gundelfinger ED (1999) Proline-Rich Synapse-Associated Protein-1 / Cortactin Binding Protein 1 (ProSAP1 / CortBP1) Is a PDZ-Domain Protein Highly Enriched in the Postsynaptic Density. J Neurosci 19:6506–6518.

Boeuf J, Trigo JM, Moreau P-H, Lecourtier L, Vogel E, Cassel J-C, Mathis C, Klosen P, Maldonado R, Simonin F (2009) Attenuated behavioural responses to acute and chronic cocaine in GASP-1-deficient mice. Eur J Neurosci 30:860–868.

Bonaglia MC, Giorda R, Mani E, Aceti G, Anderlid BM, Baroncini A, Pramparo T, Zuffardi O (2006) Identification of a recurrent breakpoint within the SHANK3 gene in the 22q13.3 deletion syndrome. J Med Genet 43:822–828.

Bourgeron T (2015) From the genetic architecture to synaptic plasticity in autism spectrum disorder. Nat Rev Neurosci 16:551–563.

Bozdagi O, Sakurai T, Papapetrou D, Wang X, Dickstein DL, Takahashi N, Kajiwara Y, Yang M, Katz AM, Scattoni M, Harris MJ, Saxena R, Silverman JL, Crawley JN, Zhou Q, Hof PR, Buxbaum JD (2010) Haploinsufficiency of the autism-associated Shank3 gene leads to deficits in synaptic function, social interaction, and social communication. Mol Autism 1:15.

Brakeman PR, Lanahan AA, O'Brien R, Roche K, Barnes CA, Huganir RL, Worley PF (1997) Homer: a protein that selectively binds metabotropic glutamate receptors. Nature 386:284–288.

Broekkamp CL, Rijk HW, Joly-Gelouin D, Lloyd KL (1986) Major tranquillizers can be distinguished from minor tranquillizers on the basis of effects on marble burying and swim-induced grooming in mice. Eur J Pharmacol 126:223–229.

Bruins Slot L a, Bardin L, Auclair AL, Depoortere R, Newman-Tancredi A (2008) Effects of antipsychotics and reference monoaminergic ligands on marble burying behavior in mice. Behav Pharmacol 19:145–152.

Butler MG, Dasouki MJ, Zhou X, Talebizadeh Z, Brown M, Takahashi TN, Miles JH, Wang CH, Stratton R, Pilarski R, Eng C (2005) Subset of individuals with autism spectrum disorders and extreme macrocephaly associated with germline PTEN tumour suppressor gene mutations. J Med Genet 42:318–321.

Butler MG, Rafi SK, Hossain W, Stephan DA, Manzardo AM (2015) Whole exome sequencing in females with autism implicates novel and candidate genes. Int J Mol Sci 16:1312–1335.

Buxbaum JD, Cai G, Chaste P, Nygren G, Goldsmith J, Reichert J, Anckarsäter H, Rastam M, Smith CJ, Silverman JM, Hollander E, Leboyer M, Gillberg C, Verloes A, Betancur C (2007) Mutation screening of the PTEN gene in patients with autism spectrum disorders and macrocephaly. Am J Med Genet Part B Neuropsychiatr Genet 144:484–491.

CDC (2014) Prevalence of autism spectrum disorder among children aged 8 years - autism and developmental disabilities monitoring network, 11 sites, United States, 2010. MMWR Surveill Summ 63:1–21.

Charman T, Pickles a, Simonoff E, Chandler S, Loucas T, Baird G (2011) IQ in children with autism spectrum disorders: data from the Special Needs and Autism Project (SNAP). Psychol Med 41:619–627.

Chen J a., Peñagarikano O, Belgard TG, Swarup V, Geschwind DH (2015) The Emerging Picture of Autism Spectrum Disorder: Genetics and Pathology. Annu Rev Pathol Mech Dis 10:111–144.

Chévere-Torres I, Maki JM, Santini E, Klann E (2012) Impaired social interactions and motor learning skills in tuberous sclerosis complex model mice expressing a dominant/negative form of tuberin. Neurobiol Dis 45:156–164.

Chih B, Engelman H, Scheiffele P (2005) Control of excitatory and inhibitory synapse formation by neuroligins. Science 307:1324–1328.

Chouinard V-A, Pingali SM, Chouinard G, Henderson DC, Mallya SG, Cypess AM, Cohen BM, Öngür D (2016) Factors associated with overweight and obesity in schizophrenia, schizoaffective and

bipolar disorders. Psychiatry Res 237:304–310.

Chuang S-C (2005) Prolonged Epileptiform Discharges Induced by Altered Group I Metabotropic Glutamate Receptor-Mediated Synaptic Responses in Hippocampal Slices of a Fragile X Mouse Model. J Neurosci 25:8048–8055.

Clement JP, Aceti M, Creson TK, Ozkan ED, Shi Y, Reish NJ, Almonte AG, Miller BH, Wiltgen BJ, Miller CA, Xu X, Rumbaugh G (2012) Pathogenic SYNGAP1 mutations impair cognitive development by disrupting maturation of dendritic spine synapses. Cell 151:709–723.

Collingridge GL, Isaac JTR, Wang YT (2004) Receptor trafficking and synaptic plasticity. Nat Rev Neurosci 5:952–962.

Collins MO, Husi H, Yu L, Brandon JM, Anderson CNG, Blackstock WP, Choudhary JS, Grant SGN (2006) Molecular characterization and comparison of the components and multiprotein complexes in the postsynaptic proteome. J Neurochem 97 Suppl 1:16–23.

Comery T a, Harris JB, Willems PJ, Oostra B a, Irwin S a, Weiler IJ, Greenough WT (1997) Abnormal dendritic spines in fragile X knockout mice. Proc Natl Acad Sci U S A 94:5401–5404.

Cristino a S, Williams SM, Hawi Z, An J-Y, Bellgrove M a, Schwartz CE, Costa LDF, Claudianos C (2014) Neurodevelopmental and neuropsychiatric disorders represent an interconnected molecular system. Mol Psychiatry 19:294–301.

CRITHCHLEY M, EARL CJC (1932) TUBEROSE SCLEROSIS AND ALLIED CONDITIONS. Brain 55:311–346.

Crowder RJ, Freeman RS (1998) Phosphatidylinositol 3-kinase and Akt protein kinase are necessary and sufficient for the survival of nerve growth factor-dependent sympathetic neurons. J Neurosci 18:2933–2943.

Curatolo P (2015) Mechanistic target of rapamycin (mTOR) in tuberous sclerosis complex-associated epilepsy. Pediatr Neurol 52:281–289.

Curley JP, Jensen CL, Franks B, Champagne FA (2012) Variation in maternal and anxiety-like behavior associated with discrete patterns of oxytocin and vasopressin 1a receptor density in the lateral septum. Horm Behav 61:454–461.

Curtin C, Bandini LG, Perrin EC, Tybor DJ, Must A (2005) Prevalence of overweight in children and adolescents with attention deficit hyperactivity disorder and autism spectrum disorders: a chart review. BMC Pediatr 5:48.

Darnell JC, Van Driesche SJ, Zhang C, Hung KYS, Mele A, Fraser CE, Stone EF, Chen C, Fak JJ, Chi SW, Licatalosi DD, Richter JD, Darnell RB (2011) FMRP stalls ribosomal translocation on mRNAs linked to synaptic function and autism. Cell 146:247–261.

Dazert E, Hall MN (2011) MTOR signaling in disease. Curr Opin Cell Biol 23:744–755.

Deacon RMJ (2006) Assessing nest building in mice. Nat Protoc 1:1117–1119.

De Filippis B, Nativio P, Fabbri A, Ricceri L, Adriani W, Lacivita E, Leopoldo M, Passarelli F, Fuso A, Laviola G (2014) Pharmacological stimulation of the brain serotonin receptor 7 as a novel

therapeutic approach for Rett syndrome. Neuropsychopharmacology 39:2506–2518.

de Hoop MJ, Huber LA, Stenmark H, Williamson E, Zerial M, Parton RG, Dotti CG (1994) The involvement of the small GTP-binding protein Rab5a in neuronal endocytosis. Neuron 13:11–22.

de la Torre-Ubieta L, Won H, Stein JL, Geschwind DH (2016) Advancing the understanding of autism disease mechanisms through genetics. Nat Med 22:345–361.

Dhami GK, Ferguson SSG (2006) Regulation of metabotropic glutamate receptor signaling, desensitization and endocytosis. Pharmacol Ther 111:260–271.

Dictenberg JB, Swanger SA, Antar LN, Singer RH, Bassell GJ (2008) A Direct Role for FMRP in Activity-Dependent Dendritic mRNA Transport Links Filopodial-Spine Morphogenesis to Fragile X Syndrome. Dev Cell 14:926–939.

Dölen G, Carpenter RL, Ocain TD, Bear MF (2010) Mechanism-based approaches to treating fragile X. Pharmacol Ther 127:78–93.

Dölen G, Osterweil E, Rao BSS, Smith GB, Auerbach BD, Chattarji S, Bear MF (2007) Correction of Fragile X Syndrome in Mice. Neuron 56:955–962.

Durand CM et al. (2007) Mutations in the gene encoding the synaptic scaffolding protein SHANK3 are associated with autism spectrum disorders. Nat Genet 39:25–27.

Durand CM, Perroy J, Loll F, Perrais D, Fagni L, Bourgeron T, Montcouquiol M, Sans N (2012) SHANK3 mutations identified in autism lead to modification of dendritic spine morphology via an actin-dependent mechanism. Mol Psychiatry 17:71–84.

Eadie BD, Zhang WN, Boehme F, Gil-Mohapel J, Kainer L, Simpson JM, Christie BR (2009) Fmr1 knockout mice show reduced anxiety and alterations in neurogenesis that are specific to the ventral dentate gyrus. Neurobiol Dis 36:361–373.

Ehlers MD (2003) Activity level controls postsynaptic composition and signaling via the ubiquitin-proteasome system. Nat Neurosci 6:231–242.

Ehninger D, Han S, Shilyansky C, Zhou Y, Li W, David J (2009) Reversal of learning deficits in a Tsc2+/- mouse model of tuberous sclerosis. Nat Med 14:843–848.

Ehninger D, Silva AJ (2011) Rapamycin for treating Tuberous sclerosis and Autism spectrum disorders. Trends Mol Med 17:78–87.

El-Hashemite N, Zhang H, Henske EP, Kwiatkowski DJ (2003) Mutation in TSC2 and activation of mammalian target of rapamycin signalling pathway in renal angiomyolipoma. Lancet (London, England) 361:1348–1349.

El-Kordi A, Winkler D, Hammerschmidt K, Kästner A, Krueger D, Ronnenberg A, Ritter C, Jatho J, Radyushkin K, Bourgeron T, Fischer J, Brose N, Ehrenreich H (2013) Development of an autism severity score for mice using Nlgn4 null mutants as a construct-valid model of heritable monogenic autism. Behav Brain Res 251:41–49.

Emamian ES, Hall D, Birnbaum MJ, Karayiorgou M, Gogos J a (2004) Convergent evidence for impaired AKT1-GSK3beta signaling in schizophrenia. Nat Genet 36:131–137.

Emr JHH and SD (2008) The Escrt Complexes: Structure and Mechanism of a Membrane- Trafficking Network. Brain Behav Immun 22:629–629.

Endersby R, Baker SJ (2008) PTEN signaling in brain: neuropathology and tumorigenesis. Oncogene 27:5416–5430.

Eng AG, Kelver DA, Hedrick TP, Swanson GT (2016) Transduction of group I mGluR-mediated synaptic plasticity by β-arrestin2 signalling. Nat Commun 7:13571.

Enquist J, Skro C (2007) Kinins Promote B 2 Receptor Endocytosis and Delay Constitutive B 1 Receptor Endocytosis. Mol Pharmacol 71:494–507.

Enriquez-Barreto L, Morales M (2016) The PI3K signaling pathway as a pharmacological target in Autism related disorders and Schizophrenia. Mol Cell Ther 4:2.

Etherton MR, Blaiss C a, Powell CM, Südhof TC (2009) Mouse neurexin-1alpha deletion causes correlated electrophysiological and behavioral changes consistent with cognitive impairments. Proc Natl Acad Sci U S A 106:17998–18003.

Falkner AL, Dollar P, Perona P, Anderson DJ, Lin D (2014) Decoding ventromedial hypothalamic neural activity during male mouse aggression. J Neurosci 34:5971–5984.

Fatemi SH, Folsom TD, Kneeland RE, Yousefi MK, Liesch SB, Thuras PD (2013) Impairment of fragile X mental retardation protein-metabotropic glutamate receptor 5 signaling and its downstream cognates ras-related C3 botulinum toxin substrate 1, amyloid beta A4 precursor protein, striatal-enriched protein tyrosine phosphatase, and h. Mol Autism 4:21.

Ferrarelli F, Tononi G (2011) The thalamic reticular nucleus and schizophrenia. Schizophr Bull 37:306–315.

Fiala JC, Spacek J, Harris KM (2002) Cause or Consequence of Neurological Disorders? Dendritic Spinen Pathol 39:1–34.

Fox MA, Panessiti MG, Hall FS, Uhl GR, Murphy DL (2013) An evaluation of the serotonin system and perseverative, compulsive, stereotypical, and hyperactive behaviors in dopamine transporter (DAT) knockout mice. Psychopharmacology (Berl) 227:685–695.

Francesconi A, Kumari R, Zukin RS (2009) Regulation of group I metabotropic glutamate receptor trafficking and signaling by the caveolar/lipid raft pathway. J Neurosci 29:3590–3602.

Fraser MM, Bayazitov IT, Zakharenko SS, Baker SJ (2008) Phosphatase and tensin homolog, deleted on chromosome 10 deficiency in brain causes defects in synaptic structure, transmission and plasticity, and myelination abnormalities. Neuroscience 151:476–488.

Fraser MM, Zhu X, Kwon CH, Uhlmann EJ, Gutmann DH, Baker SJ (2004) Pten loss causes hypertrophy and increased proliferation of astrocytes in vivo. Cancer Res 64:7773–7779.

Gai X, Xie H, Perin J, Takahashi N, Murphy K, Wenocur A, D 'arcy M, O 'hara R, Goldmuntz E, Grice D, Shaikh T, Hakonarson H, Buxbaum J, Elia J, White P (2011) Rare structural variation of synapse and neurotransmission genes in autism. Mol Psychiatry 17:402–411.

Gaugler T, Klei L, Sanders SJ, Bodea CA, Goldberg AP, Lee AB, Mahajan M, Manaa D, Pawitan Y,

Reichert J, Ripke S, Sandin S, Sklar P, Svantesson O, Reichenberg A, Hultman CM, Devlin B, Roeder K, Buxbaum JD (2014) Most genetic risk for autism resides with common variation. Nat Genet 46:881–885.

Gauthier J et al. (2010) De novo mutations in the gene encoding the synaptic scaffolding protein SHANK3 in patients ascertained for schizophrenia. Proc Natl Acad Sci U S A 107:7863–7868.

Gemelli T, Berton O, Nelson ED, Perrotti LI, Jaenisch R, Monteggia LM (2006) Postnatal loss of methyl-CpG binding protein 2 in the forebrain is sufficient to mediate behavioral aspects of Rett syndrome in mice. Biol Psychiatry 59:468–476.

Gerfen CR (2006) Short protocols in neuroscience : cellular and molecular methods : a compendium of methods from Current protocols in neuroscience. John Wiley & Sons.

Geschwind DH (2009) Advances in Autism. Annu Rev Med 60:367–380.

Giacometti E, Luikenhuis S, Beard C, Jaenisch R (2007) Partial rescue of MeCP2 deficiency by postnatal activation of MeCP2. Proc Natl Acad Sci U S A 104:1931–1936.

Gilissen C et al. (2014) Genome sequencing identifies major causes of severe intellectual disability. Nature 511:344–347.

Gimpl G, Fahrenholz F (2001) The oxytocin receptor system: structure, function, and regulation. Physiol Rev 81:629–683.

Giuffrida R (2005) A Reduced Number of Metabotropic Glutamate Subtype 5 Receptors Are Associated with Constitutive Homer Proteins in a Mouse Model of Fragile X Syndrome. J Neurosci 25:8908–8916.

Goehler H et al. (2004) A protein interaction network links GIT1, an enhancer of huntingtin aggregation, to Huntington's disease. Mol Cell 15:853–865.

Goffin A, Hoefsloot LH, Bosgoed E, Swillen A, Fryns JP (2001) PTEN mutation in a family with Cowden syndrome and autism. Am J Med Genet - Neuropsychiatr Genet 105:521–524.

Goh K-I, Cusick ME, Valle D, Childs B, Vidal M, Barabási A-L (2007) The human disease network. Proc Natl Acad Sci U S A 104:8685–8690.

Gong L, Yan Y, Xie J, Liu H, Sun X (2012a) Prediction of autism susceptibility genes based on association rules. J Neurosci Res 90:1119–1125.

Gong X, Jiang YW, Zhang X, An Y, Zhang J, Wu Y, Wang J, Sun Y, Liu Y, Gao X, Shen Y, Wu X, Qiu Z, Jin L, Wu BL, Wang H (2012b) High proportion of 22q13 deletions and SHANK3 mutations in Chinese patients with intellectual disability. PLoS One 7.

Goorden SMI, Van Woerden GM, Van Der Weerd L, Cheadle JP, Elgersma Y (2007) Cognitive deficits in Tsc1+/- mice in the absence of cerebral lesions and seizures. Ann Neurol 62:648–655.

Govek E-E, Newey SE, Akerman CJ, Cross JR, Van Der Veken L, Van Aelst L (2004) The X-linked mental retardation protein oligophrenin-1 is required for dendritic spine morphogenesis. Nat Neurosci 7:364–372.

Grabrucker AM (2013) Environmental factors in autism. Front Psychiatry 3:1–13.

Gray NW, Fourgeaud L, Huang B, Chen J, Cao H, Oswald BJ, Hémar A, McNiven MA (2003) Dynamin 3 Is a Component of the Postsynapse, Where it Interacts with mGluR5 and Homer. Curr Biol 13:510–515.

Guo W, Allan AM, Zong R, Zhang L, Johnson EB, Schaller EG, Murthy AC, Goggin SL, Eisch AJ, Oostra B a, Nelson DL, Jin P, Zhao X (2011) Ablation of Fmrp in adult neural stem cells disrupts hippocampus-dependent learning. Nat Med 17:559–565.

Guo W, Molinaro G, Collins KA, Hays SA, Paylor R, Worley PF, Szumlinski KK, Huber KM (2016) Selective Disruption of Metabotropic Glutamate Receptor 5-Homer Interactions Mimics Phenotypes of Fragile X Syndrome in Mice. J Neurosci 36:2131–2147.

Gustavson K-H, K:son HB, Holmgren G, Opitz JM, Reynolds JF (1986) Prevalence of the fragile-X syndrome in mentally retarded boys in a Swedish county. Am J Med Genet 23:581–587.

Guy J, Gan J, Selfridge J, Cobb S, Bird A (2007) Reversal of neurological defects in a mouse model of Rett syndrome. Science 315:1143–1147.

Hadley D, Wu ZL, Kao C, Kini A, Mohamed-Hadley A, Thomas K, Vazquez L, Qiu H, Mentch F, Pellegrino R, Kim C, Connolly J, Consortium AGP, Glessner J, Hakonarson H (2014) The impact of the metabotropic glutamate receptor and other gene family interaction networks on autism. Nat Commun 5:4074.

Hagerman RJ, Berry-Kravis E, Kaufmann WE, Ono MY, Tartaglia N, Lachiewicz A, Kronk R, Delahunty C, Hessl D, Visootsak J, Picker J, Gane L, Tranfaglia M (2009) Advances in the treatment of fragile X syndrome. Pediatrics 123:378–390.

Halassa MM, Chen Z, Wimmer RD, Brunetti PM, Zhao S, Zikopoulos B, Wang F, Brown EN, Wilson MA (2014) State-dependent architecture of thalamic reticular subnetworks. Cell 158:808–821.

Hamdan FF et al. (2011) Excess of de novo deleterious mutations in genes associated with glutamatergic systems in nonsyndromic intellectual disability. Am J Hum Genet 88:306–316.

Han K, Holder JL, Schaaf CP, Lu H, Chen H, Kang H, Tang J, Wu Z, Hao S, Cheung SW, Yu P, Sun H, Breman AM, Patel A, Lu H-C, Zoghbi HY (2013) SHANK3 overexpression causes manic-like behaviour with unique pharmacogenetic properties. Nature 503:72–77.

Hatton DD, Sideris J, Skinner M, Mankowski J, Bailey DB, Roberts J, Mirrett P (2006) Autistic behavior in children with fragile X syndrome: Prevalence, stability, and the impact of FMRP. Am J Med Genet Part A 140A:1804–1813.

Hayashi MK, Tang C, Verpelli C, Narayanan R, Stearns MH, Xu R, Li H, Sala C, Hayashi Y (2009a) The Postsynaptic Density Proteins Homer andShankFormaPolymericNetworkStructure. Cell 137:159–171.

Hayashi MK, Tang C, Verpelli C, Narayanan R, Stearns MH, Xu RM, Li H, Sala C, Hayashi Y (2009b) The Postsynaptic Density Proteins Homer and Shank Form a Polymeric Network Structure. Cell 137:159–171.

Heese K, Yamada T, Akatsu H, Yamamoto T, Kosaka K, Nagai Y, Sawada T (2004) Characterizing the

new transcription regulator protein p60TRP. J Cell Biochem 91:1030–1042.

Helsmoortel C, Swagemakers SMA, Vandeweyer G, Stubbs AP, Palli I, Mortier G, Kooy RF, van der Spek PJ (2016) Whole genome sequencing of a dizygotic twin suggests a role for the serotonin receptor *HTR7* in autism spectrum disorder. Am J Med Genet Part B Neuropsychiatr Genet.

Heydorn, Søndergaard, Ersbøll, Holst, Nielsen, Haft, Whistler, Schwartz (2004) A library of 7TM receptor C-terminal tails. J Biol Chem 279:54291.

Heyer MP, Feng G (2010) Engineered Mice. :211–248.

Holtmaat A, Svoboda K (2009) Experience-dependent structural synaptic plasticity in the mammalian brain. Nat Rev Neurosci 10:647–658.

Horn SC, Lalowski M, Goehler H, Dröge A, Wanker EE, Stelzl U (2006) Huntingtin interacts with the receptor sorting family protein GASP2. J Neural Transm 113:1081–1090.

Hotulainen P, Hoogenraad CC (2010) Actin in dendritic spines: Connecting dynamics to function. J Cell Biol 189:619–629.

Hou L, Antion MD, Hu D, Spencer CM, Paylor R, Klann E (2006) Dynamic Translational and Proteasomal Regulation of Fragile X Mental Retardation Protein Controls mGluR-Dependent Long-Term Depression. Neuron 51:441–454.

Huber KM (2011) Disease. Group 65:445–459.

Huber KM, Gallagher SM, Warren ST, Bear MF (2002a) Altered synaptic plasticity in a mouse model of fragile X mental retardation. Proc Natl Acad Sci U S A 99:7746–7750.

Huber KM, Gallagher SM, Warren ST, Bear MF (2002b) Altered synaptic plasticity in a mouse model of fragile X mental retardation. Proc Natl Acad Sci U S A 99:7746–7750.

Huber KM, Klann E, Costa-Mattioli M, Zukin RS (2015) Dysregulation of Mammalian Target of Rapamycin Signaling in Mouse Models of Autism. J Neurosci 35:13836–13842.

Huguenard JR, McCormick DA (2007) Thalamic synchrony and dynamic regulation of global forebrain oscillations. Trends Neurosci 30:350–356.

Huguet G, Ey E, Bourgeron T (2013) The Genetic Landscapes of Autism Spectrum Disorders. Annu Rev Genomics Hum Genet 14:191–213.

Hung AY, Futai K, Sala C, Valtschanoff JG, Ryu J, Woodworth MA, Kidd FL, Sung CC, Miyakawa T, Bear MF, Weinberg RJ, Sheng M (2008) Smaller Dendritic Spines, Weaker Synaptic Transmission, but Enhanced Spatial Learning in Mice Lacking Shank1. J Neurosci 28:1697–1708.

Hunt A, Shepherd C (1993) A prevalence study of autism in tuberous sclerosis. J Autism Dev Disord 23:323–339.

Hutsler JJ, Zhang H (2010) Increased dendritic spine densities on cortical projection neurons in autism spectrum disorders. Brain Res 1309:83–94.

Irwin SA, Patel B, Idupulapati M, Harris JB, Crisostomo RA, Larsen BP, Kooy F, Willems PJ, Cras P, Kozlowski PB, Swain RA, Weiler IJ, Greenough WT (2001) Abnormal dendritic spine characteristics in the temporal and visual cortices of patients with fragile-X syndrome: A

quantitative examination. Am J Med Genet 98:161–167.

Jamain S, Radyushkin K, Hammerschmidt K, Granon S, Boretius S, Varoqueaux F, Ramanantsoa N, Gallego J, Ronnenberg A, Winter D, Frahm J, Fischer J, Bourgeron T, Ehrenreich H, Brose N (2008) Reduced social interaction and ultrasonic communication in a mouse model of monogenic heritable autism. Proc Natl Acad Sci U S A 105:1710–1715.

Jan Y-N, Jan LY (2010) Branching out: mechanisms of dendritic arborization. Nat Rev Neurosci 11:316–328.

Jaworski J, Spangler S, Seeburg DP, Hoogenraad CC, Sheng M (2005) Control of dendritic arborization by the phosphoinositide-3'-kinase-Akt-mammalian target of rapamycin pathway. J Neurosci 25:11300–11312.

Jia J-M, Zhonghua H, Nordman J, Li Z (2014) The Schizophrenia Susceptibility Gene Dysbindin Regulates Dendritic Spine Dynamics. J Neurosci 34:13725–13736.

Jiang H, Guo W, Liang X, Rao Y (2005) Both the establishment and the maintenance of neuronal polarity require active mechanisms: Critical roles of GSK-3?? and its upstream regulators. Cell 120:123–135.

Jiang M, Deng L, Chen G (2004) High Ca(2+)-phosphate transfection efficiency enables single neuron gene analysis. Gene Ther 11:1303–1311.

Jirkof P (2014) Burrowing and nest building behavior as indicators of well-being in mice. J Neurosci Methods 234:139–146.

Jurado S et al. (2010a) PTEN is recruited to the postsynaptic terminal for NMDA receptor-dependent long-term depression. EMBO J 29:2827–2840.

Jurado S, Benoist M, Lario A, Knafo S, Petrok CN, Esteban JA (2010b) PTEN is recruited to the postsynaptic terminal for NMDA receptor-dependent long-term depression. EMBO J 29:2827–2840.

Kammermeier PJ (2008) Endogenous Homer Proteins Regulate Metabotropic Glutamate Receptor Signaling in Neurons. J Neurosci 28:8560–8567.

Kanner L (1943) Autistic disturbances of affective contact. Nerv Child 2:217–250.

Kasai H, Fukuda M, Watanabe S, Hayashi-Takagi A, Noguchi J (2010) Structural dynamics of dendritic spines in memory and cognition. Trends Neurosci 33:121–129.

Kelleher RJ, Bear MF (2008) The Autistic Neuron: Troubled Translation? Cell 135:401–406.

Kelleher RJ, Geigenmüller U, Hovhannisyan H, Trautman E, Pinard R, Rathmell B, Carpenter R, Margulies D (2012) High-throughput sequencing of mGluR signaling pathway genes reveals enrichment of rare variants in autism. PLoS One 7:11–14.

Ko SJ, Isozaki K, Kim I, Lee JH, Cho HJ, Sohn SY, Oh SR, Park S, Kim DG, Kim CH, Roche KW (2012) PKC phosphorylation regulates mGluR5 trafficking by enhancing binding of Siah-1A. J Neurosci 32:16391–16401.

Koekkoek SKE et al. (2005) Deletion of FMR1 in purkinje cells enhances parallel fiber LTD, enlarges

spines, and attenuates cerebellar eyelid conditioning in fragile X syndrome. Neuron 47:339–352.

Krumm N, Turner TN, Baker C, Vives L, Mohajeri K, Witherspoon K, Raja A, Coe BP, Stessman HA, He Z-X, Leal SM, Bernier R, Eichler EE (2015) Excess of rare, inherited truncating mutations in autism. Nat Genet 47:582–588.

Kwiatkowski DJ (2003) Tuberous sclerosis: From tubers to mTOR. Ann Hum Genet 67:87–96.

Kwon CH, Luikart BW, Powell CM, Zhou J, Matheny SA, Zhang W, Li Y, Baker SJ, Parada LF (2006) Pten Regulates Neuronal Arborization and Social Interaction in Mice. Neuron 50:377–388.

Kwon CH, Zhu X, Zhang J, Knoop LL, Tharp R, Smeyne RJ, Eberhart CG, Burger PC, Baker SJ (2001) Pten regulates neuronal soma size: a mouse model of Lhermitte-Duclos disease. Nat Genet 29:404–411.

Lakadamyali M, Rust MJ, Zhuang X (2006) Ligands for clathrin-mediated endocytosis are differentially sorted into distinct populations of early endosomes. Cell 124:997–1009.

Lang M, Wither RG, Brotchie JM, Wu C, Zhang L, Eubanks JH (2013) Selective preservation of MeCP2 in catecholaminergic cells is sufficient to improve the behavioral phenotype of male and female Mecp2-deficient mice. Hum Mol Genet 22:358–371.

Langen M, Bos D, Noordermeer SDS, Nederveen H, Van Engeland H, Durston S (2014) Changes in the development of striatum are involved in repetitive behavior in autism. Biol Psychiatry 76:405–411.

Langmead CJ, Watson J, Reavill C (2008) Muscarinic acetylcholine receptors as CNS drug targets. Pharmacol Ther 117:232–243.

Le Merrer J, Cagniard B, Cazala P (2006) Modulation of anxiety by ??-opioid receptors of the lateral septal region in mice. Pharmacol Biochem Behav 83:465–479.

Leblond CS et al. (2012) Genetic and functional analyses of SHANK2 mutations suggest a multiple hit model of autism spectrum disorders. PLoS Genet 8.

Lee J, Chung C, Ha S, Lee D, Kim D-Y, Kim H, Kim E (2015) Shank3-mutant mice lacking exon 9 show altered excitation/inhibition balance, enhanced rearing, and spatial memory deficit. Front Cell Neurosci 9:94.

Lee JH, Lee J, Choi KY, Hepp R, Lee J-Y, Lim MK, Chatani-Hinze M, Roche P a, Kim DG, Ahn YS, Kim CH, Roche KW (2008) Calmodulin dynamically regulates the trafficking of the metabotropic glutamate receptor mGluR5. Proc Natl Acad Sci U S A 105:12575–12580.

Lewis LD, Voigts J, Flores FJ, Ian Schmitt L, Wilson MA, Halassa MM, Brown EN (2015) Thalamic reticular nucleus induces fast and local modulation of arousal state. Elife 4.

LoParo D, Waldman ID (2015) The oxytocin receptor gene (OXTR) is associated with autism spectrum disorder: a meta-analysis. Mol Psychiatry 20:640–646.

Lugo JN, Smith GD, Arbuckle EP, White J, Holley AJ, Floruta CM, Ahmed N, Gomez MC, Okonkwo O (2014) Deletion of PTEN produces autism-like behavioral deficits and alterations in synaptic proteins. Front Mol Neurosci 7:27.

Luikart BW, Schnell E, Washburn EK, Bensen AL, Tovar KR, Westbrook GL (2011) Pten knockdown in vivo increases excitatory drive onto dentate granule cells. J Neurosci 31:4345–4354.

Lv J-W, Cheng T-L, Qiu Z-L, Zhou W-H (2013) Role of the PTEN signaling pathway in autism spectrum disorder. Neurosci Bull 29:773–778.

Mao L, Yang L, Tang Q, Samdani S, Zhang G, Wang JQ (2005) The Scaffold Protein Homer1b / c Links Metabotropic Glutamate Receptor 5 to Extracellular Signal-Regulated Protein Kinase Cascades in Neurons. Proteins 25:2741–2752.

Martini L, Thompson D, Kharazia V, Whistler JL (2010) Differential regulation of behavioral tolerance to WIN55,212-2 by GASP1. Neuropsychopharmacology 35:1363–1373.

McMahon JJ, Yu W, Yang J, Feng H, Helm M, McMahon E, Zhu X, Shin D, Huang Y (2015) Seizure-dependent mTOR activation in 5-HT neurons promotes autism-like behaviors in mice. Neurobiol Dis 73:296–306.

Mei Y, Monteiro P, Zhou Y, Kim J-A, Gao X, Fu Z, Feng G (2016) Adult restoration of Shank3 expression rescues selective autistic-like phenotypes. Nature 530:481–484.

Meikle L, Pollizzi K, Egnor A, Kramvis I, Lane H, Sahin M, Kwiatkowski DJ (2008) Response of a neuronal model of tuberous sclerosis to mammalian target of rapamycin (mTOR) inhibitors: effects on mTORC1 and Akt signaling lead to improved survival and function. J Neurosci 28:5422–5432.

Michalon A, Sidorov M, Ballard T, Ozmen L, Spooren W, Wettstein J, Jaeschke G, Bear M, Lindemann L (2012) Chronic Pharmacological mGlu5 Inhibition Corrects Fragile X in Adult Mice. Neuron 74:49–56.

Mishra M, Heese K (2011) P60TRP interferes with the GPCR/secretase pathway to mediate neuronal survival and synaptogenesis. J Cell Mol Med 15:2462–2477.

Moessner R, Marshall CR, Sutcliffe JS, Skaug J, Pinto D, Vincent J, Zwaigenbaum L, Fernandez B, Roberts W, Szatmari P, Scherer SW (2007) Contribution of SHANK3 mutations to autism spectrum disorder. Am J Hum Genet 81:1289–1297.

Moran LB, Graeber MB (2008) Towards a pathway definition of Parkinson's disease: A complex disorder with links to cancer, diabetes and inflammation. Neurogenetics 9:1–13.

Moretti P, Bouwknecht JA, Teague R, Paylor R, Zoghbi HY (2005) Abnormalities of social interactions and home-cage behavior in a mouse model of Rett syndrome. Hum Mol Genet 14:205–220.

Moretti P, Levenson JM, Battaglia F, Atkinson R, Teague R, Antalffy B, Armstrong D, Arancio O, Sweatt JD, Zoghbi HY (2006) Learning and memory and synaptic plasticity are impaired in a mouse model of Rett syndrome. J Neurosci 26:319–327.

Moser E, Kargl J, Whistler JL, Waldhoer M, Tschische P (2010) G protein-coupled receptor-associated sorting protein 1 regulates the postendocytic sorting of seven-transmembrane-spanning G protein-coupled receptors. Pharmacology 86:22–29.

Moy SS, Riddick N V., Nikolova VD, Teng BL, Agster KL, Nonneman RJ, Young NB, Baker LK,

Nadler JJ, Bodfish JW (2014) Repetitive behavior profile and supersensitivity to amphetamine in the C58/J mouse model of autism. Behav Brain Res 259:200–214.

Mullard A (2015) Fragile X disappointments upset autism ambitions. Nat Rev Drug Discov 14:151–153.

Nägerl UV, Eberhorn N, Cambridge SB, Bonhoeffer T (2004) Bidirectional activity-dependent morphological plasticity in hippocampal neurons. Neuron 44:759–767.

Naisbitt S, Kim E, Tu JC, Xiao B, Sala C, Valtschanoff J, Weinberg RJ, Worley PF, Sheng M, Hughes H, Hill C, Carolina N (1999) Shank , a Novel Family of Postsynaptic Density Proteins that Binds to the NMDA Receptor / PSD-95 / GKAP Complex and Cortactin University of North Carolina at Chapel Hill. Neuron 23:569–582.

Nishimori K, Takayanagi Y, Yoshida M, Kasahara Y, Young LJ, Kawamata M (2008) New aspects of oxytocin receptor function revealed by knockout mice: sociosexual behaviour and control of energy balance. Prog Brain Res 170:79–90.

Nosyreva ED, Huber KM (2006) Metabotropic receptor-dependent long-term depression persists in the absence of protein synthesis in the mouse model of fragile X syndrome. J Neurophysiol 95:3291–3295.

O'Connor EC, Bariselli S, Bellone C (2014) Synaptic basis of social dysfunction: A focus on postsynaptic proteins linking group-I mGluRs with AMPARs and NMDARs. Eur J Neurosci 39:1114–1129.

Ophir AG, Zheng D-J, Eans S, Phelps SM (2009) Social investigation in a memory task relates to natural variation in septal expression of oxytocin receptor and vasopressin receptor 1a in prairie voles (Microtus ochrogaster). Behav Neurosci 123:979–991.

Osterweil EK, Krueger DD, Reinhold K, Bear MF (2010) Hypersensitivity to mGluR5 and ERK1/2 leads to excessive protein synthesis in the hippocampus of a mouse model of fragile X syndrome. J Neurosci 30:15616–15627.

Ozonoff S, Young GS (2011) Recurrence Risk for Autism Spectrum Disorders : A Baby Siblings Research Consortium Study. Pediatrics 128:e1–e8.

Padilla SL, Reef D, Zeltser LM (2012) Defining POMC neurons using transgenic reagents: Impact of transient Pomc expression in diverse immature neuronal populations. Endocrinology 153:1219–1231.

Paluszkiewicz SM, Martin BS, Huntsman MM (2011) Fragile X syndrome: The GABAergic system and circuit dysfunction. Dev Neurosci 33:349–364.

Park M, Salgado JM, Ostroff L, Helton TD, Robinson CG, Harris KM, Ehlers MD (2006) Plasticity-Induced Growth of Dendritic Spines by Exocytic Trafficking from Recycling Endosomes. Neuron 52:817–830.

Peça J, Feliciano C, Ting JT, Wang W, Wells MF, Venkatraman TN, Lascola CD, Fu Z, Feng G (2011) Shank3 mutant mice display autistic-like behaviours and striatal dysfunction. Nature 472:437–442.

Peça J, Feng G (2012) Cellular and synaptic network defects in autism. Curr Opin Neurobiol 22:866–

872.

Peier AM, McIlwain KL, Kenneson A, Warren ST, Paylor R, Nelson DL (2000) (Over)correction of FMR1 deficiency with YAC transgenics: behavioral and physical features. Hum Mol Genet 9:1145–1159.

Pelka GJ, Watson CM, Radziewic T, Hayward M, Lahooti H, Christodoulou J, Tam PPL (2006) Mecp2 deficiency is associated with learning and cognitive deficits and altered gene activity in the hippocampal region of mice. Brain 129:887–898.

Peñagarikano O, Lázaro MT, Lu X-H, Gordon A, Dong H, Lam HA, Peles E, Maidment NT, Murphy NP, Yang XW, Golshani P, Geschwind DH (2015) Exogenous and evoked oxytocin restores social behavior in the Cntnap2 mouse model of autism. Sci Transl Med 7:271ra8.

Penzes P, Cahill ME, Jones K a, VanLeeuwen J-E, Woolfrey KM (2011) Dendritic spine pathology in neuropsychiatric disorders. Nat Neurosci 14:285–293.

Pignatelli M, Piccinin S, Molinaro G, Di Menna L, Riozzi B, Cannella M, Motolese M, Vetere G, Catania MV, Battaglia G, Nicoletti F, Nisticò R, Bruno V (2014) Changes in mGlu5 receptor-dependent synaptic plasticity and coupling to homer proteins in the hippocampus of Ube3A hemizygous mice modeling angelman syndrome. J Neurosci 34:4558–4566.

Pinault D (2004) The thalamic reticular nucleus: Structure, function and concept. Brain Res Rev 46:1–31.

Pinto D et al. (2010) Functional impact of global rare copy number variation in autism spectrum disorders. Nature 466:368–372.

Piochon C, Kloth AD, Grasselli G, Titley HK, Nakayama H, Hashimoto K, Wan V, Simmons DH, Eissa T, Nakatani J, Cherskov A, Miyazaki T, Watanabe M, Takumi T, Kano M, Wang SS-H, Hansel C (2014) Cerebellar plasticity and motor learning deficits in a copy-number variation mouse model of autism. Nat Commun 5:5586.

Piton A et al. (2011) Systematic resequencing of X-chromosome synaptic genes in autism spectrum disorder and schizophrenia. Mol Psychiatry 16:867–880.

Purpura DP (1974) Dendritic spine "dysgenesis" and mental retardation. Science 186:1126–1128.

Rácz B, Blanpied T a, Ehlers MD, Weinberg RJ (2004) Lateral organization of endocytic machinery in dendritic spines. Nat Neurosci 7:917–918.

Ramiro-Cortés Y, Israely I (2013) Long Lasting Protein Synthesis- and Activity-Dependent Spine Shrinkage and Elimination after Synaptic Depression. PLoS One 8.

Redfern RE, Daou MC, Li L, Munson M, Gericke A, Ross AH (2010) A mutant form of PTEN linked to autism. Protein Sci 19:1948–1956.

Reis DG, Scopinho A a, Guimarães FS, Corrêa FM a, Resstel LBM (2010) Involvement of the lateral septal area in the expression of fear conditioning to context. Learn Mem 17:134–138.

Reith RM, McKenna J, Wu H, Hashmi SS, Cho SH, Dash PK, Gambello MJ (2013) Loss of Tsc2 in Purkinje cells is associated with autistic-like behavior in a mouse model of tuberous sclerosis

complex. Neurobiol Dis 51:93–103.

Ritter SL, Hall RA (2009) Fine-tuning of GPCR activity by receptor-interacting proteins. Nat Rev Mol Cell Biol 10:819–830.

Ronesi JA, Collins KA, Hays S a, Tsai N-P, Guo W, Birnbaum SG, Hu J-H, Worley PF, Gibson JR, Huber KM (2012) Disrupted Homer scaffolds mediate abnormal mGluR5 function in a mouse model of fragile X syndrome. Nat Neurosci 15:431–440, S1.

Rosenberg RE, Law JK, Yenokyan G, Mcgready J, Kaufmann WE, Law PA (2009) Characteristics and Concordance of Autism Spectrum Disorders Among 277 Twin Pairs. 163:907–914.

Roussignol G, Ango F, Romorini S, Tu JC, Sala C, Worley PF, Bockaert J, 1 and LF (2005) Shank Expression Is Sufficient to Induce Functional Dendritic Spine Synapses in Aspiny Neurons. J Neurosci 25:3560–3570.

Sakai Y, Shaw CA, Dawson BC, Dugas D V., Al-Mohtaseb Z, Hill DE, Zoghbi HY (2011) Protein interactome reveals converging molecular pathways among autism disorders. Sci Transl Med 3:86ra49.

Sala C, Piëch V, Wilson NR, Passafaro M, Liu G, Sheng M (2001) Regulation of dendritic spine morphology and synaptic function by Shank and Homer. Neuron 31:115–130.

Sala C, Roussignol G, Meldolesi J, Fagni L (2005) Key Role of the Postsynaptic Density Scaffold Proteins Shank and Homer in the Functional Architecture of Ca2+ Homeostasis at Dendritic Spines in Hippocampal Neurons. J Neurosci 25:4587–4592.

Sanders SJ et al. (2012) De novo mutations revealed by whole-exome sequencing are strongly associated with autism. Nature 485:237–241.

Santini E, Huynh TN, MacAskill AF, Carter AG, Pierre P, Ruggero D, Kaphzan H, Klann E (2013) Exaggerated translation causes synaptic and behavioural aberrations associated with autism. Nature 493:411–415.

Sato A, Kasai S, Kobayashi T, Takamatsu Y, Hino O, Ikeda K, Mizuguchi M (2012a) Rapamycin reverses impaired social interaction in mouse models of tuberous sclerosis complex. Nat Commun 3:1292.

Sato D et al. (2012b) SHANK1 Deletions in Males with Autism Spectrum Disorder. Am J Hum Genet 90:879–887.

Schmeisser MJ et al. (2012) Autistic-like behaviours and hyperactivity in mice lacking ProSAP1/Shank2. Nature 486:256–260.

Schnell E, Sizemore M, Karimzadegan S, Chen L, Bredt DS, Nicoll RA (2002) Direct interactions between PSD-95 and stargazin control synaptic AMPA receptor number. Proc Natl Acad Sci U S A 99:13902–13907.

Schumann CM, Bloss CS, Barnes CC, Wideman GM, Carper RA, Akshoomoff N, Pierce K, Hagler D, Schork N, Lord C, Courchesne E (2010) Longitudinal magnetic resonance imaging study of cortical development through early childhood in autism. J Neurosci 30:4419–4427.

Sebat J et al. (2007) Strong Association of De Novo Copy Number Mutations with Autism. Science (80-) 316:445–449.

Sharma A, Hoeffer CA, Takayasu Y, Miyawaki T, McBride SM, Klann E, Zukin RS (2010) Dysregulation of mTOR signaling in fragile X syndrome. J Neurosci 30:694–702.

Sheng M, Hoogenraad CC (2007) The postsynaptic architecture of excitatory synapses: a more quantitative view. Annu Rev Biochem 76:823–847.

Shepherd CW, Beard CM, Gomez MR, Kurland LT, Whisnant JP (1991) Tuberous sclerosis complex in Olmsted County, Minnesota, 1950-1989. Arch Neurol 48:400–401.

Shiraishi-Yamaguchi Y, Furuichi T (2007) The Homer family proteins. Genome Biol 8:206.

Silverman JL, Turner SM, Barkan CL, Tolu SS, Saxena R, Hung AY, Sheng M, Crawley JN (2011) Sociability and motor functions in Shank1 mutant mice. Brain Res 1380:120–137.

Simonin F, Karcher P, Boeuf JJ, Matifas A, Kieffer BL (2004) Identification of a novel family of G protein-coupled receptor associated sorting proteins. J Neurochem 89:766–775.

Singewald GM, Rjabokon A, Singewald N, Ebner K (2011) The modulatory role of the lateral septum on neuroendocrine and behavioral stress responses. Neuropsychopharmacology 36:793–804.

Skuse DH (2005) X-linked genes and mental functioning. Hum Mol Genet 14.

Sohn JW (2015) Network of hypothalamic neurons that control appetite. BMB Rep 48:229–233.

Soloveva V, Graves R a, Rasenick MM, Spiegelman BM, Ross SR (1997) Transgenic mice overexpressing the beta 1-adrenergic receptor in adipose tissue are resistant to obesity. Mol Endocrinol 11:27–38.

Staal WG, De Krom M, De Jonge M V. (2012) Brief report: The dopamine-3-receptor gene (DRD3) is associated with specific repetitive behavior in autism spectrum disorder (ASD). J Autism Dev Disord 42:885–888.

Stoppel LJ, Auerbach BD, Senter RK, Preza AR, Lefkowitz RJ, Bear MF (2017) b -Arrestin2 Couples Metabotropic Glutamate Receptor 5 to Neuronal Protein Synthesis and Is a Potential Target to Treat Fragile X Report b -Arrestin2 Couples Metabotropic Glutamate Receptor 5 to Neuronal Protein Synthesis and Is a Potential Target to Trea. CellReports 18:2807–2814.

Sungur AÖ, Vörckel KJ, Schwarting RKW, Wöhr M (2014) Repetitive behaviors in the Shank1 knockout mouse model for autism spectrum disorder: Developmental aspects and effects of social context. J Neurosci Methods 234:92–100.

Swiech L, Perycz M, Malik A, Jaworski J (2008) Role of mTOR in physiology and pathology of the nervous system. Biochim Biophys Acta - Proteins Proteomics 1784:116–132.

Sztainberg Y, Zoghbi HY (2016) Lessons learned from studying syndromic autism spectrum disorders. Nat Neurosci 19:1408.

Takeuchi K, Gertner MJ, Zhou J, Parada LF, Bennett MVL, Zukin RS (2013) Dysregulation of synaptic plasticity precedes appearance of morphological defects in a Pten conditional knockout mouse model of autism. Proc Natl Acad Sci 110:4738–4743.

Tang G, Gudsnuk K, Kuo SH, Cotrina ML, Rosoklija G, Sosunov A, Sonders MS, Kanter E, Castagna

C, Yamamoto A, Yue Z, Arancio O, Peterson BS, Champagne F, Dwork AJ, Goldman J, Sulzer D (2014) Loss of mTOR-Dependent Macroautophagy Causes Autistic-like Synaptic Pruning Deficits. Neuron 83:1131–1143.

Tang SJ, Reis G, Kang H, Gingras A-C, Sonenberg N, Schuman EM (2002) A rapamycin-sensitive signaling pathway contributes to long-term synaptic plasticity in the hippocampus. Proc Natl Acad Sci U S A 99:467–472.

Tavazoie SF, Alvarez V a, Ridenour D a, Kwiatkowski DJ, Sabatini BL (2005) Regulation of neuronal morphology and function by the tumor suppressors Tsc1 and Tsc2. Nat Neurosci 8:1727–1734.

The European Chromosome 16 Tuberous Sclerosis Consortium (1993) Identification and characterization of the tuberous sclerosis gene on chromosome 16. Cell 75:1305–1315.

Thomas AM, Bui N, Graham D, Perkins JR, Yuva-Paylor LA, Paylor R (2011) Genetic reduction of group 1 metabotropic glutamate receptors alters select behaviors in a mouse model for fragile X syndrome. Behav Brain Res 223:310–321.

Thompson D, Martini L, Whistler JL (2010) Altered ratio of D1 and D2 dopamine receptors in mouse striatum is associated with behavioral sensitization to cocaine. PLoS One 5:e11038.

Thompson D, Pusch M, Whistler JL (2007) Changes in G protein-coupled receptor sorting protein affinity regulate postendocytic targeting of G protein-coupled receptors. J Biol Chem 282:29178–29185.

Ting JT, Peça J, Feng G (2012) Functional Consequences of Mutations in Postsynaptic Scaffolding Proteins and Relevance to Psychiatric Disorders. Annu Rev Neurosci 35:49–71.

Tost H, Kolachana B, Hakimi S, Lemaitre H, Verchinski BA, Mattay VS, Weinberger DR, Meyer-Lindenberg A (2010) A common allele in the oxytocin receptor gene (OXTR) impacts prosocial temperament and human hypothalamic-limbic structure and function. Proc Natl Acad Sci U S A 107:13936–13941.

Troca-Marín JA, Alves-Sampaio A, Montesinos ML (2012) Deregulated mTOR-mediated translation in intellectual disability. Prog Neurobiol 96:268–282.

Tsai PT, Hull C, Chu Y, Greene-Colozzi E, Sadowski AR, Leech JM, Steinberg J, Crawley JN, Regehr WG, Sahin M (2012) Autistic-like behaviour and cerebellar dysfunction in Purkinje cell Tsc1 mutant mice. Nature 488:647–651.

Tu JC, Xiao B, Naisbitt S, Yuan JP, Petralia RS, Brakeman P, Doan A, Aakalu VK, Lanahan AA, Sheng M, Worley PF (1999) Coupling of mGluR/Homer and PSD-95 complexes by the Shank family of postsynaptic density proteins. Neuron 23:583–592.

Udagawa T, Farny NG, Jakovcevski M, Kaphzan H, Alarcon JM, Anilkumar S, Ivshina M, Hurt JA, Nagaoka K, Nalavadi VC, Lorenz LJ, Bassell GJ, Akbarian S, Chattarji S, Klann E, Richter JD (2013) Genetic and acute CPEB1 depletion ameliorate fragile X pathophysiology. Nat Med 19:1473–1477.

Urdinguio RG, Lopez-Serra L, Lopez-Nieva P, Alaminos M, Diaz-Uriarte R, Fernandez AF, Esteller M

(2008) Mecp2-null mice provide new neuronal targets for rett syndrome. PLoS One 3.

Valnegri P, Sala C, Passafaro M (2012) Synaptic dysfunction and intellectual disability. Adv Exp Med Biol 970:433–449.

van de Lagemaat LN, Nijhof B, Bosch DGM, Kohansal-Nodehi M, Keerthikumar S, Heimel JA (2014) Age-related decreased inhibitory vs. excitatory gene expression in the adult autistic brain. Front Neurosci 8.

van Slegtenhorst M et al. (1997) Identification of the tuberous sclerosis gene TSC1 on chromosome 9q34. Science 277:805–808.

Ventura R, Pascucci T, Catania M V, Musumeci SA, Puglisi-Allegra S (2004) Object recognition impairment in Fmr1 knockout mice is reversed by amphetamine: involvement of dopamine in the medial prefrontal cortex. Behav Pharmacol 15:433–442.

Verkerk AJMH et al. (1991) Identification of a gene (FMR-1) containing a CGG repeat coincident with a breakpoint cluster region exhibiting length variation in fragile X syndrome. Cell 65:905–914.

Verpelli C, Dvoretskova E, Vicidomini C, Rossi F, Chiappalone M, Schoen M, Di Stefano B, Mantegazza R, Broccoli V, Böckers TM, Dityatev A, Sala C, Bockers TM, Dityatev A, Sala C (2011) Importance of Shank3 Protein in Regulating Metabotropic Glutamate Receptor 5 (mGluR5) Expression and Signaling at Synapses. J Biol Chem 286:34839–34850.

Vicidomini C, Ponzoni L, Lim D, Schmeisser M, Reim D, Morello N, Orellana D, Tozzi A, Durante V, Scalmani P, Mantegazza M, Genazzani A, Giustetto M, Sala M, Calabresi P, Boeckers T, Sala C, Verpelli C (2016) Pharmacological enhancement of mGlu5 receptors rescues behavioral deficits in SHANK3 knock-out mice. Mol Psychiatry:1–14.

Voineagu I, Wang X, Johnston P, Lowe JK, Tian Y, Horvath S, Mill J, Cantor RM, Blencowe BJ, Geschwind DH (2011) Transcriptomic analysis of autistic brain reveals convergent molecular pathology. Nature 474:380–384.

Volk L, Chiu S-L, Sharma K, Huganir RL (2015) Glutamate Synapses in Human Cognitive Disorders. Annu Rev Neurosci 38:127–149.

Waltereit R, Japs B, Schneider M, De Vries PJ, Bartsch D (2011) Epilepsy and Tsc2 haploinsufficiency lead to autistic-like social deficit behaviors in rats. Behav Genet 41:364–372.

Wang T et al. (2016a) De novo genic mutations among a Chinese autism spectrum disorder cohort. Nat Commun 7:13316.

Wang W, Li C, Chen Q, Goes M Van Der, Hawrot J, Yao AY, Gao X, Lu C, Zang Y, Zhang Q, Lyman K, Wang D, Guo B, Wu S, Gerfen CR, Fu Z, Feng G (2017) Striatopallidal dysfunction underlies repetitive behavior in Shank3- deficient model of autism. 127:25–28.

Wang X et al. (2016b) Altered mGluR5-Homer scaffolds and corticostriatal connectivity in a Shank3 complete knockout model of autism. Nat Commun 7:11459.

Wang X, McCoy PA, Rodriguiz RM, Pan Y, Je HS, Roberts AC, Kim CJ, Berrios J, Colvin JS, Bousquet-Moore D, Lorenzo I, Wu G, Weinberg RJ, Ehlers MD, Philpot BD, Beaudet AL, Wetsel WC,

Jiang YH (2011) Synaptic dysfunction and abnormal behaviors in mice lacking major isoforms of Shank3. Hum Mol Genet 20:3093–3108.

Wang Y, Cheng A, Mattson MP (2006) The PTEN phosphatase is essential for long-term depression of hippocampal synapses. Neuromolecular Med 8:329–336.

Wells MF, Wimmer RD, Schmitt LI, Feng G, Halassa MM (2016) Thalamic reticular impairment underlies attention deficit in Ptchd1(Y/-) mice. Nature 532:58–63.

Weston MC, Chen H, Swann JW (2012) Multiple roles for mammalian target of rapamycin signaling in both glutamatergic and GABAergic synaptic transmission. J Neurosci 32:11441–11452.

Whistler JL, Enquist J, Marley A, Fong J, Gladher F, Tsuruda P, Murray SR, von Zastro M (2002) Modulation of postendocytic sorting of G-protein coupled receptors. Science (80-) 297:615–620.

Wiegert JS, Oertner TG (2013) Long-term depression triggers the selective elimination of weakly integrated synapses. Proc Natl Acad Sci U S A 110:E4510–E4519.

Williams MR, DeSpenza T, Li M, Gulledge a. T, Luikart BW (2015) Hyperactivity of Newborn Pten Knock-out Neurons Results from Increased Excitatory Synaptic Drive. J Neurosci 35:943–959.

Williams SCP (2012) Drugs targeting mGluR5 receptor offer "fragile" hope for autism. Nat Med 18:840.

Willsey AJ et al. (2013) XCoexpression networks implicate human midfetal deep cortical projection neurons in the pathogenesis of autism. Cell 155:997–1007.

Winter EE, Ponting CP (2005) Mammalian BEX, WEX and GASP genes: coding and non-coding chimaerism sustained by gene conversion events. BMC Evol Biol 5:54.

Wöhr M, Roullet FI, Hung AY, Sheng M, Crawley JN (2011) Communication impairments in mice lacking shank1: Reduced levels of ultrasonic vocalizations and scent marking behavior. PLoS One 6.

Won H, Lee H-R, Gee HY, Mah W, Kim J-I, Lee J, Ha S, Chung C, Jung ES, Cho YS, Park S-G, Lee J-S, Lee K, Kim D, Bae YC, Kaang B-K, Lee MG, Kim E (2012) Autistic-like social behaviour in Shank2-mutant mice improved by restoring NMDA receptor function. Nature 486:261–265.

Wu S, Jia M, Ruan Y, Liu J, Guo Y, Shuang M, Gong X, Zhang Y, Yang X, Zhang D (2005) Positive association of the oxytocin receptor gene (OXTR) with autism in the Chinese Han population. Biol Psychiatry 58:74–77.

Wurzman R, Forcelli PA, Griffey CJ, Kromer LF (2015) Repetitive grooming and sensorimotor abnormalities in an ephrin-A knockout model for Autism Spectrum Disorders. Behav Brain Res 278:115–128.

Yan L, Shamir A, Skirzewski M, Leiva-Salcedo E, Kwon OB, Karavanova I, Paredes D, Malkesman O, Bailey KR, Vullhorst D, Crawley JN, Buonanno A (2017) Neuregulin-2 ablation results in dopamine dysregulation and severe behavioral phenotypes relevant to psychiatric disorders. Mol Psychiatry:1–11.

Yan QJ, Rammal M, Tranfaglia M, Bauchwitz RP (2005) Suppression of two major Fragile X Syndrome mouse model phenotypes by the mGluR5 antagonist MPEP. Neuropharmacology 49:1053–1066.

Yasumura M, Yoshida T, Yamazaki M, Abe M, Natsume R, Kanno K, Uemura T, Takao K, Sakimura K, Kikusui T, Miyakawa T, Mishina M (2014) IL1RAPL1 knockout mice show spine density decrease, learning deficiency, hyperactivity and reduced anxiety-like behaviours. Sci Rep 4:6613.

Yuan JP, Kiselyov K, Shin DM, Chen J, Shcheynikov N, Kang SH, Dehoff MH, Schwarz MK, Seeburg PH, Muallem S, Worley PF (2003) Homer binds TRPC family channels and is required for gating of TRPC1 by IP3 receptors. Cell 114:777–789.

Zastrow M von, Hanyaloglu AC (2008) Regulation of GPCRs by Endocytic Membrane Trafficking and Its Potential Implications. Annu Rev Pharmacol Toxicol 48:537–568.

Zeier Z, Kumar A, Bodhinathan K, Feller J a, Foster TC, Bloom DC (2009) Fragile X mental retardation protein replacement restores hippocampal synaptic function in a mouse model of fragile X syndrome. Gene Ther 16:1122–1129.

Zeng LH, Ouyang Y, Gazit V, Cirrito JR, Jansen LA, Ess KC, Yamada KA, Wozniak DF, Holtzman DM, Gutmann DH, Wong M (2007) Abnormal glutamate homeostasis and impaired synaptic plasticity and learning in a mouse model of tuberous sclerosis complex. Neurobiol Dis 28:184–196.

Zhang B, Chen LY, Liu X, Maxeiner S, Lee SJ, Gokce O, Südhof TC (2015) Neuroligins Sculpt Cerebellar Purkinje-Cell Circuits by Differential Control of Distinct Classes of Synapses. Neuron 87:781–796.

Zhou J, Blundell J, Ogawa S, Kwon C-H, Zhang W, Sinton C, Powell CM, Parada LF (2009) Pharmacological inhibition of mTORC1 suppresses anatomical, cellular, and behavioral abnormalities in neural-specific Pten knock-out mice. J Neurosci 29:1773–1783.

Zhou J, Goldberg EM, Adrian Leu N, Zhou L, Coulter DA, Jeremy Wang P (2014) Respiratory failure, cleft palate and epilepsy in the mouse model of human Xq22.1 deletion syndrome. Hum Mol Genet 23:3823–3829.

Zhou Y et al. (2016) Mice with Shank3 Mutations Associated with ASD and Schizophrenia Display Both Shared and Distinct Defects. Neuron 89:147–162.

Zoghbi HY, Bear MF (2012a) Synaptic Dysfunction in Neurodevelopmental Disorders Associated with Autism and Intellectual Disabilities. Cold Spring Harb Perspect Biol 4:a009886–a009886.

Zoghbi HY, Bear MF (2012b) Synaptic Dysfunction in Neurodevelopmental Intellectual Disabilities. Cold Spring Harb Perspect Biol 4:1–22.